

Nonequilibrium functional RG with frequency dependent vertex function – a study of the single impurity Anderson model

Severin G. Jakobs, Mikhail Pletyukhov, and Herbert Schoeller
*Institut für Theoretische Physik A, RWTH Aachen University, D-52056 Aachen, Germany and
JARA – Fundamentals of Future Information Technologies, Germany*

(Dated: November 30, 2009)

We investigate nonequilibrium properties of the single impurity Anderson model by means of the functional renormalization group (fRG) within Keldysh formalism. We present how the level broadening $\Gamma/2$ can be used as flow parameter for the fRG. This choice preserves important aspects of the Fermi liquid behaviour that the model exhibits in case of particle-hole symmetry. An approximation scheme for the Keldysh fRG is developed which accounts for the frequency dependence of the two-particle vertex in a way similar but not equivalent to a recently published approximation to the equilibrium Matsubara fRG. Our method turns out to be a rather flexible tool for the study of weak to intermediate on-site interactions $U \lesssim 3\Gamma$. In equilibrium we find excellent agreement with NRG results for the linear conductance at finite gate voltage, magnetic field, and temperature. In nonequilibrium, our results for the current agree well with TD-DMRG. For the nonlinear conductance as function of the bias voltage, we propose reliable results at finite magnetic field and finite temperature. Furthermore, we demonstrate the exponentially small scale of the Kondo temperature to appear in the second order derivative of the self-energy.

PACS numbers: 05.10.Cc, 72.10.Fk, 73.63.Kv

I. INTRODUCTION

Due to the enormous experimental progress in the investigation of nanoelectronic and molecular systems, one of the central issues of theoretical condensed matter physics is the understanding of nonequilibrium phenomena in small strongly correlated quantum systems coupled to an environment. Traditionally such systems were investigated in the context of dissipative quantum mechanics, where energy exchange of a few-level system with a single bath of phonons was considered¹. With the realization of various devices involving metallic islands², quantum dots³, single molecules⁴, or quantum wires^{5,6}, a tunneling coupling to leads was realized, which enabled the controlled study of local quantum systems coupled via particle exchange to the environment. Furthermore, in the presence of several leads, it became possible to study such systems in the presence of a finite bias voltage or temperature gradients (inhomogeneous boundary conditions), i.e. a nonequilibrium and current-carrying state can be realized in the stationary situation.

Whereas in equilibrium there are powerful numerical and analytical techniques to describe linear transport or spectral properties of mesoscopic systems, the available methods in nonequilibrium are quite restrictive and still under development in the nonperturbative regime. Exact solutions exist for some special cases^{7,8,9}. Scattering Bethe-Ansatz solutions have been applied to the interacting resonant level model¹⁰ and the Anderson impurity model¹¹, but the full understanding of the stationary state in all regimes has not yet been reached. To describe the steady state in the presence of a finite bias voltage, numerical renormalization group (NRG) methods using scattering waves¹², time-dependent density matrix renormalization group (TD-DMRG)¹³, quantum Monte Carlo (QMC) with complex chemical potentials¹⁴, and iterative path-integral approaches (ISPI)¹⁵ have been developed, but the efficiency of these methods is still not satis-

factory in the regimes of strong Coulomb interaction and/or large bias voltage. To calculate the time evolution into the stationary state, numerical techniques like time-dependent NRG (TD-NRG)^{16,17}, TD-DMRG^{8,13,18}, ISPI¹⁵, and QMC in nonequilibrium^{19,20} have been used. However, the description of finite bias or the long-time limit still remains difficult.

Naive perturbation expansions in the coupling between the local system and the reservoirs or in the Coulomb interaction on the local system can not cover the most interesting regime of quantum fluctuations and strong correlations at very low temperatures. To improve them significantly, the most promising analytic approaches are perturbative renormalization group (RG) methods for nonequilibrium systems. Several methods have been proposed, which differ significantly concerning the extent up to which nonequilibrium aspects are taken into account and how the perturbative expansion in the renormalized vertices is set up. One of the first formally exact nonequilibrium RG methods for zero-dimensional quantum systems (quantum dots) was developed in Refs. [21,22,23] and is called the real-time renormalization group method (RTRG). This technique is based on an expansion in the renormalized coupling between quantum system and reservoir, whereas the correlations on the local system are taken exactly into account. Later on, this method was formulated in pure frequency space and combined with a cutoff procedure on the imaginary frequency axis (introduced in Ref. [24]), the so-called RTRG-FS method²⁵. Within this technique it was possible to solve analytically the generic problem how RG flows are cut off by the physics of transport rates. Furthermore, it was demonstrated how all static and dynamic properties can be calculated analytically for the nonequilibrium Kondo model in weak coupling^{26,27,28} and for the interacting resonant level model (IRLM) in the scaling limit²⁹, which are two fundamental models for the physics of spin and charge fluctuations, respectively. Another perturbative RG method in nonequilibrium (called PRG-NE), which also expands in

the reservoir-system coupling, was developed in Refs. [30,31], where the slave particle approach was used in connection with Keldysh formalism and quantum Boltzmann equations. In these works it was investigated for the first time how the voltage and the magnetic field cuts off the RG flow for the Kondo model and how the frequency dependence of the vertices influences various logarithmic contributions for the susceptibility and the nonlinear conductance. A real-frequency cutoff was used and the RG was formulated purely on one part of the Keldysh-contour disregarding diagrams connecting the upper with the lower branch. This procedure turns out to be sufficient for the Kondo model to calculate logarithmic terms in leading order but the cutoff by relaxation and decoherence rates was included intuitively (recently an improved version of this method included parts of the spin relaxation and decoherence rates via self-energy insertions³²). An alternative microscopic approach to RTRG-FS for combining relaxation and decoherence rates within a nonequilibrium RG method for the Kondo model was proposed in Ref. [33], where flow-equation methods³⁴ were generalized to the nonequilibrium situation. Within this method, it was shown for the Kondo model that the cutoff of the RG flow by spin relaxation/decoherence rates occurs due to a competition of 1-loop and 2-loop terms on the r.h.s. of the RG equation for the vertex.

Whereas all of these perturbative RG methods are very successful, they have two important drawbacks. First, they expand all in the reservoir-system coupling and thus can only be used reliably in the regime of weak spin or orbital fluctuations (strong charge fluctuations seem to be covered by RTRG-FS as was demonstrated recently for the IRLM in Ref. [29]). Secondly, the RTRG-FS and the PRG-NE scheme work in a basis of the many-particle eigenfunctions of the isolated local quantum system. As a consequence larger systems like multi-level quantum dots, large molecules, or the crossover to the quantum wire case cannot be addressed due to an exponentially large number of relevant many-particle states. Therefore, another class of perturbative RG methods in nonequilibrium have been developed which are based on an expansion in the renormalized Coulomb interaction on the local quantum system by combining the Keldysh formalism with a quantum-field theoretical formulation of functional RG within the 1-particle irreducible Wetterich scheme³⁵. In the following we call this approach the fRG-NE method. It has been proposed and applied to quantum dots and quantum wires in Refs. [24,29,36,37,38]. Since the method is non-perturbative in the reservoir-system coupling and is parametrized in terms of single-particle states, it has the advantage that the strong-coupling regime of the Kondo effect can be approached and it can be applied to multi-level quantum dots and quantum wires, at least in the regime of moderate Coulomb interactions.

So far, the fRG-NE scheme was used in approximations schemes with frequency independent self-energy. This approach describes reliably the leading effects of weak interactions in an effective single-particle picture. At higher interactions the decay rates generated by inelastic effects of the interaction are no longer negligible and may drastically change the behaviour of the system. These effects can only be described

on the level of a frequency dependent self-energy, which is the subject of the present paper. We will address the problem to enhance the truncation scheme used for fRG-NE, such that it is able to describe interaction induced decay rates. The flow equations for the vertex functions are of such a structure that a frequency dependent self-energy can only result from a frequency dependent two-particle vertex. This in turn is a very complicated object, depending on four frequency, state and Keldysh indices. Conservation laws for spin, momentum, and frequency, and the symmetry properties of the vertex function discussed in Ref. [39] can be used to reduce the complexity. Nevertheless, the two-particle vertex function remains so complicated that it seems preferable to develop the methodology first for a physical system with as few interacting degrees of freedom as possible. This restricts at least the dimensionality of the state dependence of the vertex function. Insight gained at this level can later be used to attack larger systems.

We choose to investigate the single impurity Anderson model⁴⁰ (SIAM) which is considered to be a generic model for strong local correlations⁴¹ and is a minimal model to study the interplay of charge and spin fluctuations. It consists of a single-level quantum dot with spin and on-site Coulomb repulsion U , which is coupled to leads. Experimentally, it can be realized for small quantum dots or molecules. In the Coulomb-blockade regime, this model is equivalent to the Kondo model⁴² and the unitarity limit of the Kondo effect has been measured⁴³. The perturbation theory of this model in U is completely regular^{44,45,46,47}. However, the low energy behaviour at large interaction U is governed by the so called Kondo scale⁴¹ which is exponentially small in U and hence cannot be described in any finite order perturbation theory. This makes the model an interesting object of RG studies. Since the model can be described in equilibrium very accurately by the numerical renormalization group (NRG)⁴⁸ and even exact results for thermodynamic properties are available from Bethe Ansatz⁴⁹ there is the possibility given to benchmark our results at least in equilibrium.

In case of thermal equilibrium the application of the Matsubara fRG to the single-impurity Anderson model has already been studied in detail with two different truncation schemes. One of the schemes reduces the flow of the two-particle vertex to a renormalization of the static interaction strength and produces a frequency independent self-energy. This approximation is able to reproduce a Kondo scale exponentially small in U which appears e.g. in the pinning of the level to the chemical potential^{50,51}. It turned out to be a quite powerful tool for the description of static properties of diverse quantum dot geometries even at fairly large interactions⁵⁰. The approximation is however unable to describe finite frequency properties, a restriction that becomes manifest very clearly in the shape of the spectral function: the approximation of a static self-energy leads to a Lorentzian resonance peak. The sharp Kondo resonance, the side bands, the suppression of the Kondo resonance with temperature are features which cannot be described in principle by the static approximation.

The second more elaborate approximation scheme which has been used within the equilibrium fRG keeps the frequency

dependence of the two-particle vertex function and neglects the three-particle vertex^{52,53}. It yields quantitatively good results for small to intermediate interaction strengths. While finite frequencies properties are accessible to this frequency dependent fRG approximation for not too large interactions, it has been observed that the large interaction asymptotics of this refined version are worse than the ones found in the static fRG; no Kondo scale exponentially small in U has been found⁵³. Also a technical disadvantage related to the use of the Matsubara formalism becomes apparent: while the self-energy data are quite accurate on the imaginary frequency axis for small and intermediate U , the analytic continuation to the real axis was unstable for nonzero temperatures, working only for certain parameter sets. Therefore only observables which are accessible from the imaginary frequency axis (without resorting to analytic continuation) can be systematically studied at finite temperature⁵³. This finding is an additional motivation to study a frequency dependent fRG within the Keldysh formalism, being formulated on the real frequency axis from the outset.

Apart from the possibility to access real frequency properties at finite temperature we envisage the opportunity to analyze the non-equilibrium behaviour of the SIAM. This has been recently in the focus of diverse publications. Among them is also a non-equilibrium fRG study that is based on a real-frequency cut-off and a static approximation scheme^{37,38}. Results known from the Matsubara fRG could be partially reproduced by this method. It suffers however from the violation of causality related to the choice of the real-frequency cut-off. Refs. [54,55] present perturbative studies that apply to moderate interactions and the special situation of particle-hole symmetry and vanishing magnetic field. The RTRG method was used in Ref. [21] to describe the mixed valence and empty-orbital regime of the SIAM at finite bias. The results seem to be reliable but it was not possible to study the Kondo regime since essential processes describing spin fluctuations were neglected. In Ref. [14] a time independent description of non-equilibrium based on a density operator for the steady state is used to make the problem accessible by QMC. The main challenge of this method is the numerical analytic continuation of two imaginary quantities to the real axis. A recent improvement of nonequilibrium QMC applied to the SIAM at zero magnetic field and zero gate voltage²⁰ has given reliable results for $U < 3 - 5\Gamma = 6 - 10\Delta$ (in our notation $\Delta = \Gamma/2$ denotes the level broadening, i.e. Γ is the full width at half maximum of the noninteracting spectral density) for the occupations and the nonlinear current. The ISPI approach¹⁵ gives access to the current through the model for moderate U and not too low temperatures. A very promising tool is the recently introduced scattering states NRG¹². Unfortunately the results for the conductance obtained by this method bear still a considerable numerical uncertainty. Spataru et al.⁵⁶ generalized the GW approximation to non-equilibrium and concentrate on the Coulomb blockade regime of the model. In order to access the Kondo limit of the Anderson model an approach based on Hubbard-Stratonovich fields representing spin fluctuations has been used in Ref. [57]. An implementation of this idea within Matsubara fRG however has not yet been able

to reproduce the exponentially small Kondo scale. The TD-DMRG technique¹³ tries to access the steady state transport features of the model from the transient regime. Data for the current at moderate interactions have been found to agree very well with our fRG results.

In contrast to many other methods, we propose in this paper a very flexible approach which provides reliable results for moderate interactions $U \lesssim 3\Gamma = 6\Delta$. In equilibrium, we will show that the linear conductance agrees very well with NRG data at finite gate voltage, magnetic field, and temperature. In nonequilibrium at finite bias V , the nonlinear current $I(V)$ is found to agree very well with TD-DMRG data¹³. This provides the main evidence that our results can be trusted also for the nonlinear conductance $G(V)$ at finite magnetic field B and finite temperature T . In particular, at $T = B = 0$, we find that our results for $G(V)$ do not show anomalous peaks as obtained within fourth order perturbation theory⁵⁵. Furthermore, we show that even the exponentially small scale of the Kondo temperature can be identified in the second order derivative of the self-energy and the various Fermi-liquid relations are reproduced. However, the effective mass still does not contain an exponentially small scale leading to a too large broadening of the spectral density for interaction strengths $U > 3\Gamma$.

The paper is organized as follows. Section II introduces the model and its treatment within Keldysh formalism. In section III we recapitulate the core elements of the fRG for irreducible vertex functions. It follows a motivation and discussion of the choice of hybridization as flow parameter in section IV. In section V we describe the more basic frequency independent approximation of the flow equations and show that in the case of equilibrium and zero temperature we reproduce exactly the flow equations known from the Matsubara fRG. Section VI is then devoted to the fRG in frequency dependent approximation. There are three channels contributing to the flow of the two-particle vertex. We show that all three need to be taken into account and describe an approximation scheme that simplifies the functional form in which the two-particle vertex depends on frequencies. In section VII we demonstrate that the fRG approach in the chosen truncation and approximation scheme preserves the Fermi-liquid relations for the (imaginary part of the) self-energy; furthermore we determine the fRG estimate for the Fermi-liquid coefficients. Section VIII finally presents numerical results obtained from the fRG and compares them to other methods. A conclusion is given in section IX. The Appendices present some mainly technical considerations. In Appendix A we identify a set of independent components which completely determine the two-particle vertex function. The precise form of the flow equations in terms of these components is given in Appendices B and C. In Appendix D we recover within the fRG approach the nonequilibrium Fermi-liquid relation known from Ref. [58].

II. SIAM AND KELDYSH FORMALISM

The single impurity Anderson model⁴⁰ under consideration consists of a single electronic level with on-site repulsion,

which is coupled to two noninteracting reservoirs addressed as left (L) and right (R). We denote the single particle states of the impurity by $\sigma = \uparrow, \downarrow = +\frac{1}{2}, -\frac{1}{2}$ according to the state of the electron spin. The matrix element of the on-site two-particle interaction is

$$\langle \sigma'_1 \sigma'_2 | v | \sigma_1 \sigma_2 \rangle = \begin{cases} U, & \text{if } \sigma'_1 = \sigma_1 = \bar{\sigma}'_2 = \bar{\sigma}_2, \\ 0, & \text{else,} \end{cases} \quad (1)$$

with $U \geq 0$, where we used the notation $\bar{\sigma} = -\sigma$. In standard notation of second quantization the Hamiltonian is given by

$$H = H_{\text{dot}} + H_{\text{res}} + H_{\text{coup}}, \quad (2a)$$

$$H_{\text{dot}} = \sum_{\sigma} \left(eV_{\text{g}} - \sigma B - \frac{U}{2} \right) d_{\sigma}^{\dagger} d_{\sigma} + U d_{\uparrow}^{\dagger} d_{\uparrow} d_{\downarrow}^{\dagger} d_{\downarrow}, \quad (2b)$$

$$H_{\text{res}} = \sum_{r=L,R} H_{\text{res}}^{(r)} = \sum_r \sum_{\sigma} \int dk_r \epsilon_{k_r} c_{k_r, \sigma}^{\dagger} c_{k_r, \sigma}, \quad (2c)$$

$$H_{\text{coup}} = \sum_r H_{\text{coup}}^{(r)} = \sum_r \sum_{\sigma} \int dk_r (V_{k_r} d_{\sigma}^{\dagger} c_{k_r, \sigma} + \text{h.c.}), \quad (2d)$$

where the annihilators $d_{\sigma}, c_{k_r, \sigma}$ and creators $d_{\sigma}^{\dagger}, c_{k_r, \sigma}^{\dagger}$ obey the usual fermionic anti-commutation rules. The single-particle energies of the dot

$$\epsilon_{\sigma} = eV_{\text{g}} - \sigma B - U/2 \quad (3)$$

depend on the gate voltage V_{g} and the magnetic field B and are shifted by $(-U/2)$ such that particle-hole symmetry is given when eV_{g} equals the chemical potential.

We are interested in the stationary state which emerges a long time after both reservoirs have been prepared each in individual grand-canonical equilibrium described by the Fermi function

$$f_r(\omega) = \frac{1}{e^{(\omega - \mu_r)/T} + 1}. \quad (4)$$

The temperature T is assumed to be equal in both reservoirs, whereas a possible difference between the two chemical potentials accounts for a finite bias voltage,

$$eV = \mu_{\text{L}} - \mu_{\text{R}}. \quad (5)$$

We measure single-particle energies relative to the mean chemical potential by setting

$$\mu_{\text{L}} + \mu_{\text{R}} = 0. \quad (6)$$

We describe the system in the framework of Keldysh formalism^{59,60,61,62}, where the single-particle propagator between two states q' and q has four components

$$G_{q|q'}^{-|-}(t|t') = G_{q|q'}^{\text{c}}(t|t') = -i \text{Tr} \rho_0 T a_q(t) a_{q'}^{\dagger}(t') \quad (7a)$$

$$G_{q|q'}^{-|+}(t|t') = G_{q|q'}^{\text{<}}(t|t') = i \text{Tr} \rho_0 a_{q'}^{\dagger}(t') a_q(t) \quad (7b)$$

$$G_{q|q'}^{+|-}(t|t') = G_{q|q'}^{\text{>}}(t|t') = -i \text{Tr} \rho_0 a_q(t) a_{q'}^{\dagger}(t') \quad (7c)$$

$$G_{q|q'}^{+|+}(t|t') = G_{q|q'}^{\text{c}}(t|t') = -i \text{Tr} \rho_0 \tilde{T} a_q(t) a_{q'}^{\dagger}(t') \quad (7d)$$

called chronologic, lesser, greater, and anti-chronologic, respectively. Here T (\tilde{T}) denotes the time (anti-time) ordering operator and $a_q(t) = d_{\sigma}(t)$ or $c_{k_r, \sigma}(t)$ is in the Heisenberg-picture at time t . ρ_0 is the initial product density matrix at the time $t_0 \rightarrow -\infty$ of system preparation. In the time translational invariant stationary state $G(t|t') = G(t - t'|0)$ depends only on the difference of the two time arguments and we use the Fourier transform

$$G_{q|q'}^{j|j'}(\omega) = \int dt e^{i\omega t} G_{q|q'}^{j|j'}(t|0), \quad j, j' = \mp. \quad (8)$$

Instead of the contour basis with indices $j = \mp$ we use the Keldysh basis⁶³ with indices $\alpha = 1, 2$, whose components are physically more meaningful⁶⁴. The transformation to this basis is given by

$$G^{\alpha|\alpha'} = \sum_{j, j' = \mp} (D^{-1})^{\alpha|j} G^{j|j'} D^{j'|\alpha'}, \quad (9)$$

where

$$D^{-|1} = D^{\mp|2} = (D^{-1})^{1|-} = (D^{-1})^{2|\mp} = \frac{1}{\sqrt{2}}, \quad (10a)$$

$$D^{+|1} = (D^{-1})^{1|+} = -\frac{1}{\sqrt{2}}. \quad (10b)$$

The resulting components of the single particle Green function

$$G^{1|1} = 0, \quad G^{1|2} = G^{\text{Av}}, \quad G^{2|1} = G^{\text{Ret}}, \quad G^{2|2} = G^{\text{K}} \quad (11)$$

are called advanced, retarded, and Keldysh, respectively. The self-energy is transformed correspondingly,

$$\Sigma^{\alpha'|\alpha} = \sum_{j', j = \mp} (D^{-1})^{\alpha'|j'} \Sigma^{j'|j} D^{j|\alpha}, \quad (12)$$

leading to

$$\Sigma^{1|1} = \Sigma^{\text{K}}, \quad \Sigma^{1|2} = \Sigma^{\text{Ret}}, \quad \Sigma^{2|1} = \Sigma^{\text{Av}}, \quad \Sigma^{2|2} = 0. \quad (13)$$

The influence of the reservoirs onto the dot Green function can be described by self energy contributions⁷⁰

$$\Sigma_{\text{res } \sigma}^{(r) \alpha'|\alpha}(\omega) = \int dk_r V_{k_r} g_{k_r}(\omega) V_{k_r}^* \quad (14)$$

with g_{k_r} being the free propagator in the reservoir state k_r which is assumed to be independent of spin. Explicitly, the individual Keldysh components are

$$\Sigma_{\text{res } \sigma}^{(r) \text{Ret}}(\omega) = \frac{1}{2\pi} \int d\omega' \frac{\Gamma_r(\omega')}{\omega - \omega' + i\eta}, \quad (15a)$$

$$\Sigma_{\text{res } \sigma}^{(r) \text{Av}}(\omega) = \Sigma_{\text{res } \sigma}^{(r) \text{Ret}}(\omega)^*, \quad (15b)$$

$$\Sigma_{\text{res } \sigma}^{(r) \text{K}}(\omega) = -i[1 - 2f_r(\omega)]\Gamma_r(\omega), \quad (15c)$$

where we made use of the hybridization function

$$\Gamma_r(\omega) = 2\pi \int dk_r |V_{k_r}|^2 \delta(\omega - \epsilon_{k_r}). \quad (16)$$

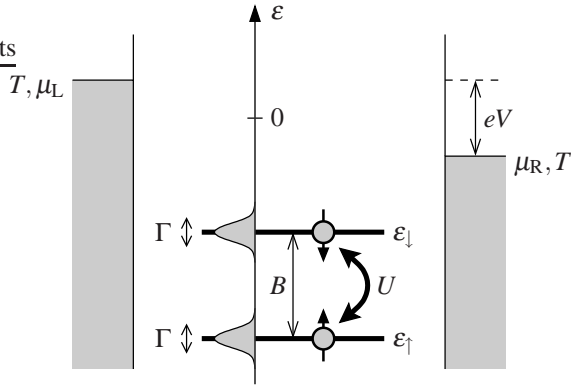


FIG. 1: Sketch of the model with single particle energy in vertical direction.

As we are neither interested in the influence of the band structure of the reservoirs nor in the momentum dependence of the hopping elements, we linearize the reservoir dispersion, $\varepsilon_{k_r} = v_r k_r$ (with $v_r = d\varepsilon_{k_r}/dk_r$ being the inverse density of states) and set the hopping to momentum independent constants, $V_{k_r} \equiv V_r$. As a result, the hybridization functions are frequency independent constants,

$$\Gamma_r(\omega) = \Gamma_r = 2\pi \frac{|V_r|^2}{v_r}. \quad (17)$$

The results presented later apply to the special case of symmetric coupling, $\Gamma_L = \Gamma_R$, which is of technical advantage for the implementation of our approximations.

Defining the total hybridization Γ via

$$\Gamma = \Gamma_L + \Gamma_R, \quad (18)$$

the reservoir-dressed noninteracting dot propagator is given by

$$g_{\sigma}^{\text{Ret}}(\omega) = \frac{1}{\omega - \varepsilon_{\sigma} + i\Gamma/2}, \quad (19a)$$

$$g_{\sigma}^{\text{Av}}(\omega) = g_{\sigma}^{\text{Ret}}(\omega)^*, \quad (19b)$$

$$g_{\sigma}^{\text{K}}(\omega) = [1 - 2f_{\text{eff}}(\omega)] [g_{\sigma}^{\text{Ret}}(\omega) - g_{\sigma}^{\text{Av}}(\omega)], \quad (19c)$$

with the effective distribution function

$$f_{\text{eff}}(\omega) = \sum_r \frac{\Gamma_r}{\Gamma} f_r(\omega). \quad (20)$$

A sketch of the model can be found in figure 1.

The current from the left reservoir through the dot to the right reservoir is given by^{54,71}

$$I = e \frac{\Gamma_L \Gamma_R}{\Gamma} \int d\omega [f_L(\omega) - f_R(\omega)] \sum_{\sigma} \rho_{\sigma}(\omega) \quad (21)$$

where the spectral density can be obtained from the interacting single-particle dot Green function as

$$\rho_{\sigma}(\omega) = -\frac{1}{\pi} \text{Im} G_{\sigma}^{\text{Ret}}(\omega). \quad (22)$$

We note that the Hamiltonian is of such a type that the dot Green function in the spin basis exhibits the special behaviour under time reversal described in section 5.5 of Ref. [39]. Therefore the Kubo-Martin-Schwinger conditions which connect the components of the Green and vertex functions in thermal equilibrium and which we apply later on take the form of a generalized fluctuation dissipation theorem as stated in section 5.6 of that reference.

III. VERTEX FUNCTIONS AND FUNCTIONAL RENORMALIZATION GROUP

A treatment of the problem with the fRG is set up by making the bare propagator g depend on a flow parameter λ . Most commonly λ is chosen to suppress low energy degrees of freedom. Being functionals of the bare propagator, the interacting Green and vertex functions acquire a dependence on λ as well, which is described by an infinite hierarchy of coupled flow equations.⁶⁶ The flow parameter is introduced in such a way that two values of λ are of particular importance: at $\lambda = \lambda_{\text{start}}$ the Green or vertex functions can be determined exactly or in reasonable approximation; at $\lambda = \lambda_{\text{stop}}$ the free propagator takes its original value, $g(\lambda_{\text{stop}}) = g$ and so do the interacting Green or vertex functions. Therefore the interacting Green or vertex functions can be found by computing (approximately) their flow from λ_{start} to λ_{stop} . In this paper we focus on the flow of the one-particle irreducible vertex functions^{35,67} which has proven to provide a successful approach to the physics of diverse low-dimensional correlated electron problems^{68,69}.

The one-particle irreducible vertex functions can be derived from generating functionals; details on this approach can be found for Matsubara formalism e.g. in Ref. [65] and for Keldysh formalism in Ref. [37]. Equivalently, the one-particle irreducible n -particle vertex function

$$\gamma_{q'_1 \dots q'_n | q_1 \dots q_n}^{\alpha'_1 \dots \alpha'_n | \alpha_1 \dots \alpha_n}(\omega'_1, \dots, \omega'_n | \omega_1, \dots, \omega_n) \quad (23)$$

can be defined diagrammatically as the sum of all one-particle irreducible diagrams with n amputated incoming lines (having states q_1, \dots, q_n , Keldysh indices $\alpha_1, \dots, \alpha_n$ and frequencies $\omega_1, \dots, \omega_n$) and n amputated outgoing lines (having states q'_1, \dots, q'_n , Keldysh indices $\alpha'_1, \dots, \alpha'_n$ and frequencies $\omega'_1, \dots, \omega'_n$). Due to frequency conservation only $(2n - 1)$ of the $2n$ frequencies are independent. By the expression (23) we refer to a function depending only on $(2n - 1)$ frequency arguments, the last one being redundant.

The vertex functions are anti-symmetric under exchange of particles. In fact, the underlying diagrammatics is meant to be of the Hugenholtz type⁶⁵, thus based on anti-symmetrized interaction vertices

$$\begin{aligned} \bar{v}_{q'_1 q'_2 | q_1 q_2}^{\alpha'_1 \alpha'_2 | \alpha_1 \alpha_2} &= \langle q'_1 q'_2 | v | q_1 q_2 \rangle - \langle q_2 q_1 \rangle \\ &\times \begin{cases} \frac{1}{2}, & \text{if } \alpha_1 + \alpha_2 + \alpha'_1 + \alpha'_2 \text{ is odd,} \\ 0, & \text{else,} \end{cases} \quad (24) \end{aligned}$$

where q, q_2 (q'_1, q'_2) are incoming (outgoing) single particle states and α_1, α_2 (α'_1, α'_2) incoming (outgoing) Keldysh indices.

In order to evaluate a specific diagram contributing to a vertex function, one determines the symmetry factor S , the number n_{eq} of equivalent lines, the number n_{loop} of internal loops and the permutation P that describes which incoming index is connected to which outgoing one. The value of the diagram is then given by

$$\frac{(-1)^{n_{\text{loop}}}(-1)^P}{2^{n_{\text{eq}}}S} \left(\frac{2\pi}{i}\right)^{n-1} \left[\prod \frac{i}{2\pi\bar{v}}\right] \prod g, \quad (25)$$

where one has to sum over all internal state and Keldysh indices and to integrate over all independent internal frequencies. Details can be found in Ref. [39]. Equation (25) defines the prefactor of the vertex functions in such a way, that they can be used themselves as vertices in diagrams with the identical prefactor rules applicable to bare n -particle interaction vertices. The self-energy is equal to the one-particle vertex, $\Sigma \equiv \gamma_{n=1}$.

A derivation of the flow equations for the vertex functions within the generating functional approach in Keldysh formalism is given in Ref. [37]. Ref. [24] describes an equivalent derivation of the flow equations based on diagrams and provides a diagram rule for their formulation. The resulting flow equations form an infinite coupled hierarchy where the flow of the n -particle vertex functions, $d\gamma_n^\lambda/d\lambda$, is a functional of $\Sigma^\lambda, \gamma_2^\lambda, \dots, \gamma_{n+1}^\lambda$. For example the flow equations for the one- and two-particle vertex function read

$$\frac{d}{d\lambda} \Sigma_{1'1}^\lambda = -\frac{i}{2\pi} \gamma_{1'2'|12}^\lambda S_{2|2'}^\lambda \quad (26)$$

and

$$\frac{d}{d\lambda} \gamma_{1'2'|12}^\lambda = -\frac{i}{2\pi} \gamma_{1'2'3'|123}^\lambda S_{3|3'}^\lambda \quad (27a)$$

$$+ \frac{i}{2\pi} \gamma_{1'2'|34}^\lambda S_{3|3'}^\lambda G_{4|4'}^\lambda \gamma_{3'4'|12}^\lambda \quad (27b)$$

$$+ \frac{i}{2\pi} \gamma_{1'4'|32}^\lambda \left[S_{3|3'}^\lambda G_{4|4'}^\lambda + G_{3|3'}^\lambda S_{4|4'}^\lambda \right] \gamma_{3'2'|14}^\lambda \quad (27c)$$

$$- \frac{i}{2\pi} \gamma_{1'3'|14}^\lambda \left[S_{3|3'}^\lambda G_{4|4'}^\lambda + G_{3|3'}^\lambda S_{4|4'}^\lambda \right] \gamma_{4'2'|32}^\lambda. \quad (27d)$$

Here we use shorthands like

$$\gamma_{1'2'|12}^\lambda \equiv (\gamma_\lambda)_{q'_1 q'_2 | q_1 q_2}^{\alpha'_1 \alpha'_2 | \alpha_1 \alpha_2} (\omega'_1 \omega'_2 | \omega_1 \omega_2), \quad (28)$$

and indices occurring twice in a product implicate summation over state and Keldysh indices and integration over independent frequencies. Furthermore,

$$S_\lambda = G_\lambda g_\lambda^{-1} s_\lambda g_\lambda^{-1} G_\lambda \quad (29)$$

with

$$s_\lambda = \frac{dg_\lambda}{d\lambda} \quad (30)$$

denotes the so called single scale propagator. We call the contributions (27b), (27c), and (27d) to the flow of $\gamma_{1'2'|12}^\lambda$ particle-particle, exchange particle-hole, and direct particle-hole channel, respectively.

For practical computations the exact infinite set of flow equations is reduced to a closed finite set of approximated flow equations. Typical approximations are to neglect the flow of higher order vertex functions by setting $d\gamma_n^\lambda/d\lambda \equiv 0$ for $n \geq n_0$ and to ascribe an effective parametrization to the remaining ones. In the present investigation of the SIAM we neglect the flow of γ_3^λ . Two different parametrizations of γ_2^λ will be discussed, a static (i.e. frequency independent) and a dynamic (frequency dependent) one.

IV. FLOW PARAMETER

In Ref. [39] it has been shown how the choice of the flow parameter determines whether certain exact properties of the vertex functions are conserved by an approximated fRG flow. For the study of the SIAM the conservation not only of causality but also of the Kubo-Martin-Schwinger (KMS) conditions characterizing thermal equilibrium is important. The correct description of thermal equilibrium is necessary in order to capture fundamental aspects of the low energy properties of the model. Consider for example the expansion of the self-energy at $eV_g = \mu = 0$, $B = 0$ in leading order in frequency, temperature, and voltage,

$$\Sigma_\sigma^{\text{Ret}}(\omega, T, V) \simeq \frac{U}{2} + \left(1 - \frac{\tilde{\chi}_s + \tilde{\chi}_c}{2}\right) \omega - i \frac{(\tilde{\chi}_s - \tilde{\chi}_c)^2}{4\Gamma} \left[\omega^2 + (\pi T)^2 + \frac{3}{4}(eV)^2 \right], \quad (31)$$

where $\tilde{\chi}_c$ and $\tilde{\chi}_s$ denote the reduced charge and spin susceptibility^{44,58}. This Fermi liquid behaviour influences important aspects of Kondo physics, like the height and width of the Kondo resonance. The derivation of (31) is based on thermal equilibrium particle statistics and hence requires the validity of the KMS conditions for a treatment within Keldysh formalism.

Hybridization can be used as a flow parameter which conserves causality and the KMS conditions³⁹. For that purpose the constants $\Gamma_{L,R}$ and Γ from equations (17, 18) are enhanced artificially by setting

$$\Gamma_\lambda = \Gamma + \lambda, \quad (32a)$$

$$\Gamma_\lambda^{(r)} = \Gamma_r + \frac{\Gamma_r}{\Gamma} \lambda, \quad r = L, R, \quad (32b)$$

where λ flows from ∞ to 0. Via the hybridization, the components of the noninteracting reservoir dressed propagator acquire the λ -dependence

$$(g_\lambda)_\sigma^{\text{Ret}}(\omega) = \frac{1}{\omega - \varepsilon_\sigma + i(\Gamma + \lambda)/2}, \quad (33a)$$

$$(g_\lambda)_\sigma^{\text{Av}}(\omega) = (g_\lambda)_\sigma^{\text{Ret}}(\omega)^*, \quad (33b)$$

$$(g_\lambda)_\sigma^{\text{K}}(\omega) = [1 - 2f_{\text{eff}}(\omega)] [(g_\lambda)_\sigma^{\text{Ret}}(\omega) - (g_\lambda)_\sigma^{\text{Av}}(\omega)], \quad (33c)$$

where $f_{\text{eff}}^{\lambda}(\omega) \equiv f_{\text{eff}}(\omega)$ does not depend on λ since $\Gamma_{\lambda}^{(r)}/\Gamma_{\lambda} = \Gamma_r/\Gamma$, compare equation (20). The components of the free single scale propagator $s_{\lambda} = dg_{\lambda}/d\lambda$ are given by

$$s_{\lambda}^{\text{Ret}}(\omega) = -\frac{i}{2} [g_{\lambda}^{\text{Ret}}(\omega)]^2, \quad (34a)$$

$$s_{\lambda}^{\text{Av}}(\omega) = s_{\lambda}^{\text{Ret}}(\omega)^{\dagger} \quad (34b)$$

$$s_{\lambda}^{\text{K}}(\omega) = [1 - 2f_{\text{eff}}(\omega)] [s_{\lambda}^{\text{Ret}}(\omega) - s_{\lambda}^{\text{Av}}(\omega)], \quad (34c)$$

and those of the full single scale propagator $S_{\lambda} = G_{\lambda} g_{\lambda}^{-1} s_{\lambda} g_{\lambda}^{-1} G_{\lambda}$ by

$$S_{\lambda}^{\text{Ret}}(\omega) = -\frac{i}{2} [G_{\lambda}^{\text{Ret}}(\omega)]^2, \quad (35a)$$

$$S_{\lambda}^{\text{Av}}(\omega) = S_{\lambda}^{\text{Ret}}(\omega)^{\dagger}, \quad (35b)$$

$$S_{\lambda}^{\text{K}}(\omega) = -\frac{i}{2} G_{\lambda}^{\text{Ret}}(\omega) G_{\lambda}^{\text{K}}(\omega) + \frac{i}{2} G_{\lambda}^{\text{K}}(\omega) G_{\lambda}^{\text{Av}}(\omega) - i[1 - 2f_{\text{eff}}(\omega)] G_{\lambda}^{\text{Ret}}(\omega) G_{\lambda}^{\text{Av}}(\omega). \quad (35c)$$

A special situation is given when

$$G_{\lambda}^{\text{K}}(\omega) = [1 - 2f_{\text{eff}}(\omega)] [G_{\lambda}^{\text{Ret}}(\omega) - G_{\lambda}^{\text{Av}}(\omega)]. \quad (36)$$

Then equation (35c) can be simplified to

$$S_{\lambda}^{\text{K}}(\omega) = [1 - 2f_{\text{eff}}(\omega)] [S_{\lambda}^{\text{Ret}}(\omega) - S_{\lambda}^{\text{Av}}(\omega)]. \quad (37)$$

The condition (36) is fulfilled for instance, due to the fluctuation dissipation theorem, in thermal equilibrium, when $\mu_{\text{L}} = \mu_{\text{R}}$ and $f_{\text{L}}(\omega) = f_{\text{R}}(\omega) = f(\omega) = f_{\text{eff}}(\omega)$. In non-equilibrium inelastic interaction processes mediated by the two-particle interaction will in general break the relation (36): via contributions to Σ^{K} and to the non-Hermitian part of Σ^{Ret} they tend to smoothen the effective distribution. Later we will feed back only the static part of the self-energy into the RG flow so that (36) is fulfilled automatically.

The starting values of the vertex functions at $\lambda = \infty$ can be determined as follows. For $\lambda \rightarrow \infty$ the propagator $g_{\lambda}^{\alpha|\alpha'}$ vanishes as $1/\lambda$ whereas $\int d\omega g_{\lambda}^{\alpha|\alpha'}(\omega)$ approaches a finite constant. Hence all diagrams having more internal lines than integrations over independent frequencies vanish. For a diagram with m two-particle vertices which contributes to the n -particle vertex function γ_n the number of internal lines is $2m - n$ while the number of integrations over independent frequencies is $m - n + 1$. Therefore only the first order contributions to the vertex functions do not vanish for $\lambda \rightarrow \infty$. This can also be understood in terms of time dependent diagrammatics: Due to the diverging decay rate $\lambda \rightarrow \infty$ only diagrams which are completely local in time do not vanish. These are exactly the first order diagrams, namely the Hartree-Fock diagram for the self-energy Σ and the bare interaction vertex for γ_2 ,

$$\gamma_n(\lambda = \infty) = 0, \quad n \geq 3, \quad (38a)$$

$$\gamma_2(\lambda = \infty) = \bar{v}, \quad (38b)$$

$$\begin{aligned} \Sigma_{\sigma}^{\text{Ret,Av}}(\lambda = \infty) &= \lim_{\lambda \rightarrow \infty} \left[-\frac{i}{2\pi} \sum_{\sigma'} \bar{v}_{\sigma\sigma'|\sigma\sigma'} \int d\omega g_{\lambda}^{\leq}(\omega) \right] \\ &= \frac{U}{2} \end{aligned} \quad (38c)$$

$$\Sigma^{\text{K}}(\lambda = \infty) = 0. \quad (38d)$$

In equation (38b), \bar{v} is given by

$$\bar{v}_{\sigma'_1\sigma'_2|\sigma_1\sigma_2}^{\alpha'_1\alpha'_2|\alpha_1\alpha_2} = \begin{cases} \frac{1}{2}\bar{v}_{\sigma'_1\sigma'_2|\sigma_1\sigma_2}, & \text{if } \alpha'_1 + \alpha'_2 + \alpha_1 + \alpha_2 \text{ is odd,} \\ 0, & \text{else,} \end{cases} \quad (39)$$

with

$$\bar{v}_{\sigma'_1\sigma'_2|\sigma_1\sigma_2} = \begin{cases} U, & \text{if } \sigma'_1 = \sigma_1 = \bar{\sigma}'_2 = \bar{\sigma}_2, \\ -U, & \text{if } \sigma'_1 = \bar{\sigma}_1 = \bar{\sigma}'_2 = \sigma_2, \\ 0 & \text{else,} \end{cases} \quad (40)$$

compare (24) and (1). The integral in (38c) has been evaluated by

$$-\frac{i}{2\pi} \int d\omega g_{\lambda}^{\leq}(\omega) = \frac{1}{\pi} \int dx \frac{f_{\text{eff}}(\varepsilon_{\sigma'} + x\Gamma_{\lambda}/2)}{x^2 + 1} \xrightarrow{\lambda \rightarrow \infty} \frac{1}{\pi} \int_{-\infty}^0 dx \frac{1}{x^2 + 1} = \frac{1}{2}, \quad (41)$$

where $x = 2(\omega - \varepsilon_{\sigma'})/\Gamma_{\lambda}$. The physical interpretation of (41) is that the mean occupation of an infinitely broadened level is $1/2$.

Hybridization as flow parameter has the advantage to conserve causality and the KMS conditions (the latter being violated for example by the imaginary frequency cut-off introduced in [24]) and to be applicable to zero-dimensional systems (as opposed to the momentum cut-off). Since it changes the free propagator in a smooth way, S_{λ} is not restricted sharply to a single scale by a delta function, as it is for step-function flow parameters like the momentum cut-off. Such a delta function simplifies the flow equations since it cancels one of the necessary integrations. The hybridization-flow thus has the disadvantage of an extra integration in the flow equations compared to step function cut-offs.

V. FRG IN STATIC APPROXIMATION

Before discussing the more elaborate frequency dependent truncation scheme, we describe a basic static approximation to the flow: the flow of the n -particle vertex functions for $n \geq 3$ is neglected and the flow of the two-particle vertex function is reduced to the flow of a frequency-independent effective interaction strength. As a consequence the self-energy remains frequency independent which means that the influence of the interaction on single-particle properties of the system is described by a mere shift of the single-particle levels. This approximation has been studied at $T = 0$ within a fRG treatment based on Matsubara formalism using an imaginary frequency cut-off^{50,51}. There it was shown to produce a Kondo scale exponentially small in U/Γ which occurs in the pinning of the renormalized level position to the chemical potential. Results for the dependence of the linear conductance on the gate voltage for different magnetic fields have been found to be in very good agreement with Bethe Ansatz and numerical renormalization group computations. It turns out that in thermal equilibrium at $T = 0$ the hybridization flow produces the identical

flow equations. Hence this Keldysh approach incorporates all features found in Ref. [51] for the Matsubara fRG.

Apart from its success in describing the linear conductance the applicability of the approximation in question is rather restricted. Given a frequency independent self-energy, the spectral density $\rho_\sigma(\omega)$ is a Lorentzian that is centered at the renormalized level position $\tilde{\varepsilon}_\sigma$ and has fixed width and height,

$$\rho_\sigma(\omega) = \frac{1}{\pi} \frac{\Gamma/2}{(\omega - \tilde{\varepsilon}_\sigma)^2 + \Gamma^2/4}. \quad (42)$$

Therefore the approximation cannot describe any features connected to details of the spectral function like the formation of a Kondo resonance with side bands and its dependence on temperature or voltage. That's why we do not elaborate in detail on this approximation but merely show that at zero temperature and in equilibrium the resulting flow equation are identical to those of Ref. [51].

Reducing the two-particle vertex function to a frequency independent effective interaction means setting

$$(\gamma_\lambda)_{\sigma'_1 \sigma'_2 | \sigma_1 \sigma_2}^{\alpha'_1 \alpha'_2 | \alpha_1 \alpha_2}(\omega'_1 \omega'_2 | \omega_1 \omega_2) = (\bar{\gamma}_\lambda)_{\sigma'_1 \sigma'_2 | \sigma_1 \sigma_2}^{\alpha'_1 \alpha'_2 | \alpha_1 \alpha_2} \quad (43)$$

where $\bar{\gamma}_\lambda$ is obtained from $\bar{\gamma}$ by replacing the bare interaction U by a renormalized one U_λ in (40). Here the effective interaction U_λ is a real number whose flow starts at

$$U_{\lambda=\infty} = U. \quad (44)$$

As a consequence of that approximation to the vertex function, the flowing self-energy remains frequency independent and real, so that we can speak of a flowing effective level position $\varepsilon_\sigma^\lambda = \varepsilon_\sigma + \Sigma_{\lambda\sigma}^{\text{Ret}}$. The initial condition for the level position is according to equations (3) and (38c)

$$\varepsilon_\sigma^{\lambda=\infty} = \varepsilon_\sigma + \Sigma_\sigma^{\text{Ret}}(\lambda = \infty) = eV_g - \sigma B. \quad (45)$$

The starting values (44) and (45) are identical to those of Ref. [51]. Note that in the framework used there the initial condition for the level position is the result of a first stage of flow from $\lambda = \infty$ to $\lambda = \lambda_0 \rightarrow \infty$, see e.g. Ref. [50]).

From equation (26) we derive the flow equation for the level position

$$\begin{aligned} \frac{d\varepsilon_\sigma^\lambda}{d\lambda} &= -\frac{i}{2\pi} \frac{U_\lambda}{2} \int d\omega S_{\lambda\bar{\sigma}}^{\text{K}}(\omega) \\ &= -\frac{U_\lambda}{8\pi} \int d\omega \text{sign}(\omega) \left\{ [G_{\lambda\bar{\sigma}}^{\text{Ret}}(\omega)]^2 + [G_{\lambda\bar{\sigma}}^{\text{Av}}(\omega)]^2 \right\}, \end{aligned} \quad (46)$$

where we used equation (37) with

$$1 - 2f_{\text{eff}}(\omega) = 1 - 2f(\omega) = \text{sign}(\omega) \quad \text{for } T = 0, \mu = 0. \quad (47)$$

Inserting

$$G_\lambda^{\text{Ret}}(\omega) = \frac{1}{\omega - \varepsilon^\lambda + i(\Gamma + \lambda)/2} = G_\lambda^{\text{Av}}(\omega)^\dagger \quad (48)$$

we can evaluate the integral in equation (46) and obtain

$$\frac{d\varepsilon_\sigma^\lambda}{d\lambda} = \frac{U_\lambda}{2\pi} \frac{\varepsilon_\sigma^\lambda}{\varepsilon_\sigma^{\lambda^2} + (\Gamma + \lambda)^2/4}. \quad (49)$$

The flow equation (27) for γ_2 generates a frequency dependent vertex function which has a richer structure in terms of Keldysh and spin indices than indicated in equation (43). After neglecting the contribution from the three-particle vertex function (27a) it can be reduced to the simple structure given in equation (43) by setting all outer frequency arguments equal to the chemical potential μ . The resulting flow equation has then the form

$$\begin{aligned} \frac{dU_\lambda}{d\lambda} &= \frac{U_\lambda^2}{2} \left[(I_\lambda^{\text{pp}})_{\uparrow\downarrow}^{22|12}(0) + (I_\lambda^{\text{pp}})_{\uparrow\downarrow}^{22|21}(0) \right. \\ &\quad \left. + (I_\lambda^{\text{ph}})_{\uparrow\downarrow}^{21|22}(0) + (I_\lambda^{\text{ph}})_{\uparrow\downarrow}^{22|12}(0) \right], \end{aligned} \quad (50)$$

where we abbreviated frequency integrals appearing in the particle-particle and particle-hole channel by

$$(I_\lambda^{\text{pp}})_{\sigma_1 \sigma_2}^{\alpha_1 \alpha_2 | \alpha'_1 \alpha'_2}(\omega) = \frac{i}{2\pi} \int d\omega' \left[G_{\lambda\sigma_1}^{\alpha_1 | \alpha'_1}(\frac{\omega}{2} + \omega') S_{\lambda\sigma_2}^{\alpha_2 | \alpha'_2}(\frac{\omega}{2} - \omega') + S_{\lambda\sigma_1}^{\alpha_1 | \alpha'_1}(\frac{\omega}{2} + \omega') G_{\lambda\sigma_2}^{\alpha_2 | \alpha'_2}(\frac{\omega}{2} - \omega') \right], \quad (51a)$$

$$(I_\lambda^{\text{ph}})_{\sigma_1 \sigma_2}^{\alpha_1 \alpha_2 | \alpha'_1 \alpha'_2}(\omega) = \frac{i}{2\pi} \int d\omega' \left[G_{\lambda\sigma_1}^{\alpha_1 | \alpha'_1}(\omega' - \frac{\omega}{2}) S_{\lambda\sigma_2}^{\alpha_2 | \alpha'_2}(\omega' + \frac{\omega}{2}) + S_{\lambda\sigma_1}^{\alpha_1 | \alpha'_1}(\omega' - \frac{\omega}{2}) G_{\lambda\sigma_2}^{\alpha_2 | \alpha'_2}(\omega' + \frac{\omega}{2}) \right]. \quad (51b)$$

Making use of equations (35a), (35b), (36), (37), (47) and (48) we evaluate the integrals and obtain

$$\frac{dU_\lambda}{d\lambda} = \frac{U_\lambda^2}{\pi} \frac{\varepsilon_\uparrow^\lambda}{\varepsilon_\uparrow^{\lambda^2} + (\Gamma + \lambda)^2/4} \frac{\varepsilon_\downarrow^\lambda}{\varepsilon_\downarrow^{\lambda^2} + (\Gamma + \lambda)^2/4}. \quad (52)$$

The substitution $\lambda \rightarrow 2\lambda$ maps the flow equations (49)

and (52) onto those of Ref. [51].

It is easy to generalize the static approximation scheme to non-equilibrium. Since the Keldysh component of the self-energy is not renormalized we merely need to replace (47) by

$$1 - 2f_{\text{eff}}(\omega) = \sum_r \frac{\Gamma^{(r)}}{\Gamma} \text{sign}(\omega - \mu_r), \quad (53)$$

which leads to a superposition of the flow equations found for thermal equilibrium in the form

$$\frac{d\varepsilon_\sigma^\lambda}{d\lambda} = \frac{U_\lambda}{2\pi} \sum_r \frac{\Gamma_r}{\Gamma} \frac{\varepsilon_\sigma^\lambda - \mu_r}{(\varepsilon_\sigma^\lambda - \mu_r)^2 + (\Gamma + \lambda)^2/4}, \quad (54a)$$

$$\frac{dU_\lambda}{d\lambda} = \frac{U_\lambda^2}{\pi} \sum_r \frac{\Gamma_r}{\Gamma} \frac{(\varepsilon_\uparrow^\lambda - \mu_r)}{(\varepsilon_\uparrow^\lambda - \mu_r)^2 + (\Gamma + \lambda)^2/4} \times \frac{(\varepsilon_\downarrow^\lambda - \mu_r)}{(\varepsilon_\downarrow^\lambda - \mu_r)^2 + (\Gamma + \lambda)^2/4}. \quad (54b)$$

This approach however does not provide a useful description of the influence of bias voltage, since it restricts the spectral function by construction to a single Lorentzian peak; no possibility to split or damp the peak is given from the outset.

VI. FRG IN DYNAMIC APPROXIMATION

In order to overcome the restrictions of the approximation described in section V, a frequency dependent self-energy is required. The flow equation (26) produces a frequency dependent self-energy only if the two-particle vertex function is frequency dependent. Therefore our aim is to extend the scheme described in section V in a way that a frequency dependent two-particle vertex function is generated. We seek for an extension which is as basic as possible; in particular we neglect the influence of the three-particle vertex function further on, such that the flow of the two-particle vertex function is induced by the three contributions (27b–27d).

A. Ladder approximations

Recent investigations of the SIAM by diagrammatic techniques have underlined the importance of exchange particle hole ladder (RPA series) for the emergence of Kondo physics^{72,74}. Let us therefore in a first step neglect all contributions to the flow of the two-particle vertex function except the exchange particle-hole channel (27c). If we suppress additionally the feedback of the self energy into the propagators except the initial Hartree term (38c) then the flow equation for the two-particle vertex functions reads

$$\begin{aligned} \frac{d}{d\lambda} (\gamma_\lambda^x)_{1'2'|12} &= \frac{i}{2\pi} (\gamma_\lambda^x)_{1'4'|32} \left[s_{3|3'}^\lambda g_{4|4'}^\lambda + g_{3|3'}^\lambda s_{4|4'}^\lambda \right] \\ &\quad \times (\gamma_\lambda^x)_{3'2'|14} \\ &= \frac{i}{2\pi} (\gamma_\lambda^x)_{1'4'|32} \frac{dg_{3|3'}^\lambda g_{4|4'}^\lambda}{d\lambda} (\gamma_\lambda^x)_{3'2'|14}, \end{aligned} \quad (55)$$

where g^λ is obtained from equation (33) replacing ε_σ by $\varepsilon_\sigma + U/2$. We marked the vertex function in this approximation with a superscript “x” which refers to “exchange”. The solution of the flow equation (55) with the initial condition $\gamma_{\lambda=\infty}^x = \bar{v}$ is given by the exchange particle-hole ladder (RPA

series)

$$\begin{aligned} (\gamma_\lambda^x)_{1'2'|12} &= \bar{v}_{1'2'|12} + \frac{i}{2\pi} \bar{v}_{1'4'|32} g_{3|3'}^\lambda g_{4|4'}^\lambda \bar{v}_{3'2'|14} + \dots \\ &= \bar{v}_{1'2'|12} + \frac{i}{2\pi} \bar{v}_{1'4'|32} g_{3|3'}^\lambda g_{4|4'}^\lambda (\gamma_\lambda^x)_{3'2'|14}. \end{aligned} \quad (56)$$

Due to frequency conservation at each interaction vertex, the frequency dependence of the ladder is reduced to a single bosonic combination of the external frequencies,

$$\gamma_\lambda^x(\omega'_1, \omega'_2 | \omega_1, \omega_2) = (\gamma_\lambda^x)(X), \quad (57)$$

with

$$X = \omega'_2 - \omega_1 = \omega_2 - \omega'_1. \quad (58)$$

We evaluate the RPA series and obtain

$$(\gamma_\lambda^x)_{\sigma\bar{\sigma}|\sigma\bar{\sigma}}^{12|22}(X) = \frac{U}{2} + \frac{U^2}{4} \frac{(B_\lambda^x)_{\sigma\bar{\sigma}}(X)}{1 - \frac{U}{2} (B_\lambda^x)_{\sigma\bar{\sigma}}(X)}, \quad (59)$$

where

$$\begin{aligned} (B_\lambda^x)_{\sigma\bar{\sigma}}(X) &= \frac{i}{2\pi} \int d\omega \left[g_{\lambda\sigma}^{\text{Ret}}(\omega - \frac{X}{2}) g_{\lambda\bar{\sigma}}^{\text{K}}(\omega + \frac{X}{2}) \right. \\ &\quad \left. + g_{\lambda\sigma}^{\text{K}}(\omega - \frac{X}{2}) g_{\lambda\bar{\sigma}}^{\text{Av}}(\omega + \frac{X}{2}) \right] \end{aligned} \quad (60)$$

denotes the particle-hole bubble (polarization operator). In the special case $T = 0$, $B = 0$, $V = 0$, $eV_g = \mu = 0$ we find

$$(B_\lambda^x)_{\sigma\bar{\sigma}}(X) = -\frac{2}{\pi} \frac{\Gamma_\lambda}{X(X - i\Gamma_\lambda)} \ln \left(1 + i \frac{X}{\Gamma_\lambda/2} \right). \quad (61)$$

Expanding $1/(B_\lambda^x)_{\sigma\bar{\sigma}}(X)$ in powers of X/Γ_λ results in

$$(\gamma_\lambda^x)_{\sigma\bar{\sigma}|\sigma\bar{\sigma}}^{12|22}(X) \simeq \frac{U}{2} - \frac{i}{2\pi} \frac{U^2}{X - i(\Gamma_\lambda/2 - U/\pi)}, \quad X \ll \Gamma_\lambda, \quad (62)$$

which features a singularity when λ reaches the value

$$\lambda = \lambda_c = 2U/\pi - \Gamma. \quad (63)$$

Additionally, for $\lambda < \lambda_c$ the function $(\gamma_\lambda^x)_{\sigma\bar{\sigma}|\sigma\bar{\sigma}}^{12|22}(X)$ exhibits the wrong analytic behaviour, being analytic in the upper half plane of X instead of the lower one as required by causality³⁹. Therefore the flow $\lambda \rightarrow 0$ can only be finished if

$$U < U_c = \pi\Gamma/2. \quad (64)$$

This limitation is not overcome when the full self energy is fed back into the flow, replacing s and g in equation (55) by S and G .

Hence we have to take into account also the other two channels (27b,27d). A parquet approach based procedure mixing the exchange particle-hole and the particle-particle channel has been set up in Ref. [72], in which the authors study the SIAM within Matsubara formalism. Essentially the particle-particle channel serves them to renormalize the interaction U which enters the exchange channel to an effective value U_{eff}

which is always lesser than U_c . The difference $U_c - U_{\text{eff}}$ is then used as a measure for the Kondo scale.

We aim to implement a similar proceeding within the framework of the functional RG. We consider it appropriate to include also contributions from the direct particle-hole channel, because this channel bears the same singularity as the exchange channel. In order to see this let us define the particle-particle and the direct particle-hole ladder on the analogy of equation (55) by the flow equations

$$\frac{d}{d\lambda}(\gamma_\lambda^p)_{1'2'|12} = \frac{i}{4\pi}(\gamma_\lambda^p)_{1'2'|34} \frac{dg_{3|3'}^\lambda g_{4|4'}^\lambda}{d\lambda} (\gamma_\lambda^p)_{3'4'|12}, \quad (65a)$$

$$\frac{d}{d\lambda}(\gamma_\lambda^d)_{1'2'|12} = -\frac{i}{2\pi}(\gamma_\lambda^d)_{1'3'|14} \frac{dg_{3|3'}^\lambda g_{4|4'}^\lambda}{d\lambda} (\gamma_\lambda^d)_{4'2'|32}. \quad (65b)$$

In correspondence to equation (56) the solutions of these flow equations satisfy

$$(\gamma_\lambda^p)_{1'2'|12} = \bar{v}_{1'2'|12} + \frac{i}{4\pi} \bar{v}_{1'2'|34} g_{3|3'} g_{4|4'} (\gamma_\lambda^p)_{3'4'|12}, \quad (66a)$$

$$(\gamma_\lambda^d)_{1'2'|12} = \bar{v}_{1'2'|12} - \frac{i}{2\pi} \bar{v}_{1'3'|14} g_{3|3'} g_{4|4'} (\gamma_\lambda^d)_{4'2'|32}. \quad (66b)$$

Their frequency dependence takes the form

$$(\gamma_\lambda^p)(\omega'_1, \omega'_2 | \omega_1, \omega_2) = (\gamma_\lambda^p)(\Pi), \quad (67a)$$

$$(\gamma_\lambda^d)(\omega'_1, \omega'_2 | \omega_1, \omega_2) = (\gamma_\lambda^d)(\Delta), \quad (67b)$$

with

$$\Pi = \omega_1 + \omega_2 = \omega'_1 + \omega'_2, \quad (68a)$$

$$\Delta = \omega'_1 - \omega_1 = \omega_2 - \omega'_2. \quad (68b)$$

Evaluating (66a) one finds

$$(\gamma_\lambda^p)_{\sigma\bar{\sigma}|\sigma\bar{\sigma}}^{12|22}(\Pi) = \frac{U}{2} + \frac{U^2}{4} \frac{(B_\lambda^p)_{\sigma\bar{\sigma}}(\Pi)}{1 - \frac{U}{2}(B_\lambda^p)_{\sigma\bar{\sigma}}(\Pi)}, \quad (69)$$

where at $T=0, B=0, V=0, eV_g = \mu = 0$ the particle-particle bubble B_λ^p takes the form

$$(B_\lambda^p)_{\sigma\bar{\sigma}}(\Pi) = \frac{2}{\pi} \frac{\Gamma_\lambda}{\Pi(\Pi + i\Gamma_\lambda)} \ln \left(1 - i \frac{\Pi}{\Gamma_\lambda/2} \right) \quad (70)$$

such that γ_λ^p is a regular function on the real Π -axis for all values of U . In contrast, $(\gamma_\lambda^d)^{12|22}$ satisfies

$$(\gamma_\lambda^d)_{\sigma\bar{\sigma}|\sigma\bar{\sigma}}^{12|22}(\Delta) = \frac{1}{2} \left[(\gamma^p)_{\sigma\bar{\sigma}|\sigma\bar{\sigma}}^{12|22}(\Delta) + (\gamma^x)_{\sigma\bar{\sigma}|\sigma\bar{\sigma}}^{12|22}(\Delta)^* \right], \quad (71)$$

$$(\gamma_\lambda^d)_{\sigma\sigma|\sigma\sigma}^{12|22}(\Delta) = \frac{1}{2} \left[(\gamma^p)_{\sigma\bar{\sigma}|\sigma\bar{\sigma}}^{12|22}(\Delta) - (\gamma^x)_{\sigma\bar{\sigma}|\sigma\bar{\sigma}}^{12|22}(\Delta)^* \right] \quad (72)$$

and thus possesses the same singularity as the exchange particle-hole channel.

B. Approximated mixing of the channels

In an approximation taking into account all three channels (27b–27d), the two-particle vertex function will depend on all three frequencies, $\gamma(\Pi, X, \Delta)$. Due to frequency conservation these three are indeed sufficient to express the general frequency dependence. In the following the three bosonic frequency arguments of the vertex function will always be indicated in the order (Π, X, Δ) . When all three contributions (27b–27d) to the flow are taken into account simultaneously, then the dependence on Π, Δ, X is mixed through the feedback of the vertex function on the right hand side of the flow equation that reads

$$\frac{d}{d\lambda} \gamma_{1'2'|12}^\lambda(\Pi, X, \Delta) = \frac{i}{2\pi} \int d\omega \left\{ \gamma_{1'2'|34}^\lambda \left(\Pi, \omega + \frac{X-\Delta}{2}, \omega - \frac{X-\Delta}{2} \right) S_{3|3'}^\lambda \left(\frac{\Pi}{2} - \omega \right) G_{4|4'}^\lambda \left(\frac{\Pi}{2} + \omega \right) \gamma_{3'4'|12}^\lambda \left(\Pi, \frac{X+\Delta}{2} + \omega, \frac{X+\Delta}{2} - \omega \right) \right. \quad (73a)$$

$$+ \gamma_{1'4'|32}^\lambda \left(\frac{\Pi+\Delta}{2} + \omega, X, \frac{\Pi+\Delta}{2} - \omega \right) \left[S_{3|3'}^\lambda \left(\omega - \frac{X}{2} \right) G_{4|4'}^\lambda \left(\omega + \frac{X}{2} \right) + G_{3|3'}^\lambda \left(\omega - \frac{X}{2} \right) S_{4|4'}^\lambda \left(\omega + \frac{X}{2} \right) \right] \gamma_{3'2'|14}^\lambda \left(\omega + \frac{\Pi-\Delta}{2}, X, \omega - \frac{\Pi-\Delta}{2} \right) \quad (73b)$$

$$\left. - \gamma_{1'3'|14}^\lambda \left(\omega + \frac{\Pi-X}{2}, \omega - \frac{\Pi-X}{2}, \Delta \right) \left[S_{3|3'}^\lambda \left(\omega - \frac{\Delta}{2} \right) G_{4|4'}^\lambda \left(\omega + \frac{\Delta}{2} \right) + G_{3|3'}^\lambda \left(\omega - \frac{\Delta}{2} \right) S_{4|4'}^\lambda \left(\omega + \frac{\Delta}{2} \right) \right] \gamma_{3'2'|32}^\lambda \left(\frac{\Pi+X}{2} + \omega, \frac{\Pi+X}{2} - \omega, \Delta \right) \right\}. \quad (73c)$$

Here we use shorthands like

$$\gamma_{1'2'|12}^\lambda \equiv \gamma_{\sigma_1' \sigma_2' | \sigma_1 \sigma_2}^{\lambda \alpha_1' \alpha_2' | \alpha_1 \alpha_2} \quad (74)$$

and indices occurring twice in a product implicate summation over state and Keldysh indices. The flow equation (73)

leads to a complicated dependence of the vertex function on the three frequencies (Π, X, Δ) . As a consequence a numerical solution of the flow equation requires a sampling of three dimensional frequency space which constitutes a high computational effort. The structure of the flow equation suggests

to approximate the frequency dependence of the two-particle vertex function by

$$\gamma_\lambda(\Pi, X, \Delta) \simeq \bar{\nu} + \varphi_\lambda^p(\Pi) + \varphi_\lambda^x(X) + \varphi_\lambda^d(\Delta), \quad (75)$$

where the bare interaction vertex $\bar{\nu}$ is the initial value at the beginning of the flow, $\bar{\nu} = \gamma_{\lambda=\infty}$, and where $\varphi_\lambda^p(\Pi)$, $\varphi_\lambda^x(X)$, $\varphi_\lambda^d(\Delta)$ are approximations to the parts of γ produced by (73a), (73b), (73c), respectively. An analogous approximation has been investigated in studies of the SIAM based on the equilibrium Matsubara fRG⁵³. The results achieved with and without this approximation were of the same quality. Reliable results were obtained for small and intermediate U/Γ . The limiting effect for large U/Γ seems to stem from omitting the three-particle vertex function. For small U/Γ the system can be described by second order perturbation theory which also produces a two-particle vertex function of the form (75). Our fRG treatment will comprise the diagrams of second order perturbation theory for the self energy and for the vertex function. For $U \rightarrow 0$ the fRG results asymptotically approach those of second order perturbation theory.

In order to achieve the form (75) where the frequency dependence is split up onto three functions we have to eliminate X and Δ from (73a), Π and Δ from (73b), and Π and X from (73c). It is obvious that any manipulation of this type can only yield convincing results if the frequency dependence of the vertex functions is not very pronounced. This limits the range of applicability of the approximation to small and intermediate interaction strengths. Kondo physics emerging for large U/Γ cannot be described in general: we expect $\gamma(\Pi, X, \Delta)$ to exhibit a sharp resonance as function of X in this regime (cf. Ref. [72] and section VI.A); furthermore omitting the three particle vertex is not justified for large U/Γ .

Different approaches in order to get rid of the frequency mixing on the right hand side of (73) are conceivable. The variety of reasonable replacements is however restricted by the necessity that the components of the vertex function maintain their fundamental features concerning exchange of particles, causality and the KMS conditions as described in Ref. [39]. We have tested different possibilities. Here we present only the one which provided the most convincing results. It is based on a procedure to assign a static vertex to the functions $\varphi_\lambda^{p,x,d}$,

$$\varphi_\lambda^p(\Pi) \rightarrow \Phi_\lambda^p, \quad (76a)$$

$$\varphi_\lambda^x(X) \rightarrow \Phi_\lambda^x, \quad (76b)$$

$$\varphi_\lambda^d(\Delta) \rightarrow \Phi_\lambda^d. \quad (76c)$$

The $\Phi_\lambda^{p,x,d}$ are frequency independent and represent effective static interactions between particles of either opposite or identical spin state. Since permutations of the incoming indices map the exchange particle-hole channel onto the direct particle-hole channel and vice versa, the $\Phi^{x,d}$ have to satisfy

$$(\Phi_\lambda^x)_{\sigma\bar{\sigma}|\sigma\bar{\sigma}}^{\alpha'_1\alpha'_2|\alpha_2\alpha_1} = -(\Phi_\lambda^d)_{\sigma\bar{\sigma}|\bar{\sigma}\sigma}^{\alpha'_1\alpha'_2|\alpha_1\alpha_2}, \quad (77a)$$

$$(\Phi_\lambda^x)_{\bar{\sigma}\bar{\sigma}|\bar{\sigma}\bar{\sigma}}^{\alpha'_1\alpha'_2|\alpha_1\alpha_2} = -(\Phi_\lambda^d)_{\sigma\bar{\sigma}|\sigma\bar{\sigma}}^{\alpha'_1\alpha'_2|\alpha_2\alpha_1}, \quad (77b)$$

$$(\Phi_\lambda^x)_{\sigma\sigma|\sigma\sigma}^{\alpha'_1\alpha'_2|\alpha_1\alpha_2} = -(\Phi_\lambda^d)_{\sigma\sigma|\sigma\sigma}^{\alpha'_1\alpha'_2|\alpha_2\alpha_1}. \quad (77c)$$

This is achieved by the form

$$(\Phi_\lambda^p)_{\sigma'_1\sigma'_2|\sigma_1\sigma_2} = \begin{cases} U_\lambda^p, & \text{if } \sigma'_1 = \sigma_1 = \bar{\sigma}'_2 = \bar{\sigma}_2, \\ -U_\lambda^p, & \text{if } \sigma'_1 = \bar{\sigma}_1 = \bar{\sigma}'_2 = \sigma_2, \\ 0, & \text{else,} \end{cases} \quad (78a)$$

$$(\Phi_\lambda^x)_{\sigma'_1\sigma'_2|\sigma_1\sigma_2} = \begin{cases} U_\lambda^x, & \text{if } \sigma'_1 = \sigma_1 = \bar{\sigma}'_2 = \bar{\sigma}_2, \\ -U_\lambda^d, & \text{if } \sigma'_1 = \bar{\sigma}_1 = \bar{\sigma}'_2 = \sigma_2, \\ -W_{\lambda\sigma_1}^d, & \text{if } \sigma'_1 = \sigma_1 = \sigma'_2 = \sigma_2, \\ 0, & \text{else,} \end{cases} \quad (78b)$$

$$(\Phi_\lambda^d)_{\sigma'_1\sigma'_2|\sigma_1\sigma_2} = \begin{cases} U_\lambda^d, & \text{if } \sigma'_1 = \sigma_1 = \bar{\sigma}'_2 = \bar{\sigma}_2, \\ -U_\lambda^x, & \text{if } \sigma'_1 = \bar{\sigma}_1 = \bar{\sigma}'_2 = \sigma_2, \\ W_{\lambda\sigma_1}^d, & \text{if } \sigma'_1 = \sigma_1 = \sigma'_2 = \sigma_2, \\ 0, & \text{else,} \end{cases} \quad (78c)$$

and

$$(\Phi_\lambda^{p,x,d})_{\sigma'_1\sigma'_2|\sigma_1\sigma_2}^{\alpha'_1\alpha'_2|\alpha_1\alpha_2} = \begin{cases} \frac{1}{2}(\Phi_\lambda^{p,x,d})_{\sigma'_1\sigma'_2|\sigma_1\sigma_2}, & \text{if } \alpha'_1 + \alpha'_2 + \alpha_1 + \alpha_2 \text{ is odd} \\ 0, & \text{else,} \end{cases} \quad (79)$$

with $U_\lambda^{p,x,d}$ and $W_{\lambda\sigma}^d$ being real numbers, compare (39) and (40). The detailed procedure to determine appropriate constants $U_\lambda^{p,x,d}$, $W_{\lambda\sigma}^d$ has to be consistent with the flow equations and is discussed below in section VI.C. In (78a) we exclude the possibility that an effective interaction between two particles of identical spin state could result from the particle-particle channel. The reason is that a static interaction vertex between particles of identical spin state vanishes when being anti-symmetrized since the direct and exchange terms cancel each other. This is consistent with the fact that such a contribution is not generated by the flow equation (80a) below, since $\bar{\nu} + \Phi_\lambda^x + \Phi_\lambda^d$ allows only interactions of particles in opposite spin states. Also the fact that $U_\lambda^{p,x,d}$ are independent of the spin (while $W_{\lambda\sigma}^d$ is not) is consistent with the structure of an effective interaction vertex, compare (40), and will be reproduced by the flow equations below.

When inserting now the form (75) on the right hand side of the flow equation (73), the sum structure is reproduced by the flow if we replace $\varphi_\lambda^x(X)$ and $\varphi_\lambda^d(\Delta)$ in the particle-particle channel (73a) by the constant vertices Φ_λ^x , Φ_λ^d and proceed analogously for the other channels: in the flow of any channel the other two channels are reduced to constant vertices. The flow equations for $\varphi_\lambda^{p,x,d}$ are then given by

$$\begin{aligned} \frac{d}{d\lambda}(\varphi_\lambda^p)_{1'2'|12}(\Pi) &= \frac{1}{2}(\bar{\nu} + \varphi_\lambda^p(\Pi) + \Phi_\lambda^x + \Phi_\lambda^d)_{1'2'|34} \\ &\times (I_\lambda^{pp})_{34|3'4'}(\Pi)(\bar{\nu} + \varphi_\lambda^p(\Pi) + \Phi_\lambda^x + \Phi_\lambda^d)_{3'4'|12}, \end{aligned} \quad (80a)$$

$$\begin{aligned} \frac{d}{d\lambda}(\varphi_\lambda^x)_{1'2'|12}(X) &= (\bar{\nu} + \Phi_\lambda^p + \varphi_\lambda^x(X) + \Phi_\lambda^d)_{1'4'|32} \\ &\times (I_\lambda^{ph})_{34|3'4'}(X)(\bar{\nu} + \Phi_\lambda^p + \varphi_\lambda^x(X) + \Phi_\lambda^d)_{3'2'|14}, \end{aligned} \quad (80b)$$

$$\begin{aligned} \frac{d}{d\lambda} (\varphi_\lambda^d)_{1'2'|12}(\Delta) &= -(\bar{v} + \Phi_\lambda^p + \Phi_\lambda^x + \varphi_\lambda^d(\Delta))_{1'3'|14} \\ &\times (I_\lambda^{\text{ph}})_{34|3'4'}(\Delta) (\bar{v} + \Phi_\lambda^p + \Phi_\lambda^x + \varphi_\lambda^d(\Delta))_{4'2'|32}, \end{aligned} \quad (80c)$$

where we used a summation convention for index numbers representing the state σ and the Keldysh index α , and

$$(I_\lambda^{\text{pp,ph}})_{34|3'4'} = \delta_{\sigma_3\sigma_3'} \delta_{\sigma_4\sigma_4'} (I_\lambda^{\text{pp,ph}})_{\sigma_3\sigma_4}^{\alpha_3\alpha_4|\alpha_3'\alpha_4'} \quad (81)$$

refers to (51).

The different spin and Keldysh components of the functions $\varphi^{\text{p,x,d}}$ are not all independent of each other: there exist identities connecting them which are related to the exchange of particles and to complex conjugation³⁹. Further identities follow from spin conservation and from the special structure of the flow equations (80). In Appendix A we determine a set of independent spin and Keldysh components of the functions $\varphi^{\text{p,x,d}}$ from which all other components can be derived. It is then sufficient to compute the RG flow of these independent components; the corresponding flow equations are presented in the Appendices B and C.

C. How to determine $U_\lambda^{\text{p,x,d}}$ and W_λ^d

The approximation scheme described above requires a procedure which assigns effective constant interaction vertices $\Phi_\lambda^{\text{p,x,d}}$ to the functions $\varphi_\lambda^p(\Pi)$, $\varphi_\lambda^x(X)$, $\varphi_\lambda^d(\Delta)$. Hence it is a central question how to determine appropriate real numbers $U_\lambda^{\text{p,x,d}}$, W_λ^d which characterize the vertices $\Phi_\lambda^{\text{p,x,d}}$ in equations (78). We propose a very simple scheme for the case of thermal equilibrium. In order to generalize this approach to non-equilibrium however we will need to formulate additional constrictions.

Let us first assume thermal equilibrium. Then we can show that

$$\Phi_\lambda^p = \varphi_\lambda^p(\Pi = 0), \quad (82a)$$

$$\Phi_\lambda^x = \varphi_\lambda^x(X = 0), \quad (82b)$$

$$\Phi_\lambda^d = \varphi_\lambda^d(\Delta = 0) \quad (82c)$$

have exactly the structure given in equations (78) and (79). For the proof we make use of the special spin and Keldysh structure of $\varphi^{\text{p,x,d}}$ that is described in Appendix A.

We first discuss the particle-hole channel. From equations (A15a) and (A18a) we infer that $(a_\lambda^d)_{\sigma\bar{\sigma}}(0)$ and $(a_\lambda^d)_{\sigma\sigma}(0)$ are real numbers. Using the KMS conditions (A16) and (A19) combined with equation (C8) we conclude further that $(b_\lambda^d)_{\sigma\bar{\sigma}}(0) = 0$ and $(b_\lambda^d)_{\sigma\sigma}(0) = 0$. In thermal equilibrium we can use the fluctuation dissipation theorem

$$G_\lambda^K(\omega) = [1 - 2f(\omega)] [G_\lambda^{\text{Ret}}(\omega) - G_\lambda^{\text{Av}}(\omega)], \quad (83a)$$

$$S_\lambda^K(\omega) = [1 - 2f(\omega)] [S_\lambda^{\text{Ret}}(\omega) - S_\lambda^{\text{Av}}(\omega)], \quad (83b)$$

to show that

$$\begin{aligned} (I_\lambda^{\text{ph}})_{\sigma\bar{\sigma}}^{21|22}(0) + (I_\lambda^{\text{ph}})_{\sigma\bar{\sigma}}^{22|12}(0) = \\ -2\text{Re} \left\{ \frac{i}{2\pi} \int d\omega [G_\sigma^{\text{Av}}(\omega) S_\sigma^{\text{Av}}(\omega) + S_\sigma^{\text{Av}}(\omega) G_\sigma^{\text{Av}}(\omega)] \right. \\ \left. \times [1 - 2f(\omega)] \right\} \end{aligned} \quad (84)$$

is a real number. From the flow equation (C6a) it follows that $(a_\lambda^x)_{\sigma\bar{\sigma}}(0)$ is real. The KMS condition (A13) then entails that $(b_\lambda^x)_{\sigma\bar{\sigma}}(0) = 0$. In total this means that we can set

$$\Phi_\lambda^d = \varphi_\lambda^d(0) \quad \text{and} \quad \Phi_\lambda^x = \varphi_\lambda^x(0), \quad (85)$$

with

$$U_\lambda^x = 2(a_\lambda^x)_{\sigma\bar{\sigma}}(0), \quad (86a)$$

$$U_\lambda^d = 2(a_\lambda^d)_{\sigma\bar{\sigma}}(0), \quad (86b)$$

$$W_\lambda^d = 2(a_\lambda^d)_{\sigma\sigma}(0). \quad (86c)$$

When we insert (86c) into (C7a) this yields in particular $d(a_\lambda^d)_{\sigma\bar{\sigma}}/d\lambda = 0$. Combining this with the initial condition $(a_{\lambda=\infty}^d)_{\sigma\bar{\sigma}} = 0$ we conclude from (86b) that

$$U_\lambda^d \equiv 0. \quad (87)$$

For the particle-particle channel we combine the fluctuation dissipation theorem (83) and (37) with

$$1 - 2f(\omega) = -[1 - 2f(-\omega)] \quad (88)$$

(mind the convention $\mu = 0$) to find that

$$\begin{aligned} (I_\lambda^{\text{pp}})_{\sigma\bar{\sigma}}^{22|12}(0) + (I_\lambda^{\text{pp}})_{\sigma\bar{\sigma}}^{22|21}(0) = \\ 2\text{Re} \left\{ \frac{i}{2\pi} \int d\omega [G_\sigma^{\text{Ret}}(\omega) S_\sigma^{\text{Av}}(-\omega) + S_\sigma^{\text{Ret}}(\omega) G_\sigma^{\text{Av}}(-\omega)] \right. \\ \left. \times [1 - 2f(\omega)] \right\} \end{aligned} \quad (89)$$

is a real number. Hence it follows from the flow equation (C3a) that $(a_\lambda^p)_{\sigma\bar{\sigma}}(0)$ is real. The KMS condition (A10) then demands that $(b_\lambda^p)_{\sigma\bar{\sigma}}(0) = 0$. Therefore we can set

$$\Phi_\lambda^p = \varphi_\lambda^p(0) \quad (90)$$

with

$$U_\lambda^p = 2(a_\lambda^p)_{\sigma\bar{\sigma}}(0). \quad (91)$$

Note that $(\bar{v} + \Phi_\lambda^p + \Phi_\lambda^x + \Phi_\lambda^d) = \bar{v}_\lambda$ is exactly the flowing effective interaction vertex used in the static approximation scheme in section V.

In the case of non-equilibrium with $\mu_L + \mu_R = 0$ we will also use (86) and (91). While U_λ^d and W_λ^d are then again guaranteed to be real valued by (A15a) and (A18a), additional assumptions are necessary to ensure this for U_λ^x and U_λ^p . If

the propagator which we feed back into the flow of the two-particle vertex satisfies equation (36), then equation (84) is still valid in non-equilibrium, with $f_{\text{eff}}(\omega)$ replacing $f(\omega)$; this warrants that U_λ^λ is real. Under the additional assumptions

$$\Gamma_L = \Gamma_R \quad \text{and} \quad T_L = T_R \quad (92)$$

also equation (89) can be maintained; in that case also U_λ^p is real.

D. Self-energy feedback

The propagators S, G appearing in the flow equation for the self-energy and for the vertex function are full propagators, which means that they are dressed with the current value of the self-energy $\Sigma^\lambda(\omega)$. In this way the self-energy feeds back into its own flow and into the flow of the vertex function. In the preceding section we described that our flow scheme requires the validity of the fluctuation dissipation theorem like equation (36), or, equivalently,

$$\Sigma_\lambda^K(\omega) = [1 - 2f_{\text{eff}}(\omega)] [\Sigma_\lambda^{\text{Ret}}(\omega) - \Sigma_\lambda^{\text{Av}}(\omega)]. \quad (93)$$

While this identity is guaranteed in equilibrium by the KMS conditions, it constitutes an approximation in non-equilibrium; interaction effects that lead to a redistribution of particle statistics are neglected.

The results discussed in section VIII below show that the feedback of the full frequency dependent self-energy into the flow leads to an artificial smoothing of spectral features. The Kondo resonance at $\omega = 0$ for instance acquires a much broader shape than expected. Better results are achieved with a different feedback scheme for the self-energy which reduces its back-coupling into the flow to a simple shift of the single-particle levels. In analogy to the way how we determine an effective static interaction vertex from the vertex function in section VI.C, we assign a real and static level shift E to the self-energy by setting

$$E_\sigma^{\text{Ret}\lambda} = E_\sigma^{\text{Av}\lambda} = \text{Re} \Sigma_\sigma^{\text{Ret}\lambda}(\omega = 0), \quad (94a)$$

$$E_\sigma^{\text{K}\lambda} = 0. \quad (94b)$$

Only this static renormalization enters the propagators on the right hand side of the flow equations for Σ^λ and γ^λ . Due to the missing Keldysh component of E_σ^λ the condition (36) is then readily fulfilled.

It turns out that this static self-energy feedback produces results distinctively better than in case of the full frequency dependent self-energy feedback. We also studied mixed schemes, for instance to feed the static self-energy into the flow of γ^λ while the full self-energy is used for the flow of Σ^λ , or vice versa. However, static feedback into both flow equations performed better. Hence all results shown in section VIII are computed with this scheme.

VII. APPROXIMATE SOLUTION IN THE PARTICLE-HOLE SYMMETRIC POINT

In this section we discuss the special case of vanishing magnetic field, $B = 0$, and particle-hole symmetry; the latter is given for $eV_g = (\mu_L + \mu_R)/2 = 0$. Note that we already introduced before the restriction $\Gamma_L = \Gamma_R$. In that symmetric situation the RG flow does not generate any contribution to $\text{Re} \Sigma_\lambda^{\text{Ret}}(\omega = 0)$ which hence remains at its initial value $U/2$ given in equation (38c). The renormalized effective level position is then given by

$$\varepsilon_\sigma^\lambda = \varepsilon_\sigma + \text{Re} \Sigma_{\lambda\sigma}^{\text{Ret}}(\omega = 0) = 0, \quad (95)$$

compare equations (3) and (94a). Hence the effective single-particle levels for the two spin-states are degenerate and fixed in the middle of the two chemical potentials throughout the flow.

This section is organized as follows. At first, we discuss the structure of the vertex functions in the particle-particle (PP) and exchange particle-hole (PH(e)) channels. At second, we focus on the vertex functions in the direct particle-hole (PH(d)) channel. We distinguish this case from the other two channels because of a bit more involved spin structure. At third, we formulate a simplified version of the flow equation (26) for the self-energy. On its basis we recover the Fermi-liquid relations^{44,58} for the (imaginary part of) self-energy providing an analytical fRG estimate for a characteristic energy scale of the quasiparticle resonance at zero frequency.

A. Particle-particle and exchange particle-hole channels

Let us first discuss the structure of the vertex functions in the particle-particle and exchange particle-hole channels characterized by energy exchange frequencies Π and X , respectively.

From Eqs. (86b) and (87) we establish the property

$$(a_\lambda^d)_{\sigma\bar{\sigma}}(0) \equiv U_\lambda^d/2 = 0, \quad (96)$$

which leads, as we will show below, to decoupling of PP and PH(e) channels from PH(d) channel.

Taking into account (96) we introduce for convenience the following shorthand notations (cf. Eqs. (78), (A9) and (A12))

$$a_1(\Pi) = (a_\lambda^p)_{\sigma\bar{\sigma}}(\Pi) + \frac{U + U_\lambda^x}{2}, \quad (97)$$

$$F_1(\Pi) = (I_\lambda^{\text{pp}})_{\sigma\bar{\sigma}}^{22|12}(\Pi) + (I_\lambda^{\text{pp}})_{\sigma\bar{\sigma}}^{22|21}(\Pi), \quad (98)$$

$$b_1(\Pi) = (b_\lambda^p)_{\sigma\bar{\sigma}}(\Pi), \quad (99)$$

$$H_1(\Pi) = 2i \text{Im} \left[(I_\lambda^{\text{pp}})_{\sigma\bar{\sigma}}^{22|11}(\Pi) + \frac{1}{2} (I_\lambda^{\text{pp}})_{\sigma\bar{\sigma}}^{22|22}(\Pi) \right] \quad (100)$$

and

$$a_3(X) = \frac{U + U_\lambda^P}{2} + (a_\lambda^x)_{\sigma\bar{\sigma}}(X), \quad (101)$$

$$F_3(X) = (I_\lambda^{\text{ph}})_{\sigma\bar{\sigma}}^{21|22}(X) + (I_\lambda^{\text{ph}})_{\sigma\bar{\sigma}}^{22|12}(X), \quad (102)$$

$$b_3(X) = (b_\lambda^x)_{\sigma\bar{\sigma}}(X), \quad (103)$$

$$H_3(X) = 2i \text{Im} \left[(I_\lambda^{\text{ph}})_{\sigma\bar{\sigma}}^{12|21}(X) + \frac{1}{2} (I_\lambda^{\text{ph}})_{\sigma\bar{\sigma}}^{22|22}(X) \right], \quad (104)$$

where the functions (97) and (101) are specifically defined to fulfill $a_1(0) = a_3(0)$. The flow equations (C3a) and (C6a) can be then transformed into

$$\frac{\partial a_1(\Pi)}{\partial \lambda} = [a_1(\Pi)]^2 F_1(\Pi) + \left(\frac{\tilde{U}_\lambda}{2} \right)^2 F_3(0), \quad (105)$$

$$\frac{\partial a_3(X)}{\partial \lambda} = \left(\frac{\tilde{U}_\lambda}{2} \right)^2 F_1(0) + [a_3(X)]^2 F_3(X), \quad (106)$$

where the static part

$$\tilde{U}_\lambda = U + U_\lambda^P + U_\lambda^x = 2a_1(0) = 2a_3(0) \quad (107)$$

obeys the equation

$$\frac{\partial \tilde{U}_\lambda}{\partial \lambda} = \frac{\tilde{U}_\lambda^2}{2} [\tilde{F}_1(0) + F_3(0)]. \quad (108)$$

In case of particle-hole symmetry and zero magnetic field the following property holds

$$F_3(X) = -F_1(-X), \quad (109)$$

which, in particular, implies $F_1(0) + F_3(0) = 0$. Therefore the static component $\tilde{U}_\lambda \equiv U$ does not flow within the approximation introduced in subsection VI.B.

The flow equations (C3b) and (C6b) for the functions (99) and (103) read in the new notations

$$\frac{\partial b_1(\Pi)}{\partial \lambda} = |\tilde{a}_1(\Pi)|^2 H_1(\Pi) + 2i \text{Im} \{ a_1(\Pi) b_1(\Pi) F_1(\Pi) \}, \quad (110)$$

$$\frac{\partial b_3(X)}{\partial \lambda} = |a_3(X)|^2 H_3(X) + 2i \text{Im} \{ a_3(X) b_3(X) F_3(X) \}. \quad (111)$$

The functions $F_{1,3}$ and $H_{1,3}$ are given by

$$F_1(\Pi) = \frac{i}{2\pi} \frac{\partial}{\partial \lambda} \int d\omega' \left[G_\sigma^{\text{Ret}} \left(\frac{\Pi}{2} + \omega' \right) G_\sigma^K \left(\frac{\Pi}{2} - \omega' \right) + G_\sigma^K \left(\frac{\Pi}{2} + \omega' \right) G_\sigma^{\text{Ret}} \left(\frac{\Pi}{2} - \omega' \right) \right], \quad (112)$$

$$F_3(X) = \frac{i}{2\pi} \frac{\partial}{\partial \lambda} \int d\omega' \left[G_\sigma^{\text{Ret}} \left(\omega' - \frac{X}{2} \right) G_\sigma^K \left(\omega' + \frac{X}{2} \right) + G_\sigma^K \left(\omega' - \frac{X}{2} \right) G_\sigma^{\text{Av}} \left(\omega' + \frac{X}{2} \right) \right] \quad (113)$$

and

$$H_1(\Pi) = \frac{i}{2\pi} \frac{\partial}{\partial \lambda} \int d\omega' \times [G_\sigma^{\text{Ret}} G_\sigma^{\text{Ret}} + G_\sigma^{\text{Av}} G_\sigma^{\text{Av}} + G_\sigma^K G_\sigma^K], \quad (114)$$

$$H_3(X) = \frac{i}{2\pi} \frac{\partial}{\partial \lambda} \int d\omega' \times [G_\sigma^{\text{Ret}} G_\sigma^{\text{Av}} + G_\sigma^{\text{Av}} G_\sigma^{\text{Ret}} + G_\sigma^K G_\sigma^K], \quad (115)$$

where the partial derivative $\partial/\partial\lambda$ is supposed to act only on explicitly λ -dependent term within G 's, and the arguments of Green functions in (114) and (115) correspond to those in (112) and (113), respectively. (For brevity we also denote $G_\lambda \equiv G$.) By a straightforward evaluation one can check that in equilibrium the following identities hold

$$H_1(\Pi) = \coth \left(\frac{\Pi}{2T} \right) [F_1(\Pi) - F_1^*(\Pi)], \quad (116)$$

$$H_3(X) = -\coth \left(\frac{X}{2T} \right) [F_3(X) - F_3^*(X)]. \quad (117)$$

With their help we can establish that the combinations

$$c_1(\Pi) = b_1(\Pi) - \coth \left(\frac{\Pi}{2T} \right) [a_1(\Pi) - a_1^*(\Pi)], \quad (118)$$

$$c_3(X) = b_3(X) + \coth \left(\frac{X}{2T} \right) [a_3(X) - a_3^*(X)] \quad (119)$$

obey the equations

$$\frac{\partial c_1}{\partial \lambda} = 2 \text{Re} \{ a_1 F_1 \} c_1, \quad (120)$$

$$\frac{\partial c_3}{\partial \lambda} = 2 \text{Re} \{ a_3 F_3 \} c_3, \quad (121)$$

respectively. Since initially $c_1(\Pi) = c_3(X) \equiv 0$, they also remain zero during the flow, accordingly to (120) and (121). This proves that the KMS relations (A10) and (A13) inherent to the equilibrium state are exactly preserved under the fRG flow in the chosen approximation.

The derivative of the function F_3 at zero temperature reads

$$\begin{aligned} \frac{\partial F_3(X)}{\partial X} \Big|_{X=0} &\equiv F_3'(0) = -\frac{1}{\pi} \frac{\partial}{\partial \lambda} \int d\omega' \\ &\times \left\{ 2\delta(\omega') [G_\sigma^{\text{Ret}}(\omega') \text{Im} G_\sigma^R(\omega') - \text{Im} G_\sigma^{\text{Ret}}(\omega') G_\sigma^{\text{Av}}(\omega')] \right. \\ &\left. + h_F(\omega') \left[G_\sigma^{\text{Ret}}(\omega') \text{Im} \frac{\partial G_\sigma^{\text{Ret}}(\omega')}{\partial \omega'} - \text{Im} \frac{\partial G_\sigma^{\text{Ret}}(\omega')}{\partial \omega'} G_\sigma^{\text{Av}}(\omega') \right] \right\}, \end{aligned} \quad (122)$$

where $h_F(\omega) \equiv 1 - 2f(\omega) \stackrel{T \rightarrow 0}{=} \text{sign}(\omega)$. Under constraints adopted in this section the formula (122) simplifies to

$$\begin{aligned} F_3'(0) &= -\frac{i}{\pi} \frac{\partial}{\partial \lambda} \int d\omega' \\ &\times \left\{ 4\delta(\omega') [\text{Im} G_\sigma^{\text{Ret}}(\omega')]^2 + h_F(\omega') \frac{\partial}{\partial \omega'} [\text{Im} G_\sigma^{\text{Ret}}(\omega')]^2 \right\} \\ &= -\frac{2i}{\pi} \frac{\partial}{\partial \lambda} [\text{Im} G_\sigma^{\text{Ret}}(0)]^2 = \frac{16i}{\pi \Gamma_\lambda^3}. \end{aligned} \quad (123)$$

In the approximation achieved by neglecting the self-energy feedback $G_\lambda \rightarrow g_\lambda$ we find that

$$F_3(X) = \frac{\partial}{\partial \lambda} \left[-\frac{2}{\pi} \frac{\Gamma_\lambda}{X(X - i\Gamma_\lambda)} \ln \left(1 + i \frac{X}{\Gamma_\lambda/2} \right) \right] \quad (124)$$

is given by the λ -derivative of the particle-hole bubble (61). In particular, we obtain $F_3(0) = -4/(\pi\Gamma_\lambda^2)$, and at small $X \leq \Gamma_\lambda$ we approximately have

$$F_3(X) \approx \frac{4}{\pi(2X - i\Gamma_\lambda)^2}. \quad (125)$$

This leads to an approximate solution of the equation (106)

$$a_3(X) \approx -\frac{U X + iB(U, \lambda)}{2 X - iB(U, \lambda)}, \quad (126)$$

where the width of the Lorentzian is given by

$$B(U, \lambda) = \frac{4U}{\pi} e^{-\frac{4U}{\pi\lambda}}. \quad (127)$$

It explicitly manifests that the exponential scale develops in the broadening of the renormalized frequency-dependent vertex function in the exchange particle-hole channel.

B. Direct particle-hole channel

The flow equations for the vertex functions in this channel are split off those considered in the previous subsection. We analogously introduce the new notations (cf. (A15) and (A18))

$$a_{20}(\Delta) = \frac{U + U_\lambda^p + U_\lambda^x}{2} + (a_\lambda^d)_{\sigma\bar{\sigma}}(\Delta), \quad (128)$$

$$a_{2\sigma}(\Delta) = (a_\lambda^d)_{\sigma\sigma}(\Delta) - \frac{W_\lambda^d}{2}, \quad (129)$$

$$F_{2\sigma}(\Delta) = (I_\lambda^{\text{ph}})_{\sigma\sigma}^{22|21}(\Delta) + (I_\lambda^{\text{ph}})_{\sigma\sigma}^{12|22}(\Delta), \quad (130)$$

$$b_{20}(\Delta) = (b_\lambda^d)_{\sigma\bar{\sigma}}(\Delta), \quad (131)$$

$$b_{2\sigma}(\Delta) = (b_\lambda^d)_{\sigma\sigma}(\Delta), \quad (132)$$

$$H_{2\sigma}(\Delta) = 2i \text{Im} \left\{ (I_\lambda^{\text{ph}})_{\sigma\sigma}^{12|21}(\Delta) + \frac{1}{2} (I_\lambda^{\text{ph}})_{\sigma\sigma}^{22|22}(\Delta) \right\}, \quad (133)$$

and rewrite the corresponding equations (C7) and (C9)

$$\begin{aligned} \frac{\partial a_{20}(\Delta)}{\partial \lambda} &= -a_{20}(\Delta) \sum_{s=\uparrow, \downarrow} a_{2s}(\Delta) F_{2s}(\Delta) \\ &\quad + \left(\frac{\tilde{U}_\lambda}{2} \right)^2 [\tilde{F}_1(0) + F_3(0)], \end{aligned} \quad (134)$$

$$\begin{aligned} \frac{\partial a_{2\sigma}(\Delta)}{\partial \lambda} &= -[a_{20}(\Delta)]^2 F_{2\bar{\sigma}}(\Delta) - [a_{2\sigma}(\Delta)]^2 F_{2\sigma}(\Delta) \\ &\quad + \left(\frac{\tilde{U}_\lambda}{2} \right)^2 F_{2\bar{\sigma}}(0), \end{aligned} \quad (135)$$

$$\begin{aligned} \frac{\partial b_{20}(\Delta)}{\partial \lambda} &= -a_{20}(\Delta) a_{2\bar{\sigma}}^*(\Delta) H_{2\bar{\sigma}}(\Delta) - a_{20}^*(\Delta) a_{2\sigma}(\Delta) H_{2\sigma}(\Delta) \\ &\quad - a_{20}(\Delta) b_{2\bar{\sigma}}(\Delta) F_{2\bar{\sigma}}(\Delta) - a_{20}^*(\Delta) b_{2\sigma}(\Delta) F_{2\sigma}^*(\Delta) \\ &\quad - a_{2\bar{\sigma}}^*(\Delta) b_{20}(\Delta) F_{2\bar{\sigma}}^*(\Delta) - a_{2\sigma}(\Delta) b_{20}(\Delta) F_{2\sigma}(\Delta), \end{aligned} \quad (136)$$

$$\begin{aligned} \frac{\partial b_{2\sigma}(\Delta)}{\partial \lambda} &= -|a_{20}(\Delta)|^2 H_{2\bar{\sigma}}(\Delta) - |a_{2\sigma}(\Delta)|^2 H_{2\sigma}(\Delta) \\ &\quad - 2 \text{Re}\{a_{2\sigma}(\Delta) F_{2\sigma}(\Delta)\} b_{2\sigma}(\Delta) \\ &\quad - 2i \text{Im}\{a_{20}^*(\Delta) b_{20}(\Delta) F_{2\bar{\sigma}}^*(\Delta)\}. \end{aligned} \quad (137)$$

We note that $a_{20}(0) = \tilde{U}_\lambda/2$ and $a_{2\sigma}(0) = 0$ as well as $F_{2\sigma}(\Delta) = F_3(-\Delta)$ and $H_{2\sigma}(\Delta) = H_3(-\Delta)$. One can also observe that $b_{20}(\Delta)$ contains both real $b_{20}^r(\Delta) = \text{Re} b_{20}(\Delta)$ and imaginary $b_{20}^i(\Delta) = \text{Im} b_{20}(\Delta)$ parts, while $b_{2\sigma}(\Delta)$ is purely imaginary.

Analogously to (117) the following identity holds in equilibrium

$$H_{2\sigma}(\Delta) = \coth \left(\frac{\Delta}{2T} \right) [F_{2\sigma}(\Delta) - F_{2\sigma}^*(\Delta)]. \quad (138)$$

It allows us to express the equations for $b_{20}^r(\Delta)$ and for the combinations

$$c_{20}(\Delta) = i b_{20}^i(\Delta) - \coth \left(\frac{\Delta}{2T} \right) [a_{20}(\Delta) - a_{20}^*(\Delta)] \quad (139)$$

$$c_{2\sigma}(\Delta) = b_{2\sigma}(\Delta) - \coth \left(\frac{\Delta}{2T} \right) [a_{2\sigma}(\Delta) - a_{2\sigma}^*(\Delta)] \quad (140)$$

in the following form

$$\begin{aligned} \frac{\partial b_{20}^r}{\partial \lambda} &= -\text{Re}\{F_{2\sigma} a_{2\sigma} + F_{2\bar{\sigma}} a_{2\bar{\sigma}}\} b_{20}^r \\ &\quad - i \text{Im}\{F_{2\sigma} a_{2\sigma} - F_{2\bar{\sigma}} a_{2\bar{\sigma}}\} c_{20} \\ &\quad + i \text{Im}\{F_{2\sigma} a_{20}\} c_{2\sigma} - i \text{Im}\{F_{2\bar{\sigma}} a_{20}\} c_{2\bar{\sigma}}, \end{aligned} \quad (141)$$

$$\begin{aligned} \frac{\partial c_{20}}{\partial \lambda} &= -i \text{Im}\{F_{2\sigma} a_{2\sigma} - F_{2\bar{\sigma}} a_{2\bar{\sigma}}\} b_{20}^r \\ &\quad - \text{Re}\{F_{2\sigma} a_{2\sigma} + F_{2\bar{\sigma}} a_{2\bar{\sigma}}\} c_{20} \\ &\quad - \text{Re}\{F_{2\sigma} a_{20}\} c_{2\sigma} - \text{Re}\{F_{2\bar{\sigma}} a_{20}\} c_{2\bar{\sigma}}, \end{aligned} \quad (142)$$

$$\begin{aligned} \frac{\partial c_{2\sigma}}{\partial \lambda} &= 2i \text{Im}\{F_{2\bar{\sigma}} a_{20} + F_{2\sigma} a_{2\sigma}\} b_{20}^r \\ &\quad - 2 \text{Re}\{F_{2\bar{\sigma}} a_{20}\} c_{20} - 2 \text{Re}\{F_{2\sigma} a_{2\sigma}\} c_{2\sigma}. \end{aligned} \quad (143)$$

Since initially $b_{20}^r(\Delta) = c_{20}(\Delta) = c_{2\sigma}(\Delta) = 0$, they remain zero during the flow [cf. Eq. (A16)]. This observation completes the proof of the statement that the KMS relations are preserved in the chosen approximation scheme.

C. Fermi-liquid relations for the self-energy

In the case of particle-hole symmetry it is convenient to introduce the notations

$$\bar{a}_1(\Pi) = -a_1(-\Pi), \quad (144)$$

$$\bar{a}_{2\sigma}(\Delta) = -a_{2\sigma}(-\Delta), \quad (145)$$

and rewrite an equilibrium version of the equation (B1) for the retarded self-energy in a simplified form

$$\begin{aligned} \frac{\partial}{\partial \lambda} \Sigma_{\sigma}^{\text{Ret}}(\omega) = & \frac{1}{\pi} \int d\tilde{\omega} \left[-\frac{U}{2} h_F(\tilde{\omega}) \text{Im} s_{\sigma}^{\text{Ret}}(\tilde{\omega}) \right. \\ & + h_F(\tilde{\omega}) \bar{a}_1(\tilde{\omega} - \omega) \text{Im} s_{\sigma}^{\text{Ret}}(-\tilde{\omega}) \\ & + h_B(\tilde{\omega} - \omega) \text{Im} \bar{a}_1(\tilde{\omega} - \omega) s_{\sigma}^{\text{Av}}(-\tilde{\omega}) \\ & + h_F(\tilde{\omega}) a_3(\tilde{\omega} - \omega) \text{Im} s_{\sigma}^{\text{Ret}}(\tilde{\omega}) \\ & - h_B(\tilde{\omega} - \omega) \text{Im} a_3(\tilde{\omega} - \omega) s_{\sigma}^{\text{Ret}}(\tilde{\omega}) \\ & + h_F(\tilde{\omega}) \bar{a}_{2\sigma}(\tilde{\omega} - \omega) \text{Im} s_{\sigma}^{\text{Ret}}(\tilde{\omega}) \\ & \left. - h_B(\tilde{\omega} - \omega) \text{Im} \bar{a}_{2\sigma}(\tilde{\omega} - \omega) s_{\sigma}^{\text{Ret}}(\tilde{\omega}) \right] \end{aligned} \quad (146)$$

where $h_B(\omega) = \coth \frac{\omega}{2T}$. In this equation the self-energy feedback is neglected as well by replacing $S_{\lambda} \rightarrow s_{\lambda} = \frac{\partial g_{\lambda}}{\partial \lambda}$.

Comparing Eqs. (105) and (106) with (134) and (135), one can observe that the relation

$$\bar{a}_{2\sigma}(\omega) = \frac{\bar{a}_1(\omega) + a_3(\omega)}{2} \quad (147)$$

holds at every λ . The identities $\text{Im} s^{\text{Ret}}(\omega) = \text{Im} s^{\text{Ret}}(-\omega)$, $s^{\text{Av}}(-\omega) = -s^{\text{Ret}}(\omega)$ are fulfilled as well. Therefore (146) reduces to the form

$$\begin{aligned} \frac{\partial}{\partial \lambda} \Sigma_{\sigma}^{\text{Ret}}(\omega) = & \frac{3}{2\pi} \int d\tilde{\omega} \\ & \times \left[h_F(\tilde{\omega}) \bar{a}_1(\tilde{\omega} - \omega) \text{Im} s_{\sigma}^{\text{Ret}}(\tilde{\omega}) \right. \\ & - h_B(\tilde{\omega} - \omega) \text{Im} \bar{a}_1(\tilde{\omega} - \omega) s_{\sigma}^{\text{Ret}}(\tilde{\omega}) \\ & + h_F(\tilde{\omega}) a_3(\tilde{\omega} - \omega) \text{Im} s_{\sigma}^{\text{Ret}}(\tilde{\omega}) \\ & \left. - h_B(\tilde{\omega} - \omega) \text{Im} a_3(\tilde{\omega} - \omega) s_{\sigma}^{\text{Ret}}(\tilde{\omega}) \right] \end{aligned} \quad (148)$$

In particular, its imaginary part reads

$$\begin{aligned} \frac{\partial}{\partial \lambda} \text{Im} \Sigma_{\sigma}^{\text{Ret}}(\omega) = & \frac{3}{2\pi} \int d\tilde{\omega} [h_F(\tilde{\omega}) - h_B(\tilde{\omega} - \omega)] \\ & \times \text{Im} [\bar{a}_1(\tilde{\omega} - \omega) + a_3(\tilde{\omega} - \omega)] \text{Im} s_{\sigma}^{\text{Ret}}(\tilde{\omega}), \end{aligned} \quad (149)$$

which at $T = 0$ amounts to

$$\begin{aligned} \frac{\partial}{\partial \lambda} \text{Im} \Sigma_{\sigma}^{\text{Ret}}(\omega) & \\ = & \frac{3}{\pi} \int_0^{\omega} d\tilde{\omega} \text{Im} [\bar{a}_1(\tilde{\omega} - \omega) + a_3(\tilde{\omega} - \omega)] \text{Im} s_{\sigma}^{\text{Ret}}(\tilde{\omega}). \end{aligned} \quad (150)$$

Differentiating the latter expression with respect to ω and taking into account symmetries of integrands we obtain

$$\frac{\partial}{\partial \lambda} \text{Im} \Sigma'' = -\frac{3}{\pi} \text{Im} \left[\frac{\partial \bar{a}_1}{\partial \omega} + \frac{\partial a_3}{\partial \omega} \right]_{\omega=0} \text{Im} s_{\sigma}^{\text{Ret}}(0),$$

where $\text{Im} \Sigma'' = \text{Im} \frac{\partial^2 \Sigma_{\sigma}^{\text{Ret}}}{\partial \omega^2} \Big|_{\omega=0}$. Note that the first derivative $\text{Im} \Sigma' = \text{Im} \frac{\partial \Sigma_{\sigma}^{\text{Ret}}}{\partial \omega} \Big|_{\omega=0}$ vanishes. It means that ω -expansion of $\text{Im} \Sigma^{\text{Ret}}(\omega) \approx \frac{1}{2} \text{Im} \Sigma'' \omega^2$ starts from the quadratic term, in compliance with the Fermi-liquid expression (31).

In order to find an fRG estimate for $\text{Im} \Sigma''$, we need to establish equations for $\bar{a}'_1 = \text{Im} \frac{\partial \bar{a}_1}{\partial \omega} \Big|_{\omega=0}$ and $a'_3 = \text{Im} \frac{\partial a_3}{\partial \omega} \Big|_{\omega=0}$. This is achieved by differentiating (105) and (106)

$$\frac{\partial \bar{a}'_1}{\partial \lambda} = -U \bar{a}'_1 F_3(0) + \frac{U^2}{4} \text{Im} F_3'(0), \quad (151)$$

$$\frac{\partial a'_3}{\partial \lambda} = U a'_3 F_3(0) + \frac{U^2}{4} \text{Im} F_3'(0). \quad (152)$$

Using (122) and $\text{Im} s^{\text{Ret}}(0) = 2/\Gamma_{\lambda}^2$, we obtain the following set of equations

$$\frac{\partial \text{Im} \Sigma''}{\partial \lambda} = -(\bar{a}'_1 + a'_3) \frac{6}{\pi \Gamma_{\lambda}^2}, \quad (153)$$

$$\frac{\partial \bar{a}'_1}{\partial \lambda} = \bar{a}'_1 \frac{4U}{\pi \Gamma_{\lambda}^2} + \frac{4U^2}{\pi \Gamma_{\lambda}^3}, \quad (154)$$

$$\frac{\partial a'_3}{\partial \lambda} = -a'_3 \frac{4U}{\pi \Gamma_{\lambda}^2} + \frac{4U^2}{\pi \Gamma_{\lambda}^3}. \quad (155)$$

The solution of the last equations is given by

$$\bar{a}'_1 = \frac{\pi}{4} \left[1 - \frac{4U}{\pi \Gamma_{\lambda}} - e^{-\frac{4U}{\pi \Gamma_{\lambda}}} \right], \quad (156)$$

$$a'_3 = \frac{\pi}{4} \left[1 + \frac{4U}{\pi \Gamma_{\lambda}} - e^{+\frac{4U}{\pi \Gamma_{\lambda}}} \right], \quad (157)$$

and therefore

$$\bar{a}'_1 + a'_3 = \frac{\pi}{2} \left[1 - \cosh \frac{4U}{\pi \Gamma_{\lambda}} \right]. \quad (158)$$

Integrating the equation for $\text{Im} \Sigma''$, we obtain at $\lambda = 0$

$$\text{Im} \Sigma'' = \frac{3}{\Gamma} \left[1 - \frac{\pi \Gamma}{4U} \sinh \frac{4U}{\pi \Gamma} \right]. \quad (159)$$

At large $U \gg \Gamma$ an exponentially large scale emerges in $a'_3 \approx -\frac{\pi}{4} e^{\frac{4U}{\pi \Gamma}}$ and in $\text{Im} \Sigma'' \approx -\frac{3\pi}{8U} e^{\frac{4U}{\pi \Gamma}}$. We also note that a'_3 determines the width $B = -U/a'_3$ given in Eq. (127).

In a similar way we can establish the Fermi-liquid coefficient corresponding to small-temperature expansion. Let us set $\omega = 0$ in Eq. (149) and rescale the integration variable $\tilde{\omega} = xT$. Then

$$\begin{aligned} \frac{\partial}{\partial \lambda} \text{Im} \Sigma_{\sigma}^{\text{Ret}}(0) & \\ = & -\frac{3}{\pi} \int \frac{d\tilde{\omega}}{\sinh \tilde{\omega}/T} \text{Im} [\bar{a}_1(\tilde{\omega}) + a_3(\tilde{\omega})] \text{Im} s_{\sigma}^{\text{Ret}}(\tilde{\omega}) \\ = & -\frac{3T}{\pi} \int \frac{dx}{\sinh x} \text{Im} [\bar{a}_1(xT) + a_3(xT)] \text{Im} s_{\sigma}^{\text{Ret}}(xT). \end{aligned} \quad (160)$$

Differentiating it twice with respect to T we obtain

$$\begin{aligned} \frac{\partial}{\partial \lambda} \text{Im} \frac{\partial^2 \Sigma_{\sigma}^{\text{Ret}}(0)}{\partial T^2} \Big|_{T=0} & \\ = & -\frac{3}{\pi} \left(\int \frac{2xdx}{\sinh x} \right) \text{Im} \left[\frac{\partial \bar{a}_1}{\partial \omega} + \frac{\partial a_3}{\partial \omega} \right]_{\omega=0} \text{Im} s_{\sigma}^{\text{Ret}}(0), \end{aligned} \quad (161)$$

where $\int_{-\infty}^{\infty} \frac{2x dx}{\sinh x} = \pi^2$. Comparing this expression with (153) we establish [cf. Eq. (31)]

$$\text{Im} \left. \frac{\partial^2 \Sigma_{\sigma}^{\text{Ret}}}{\partial T^2} \right|_{\omega, T=0} = \pi^2 \text{Im} \Sigma''. \quad (162)$$

Calculation of the Fermi-liquid coefficient corresponding to small-bias expansion is presented in the Appendix D.

VIII. RESULTS OF THE FREQUENCY DEPENDENT FRG

We start the discussion of numerical results with the particle-hole symmetric model in thermal equilibrium at $B = 0$. The low energy expansion of the retarded self-energy is then given by equation (31). The reduced susceptibilities serving as coefficients of this expansion are known exactly from Bethe Ansatz and are⁴⁷

$$\tilde{\chi}_s = \exp\left(\frac{\pi U}{4\Gamma}\right) \sqrt{\frac{\Gamma}{U}} \int_0^{\infty} dx \exp\left(-\frac{\pi \Gamma}{4U} x^2\right) \frac{\cos(\pi x/2)}{1-x^2}, \quad (163a)$$

$$\tilde{\chi}_c = \exp\left(-\frac{\pi U}{4\Gamma}\right) \sqrt{\frac{\Gamma}{U}} \int_0^{\infty} dx \exp\left(-\frac{\pi \Gamma}{4U} x^2\right) \frac{\cosh(\pi x/2)}{1+x^2}. \quad (163b)$$

For $U \gtrsim \pi\Gamma$ the reduced susceptibilities acquire their asymptotic form where⁴⁷

$$\tilde{\chi}_s \pm \tilde{\chi}_c \simeq \tilde{\chi}_s \simeq \frac{\pi}{2} \sqrt{\frac{\Gamma}{U}} \exp\left(\frac{\pi}{4} \left[\frac{U}{\Gamma} - \frac{\Gamma}{U}\right]\right), \quad U \gtrsim \pi\Gamma. \quad (164)$$

This exponential behaviour governs the width of the Kondo resonance, which can be seen as follows. At $eV_g = 0$ ($= \mu$), $T = 0$, $B = 0$, $V = 0$ the retarded Green function can be approximated for ω close to 0 by

$$G_{\sigma}^{\text{Ret}}(\omega) \simeq \frac{1}{m^* \omega + i\Gamma/2}, \quad (165)$$

compare (3) and (31), the effective mass m^* being defined as

$$m^* = 1 - \left. \frac{\partial \Sigma^{\text{Ret}}}{\partial \omega} \right|_{\omega=0}. \quad (166)$$

Hence

$$\rho_{\sigma}(\omega) = -\frac{1}{\pi} \text{Im} G_{\sigma}^{\text{Ret}}(\omega) \simeq \frac{1}{\pi} \frac{\Gamma/2}{(m^* \omega)^2 + \Gamma^2/4}, \quad (167)$$

so that the full width at half maximum of the peak within this approximation is given by

$$T_K = \frac{\Gamma}{m^*}. \quad (168)$$

From (31) and (164) we deduce

$$m^* = \frac{\tilde{\chi}_s + \tilde{\chi}_c}{2} \quad (169a)$$

$$\simeq \frac{\pi}{4} \sqrt{\frac{\Gamma}{U}} \exp\left(\frac{\pi}{4} \left[\frac{U}{\Gamma} - \frac{\Gamma}{U}\right]\right), \quad U \gtrsim \pi\Gamma, \quad (169b)$$

and thus

$$T_K = \frac{4}{\pi} \sqrt{U\Gamma} \exp\left(-\frac{\pi}{4} \left[\frac{U}{\Gamma} - \frac{\Gamma}{U}\right]\right). \quad (170)$$

Figure 2 shows a comparison of the effective mass computed by the fRG to that obtained from second order perturbation theory and to the exact Bethe Ansatz result. Since second order perturbation theory will serve us several times as comparison we briefly sketch how it is determined. When evaluating the frequency dependent second order diagram for the self-energy we use propagators dressed with the restricted self-consistent Hartree-Fock self-energy as lines. Self-consistent Hartree-Fock is obtained as solution of the self-consistency equation

$$\Sigma_{\sigma}^{\text{Ret}} = U \langle n_{\bar{\sigma}} \rangle \quad (171a)$$

$$= -\frac{i}{2\pi} U \int d\omega G_{\bar{\sigma}}^{\leq}(\omega) \quad (171b)$$

$$= \frac{U}{2\pi} \int d\omega N(\omega) \frac{\Gamma}{(\omega - \varepsilon_{\bar{\sigma}} - \Sigma_{\bar{\sigma}}^{\text{Ret}})^2 + \Gamma^2/4}. \quad (171c)$$

This equation has a unique solution for small U , but there are three solutions at larger values of U (e.g. for $U > \pi\Gamma/2$ for $T = 0$, $B = 0$). Two of them feature a local moment, $\Sigma_{\uparrow}^{\text{Ret}} \neq \Sigma_{\downarrow}^{\text{Ret}}$, even for $B = 0$.⁴⁰ Restricted Hartree-Fock refers to the third solution which is energetically unfavorable compared to the other two ones but which has the advantage not to break spin symmetry, $\Sigma_{\uparrow}^{\text{Ret}} = \Sigma_{\downarrow}^{\text{Ret}}$. In the particle-hole symmetric case for instance the restricted Hartree-Fock self-energy is $\Sigma_{\uparrow}^{\text{Ret}} = \Sigma_{\downarrow}^{\text{Ret}} = U/2$ and aligns the single-particle levels with the chemical potential. We use this perturbation theory only for $B = 0$. For finite magnetic field it is not clear which solution of the self-consistency equation ought to be used to dress the propagators.

In Figure 2 we see that the effective mass computed from the fRG does not increase exponentially for large U , but is comparable to the one computed with second order perturbation theory. As a consequence the width of the Kondo resonance of the spectral function resulting from the fRG approximation does not decrease exponentially for increasing U . Figure 2 also shows the effective mass obtained from the fRG with full frequency dependent back-coupling of the self-energy into the flow. As mentioned in section VI.D this feedback leads to an artificial broadening of spectral features which becomes apparent here by too low values for the effective mass.

From the expansion (31) and from (164) and (169) it follows that also

$$\frac{i\Gamma}{2} \left. \frac{\partial^2 \Sigma_{\sigma}^{\text{Ret}}}{\partial \omega^2} \right|_{\omega=0} = \frac{(\tilde{\chi}_s - \tilde{\chi}_c)^2}{4} \quad (172a)$$

$$\simeq m^{*2}, \quad U \gtrsim \pi\Gamma, \quad (172b)$$

increases exponentially with U in the Kondo regime. Figure 3 presents the respective data obtained by fRG and second order perturbation theory in comparison to the exact result. In contrast to second order perturbation theory the fRG produces an exponential scale as has been proven already in

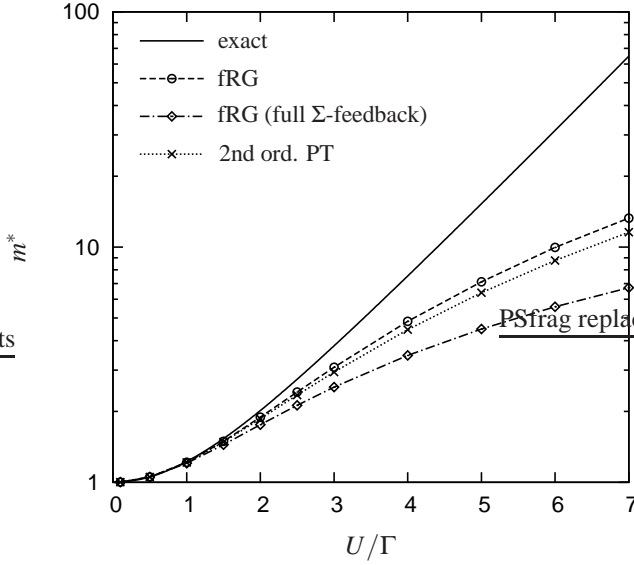


FIG. 2: The effective mass $m^* = 1 - \Sigma_{\sigma}^{\text{Ret}}|_{\omega=0}$ as function of U for $V_g = 0, T = 0, B = 0, V = 0$. The exponential behaviour exhibited by the exact result obtained from equations (169a) and (163) at large U/Γ is neither reproduced by the fRG nor by second order perturbation theory. While the effective mass computed from the fRG with the (standard) static feedback scheme is comparable to the one found in second order perturbation theory, the values obtained from the fRG with full self-energy feedback (see section VI.D) are clearly worse.

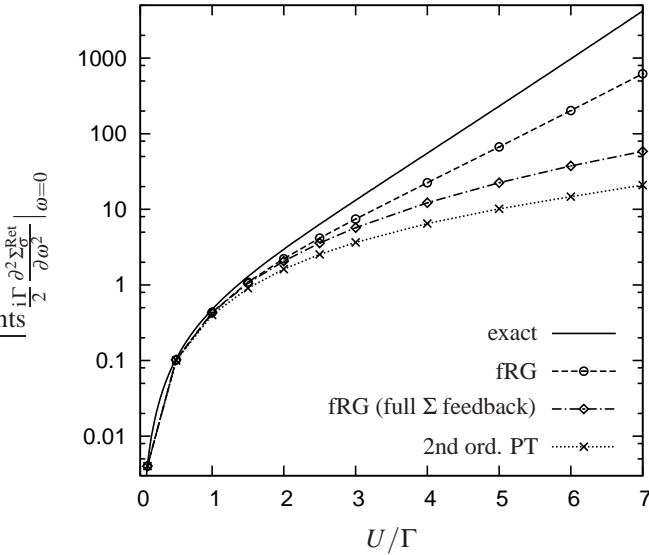


FIG. 3: The second derivative of the self-energy as function of U for $V_g = 0, T = 0, B = 0, V = 0$. The fRG produces an exponential increase with the exponent $4U/\pi\Gamma$, whereas the exact exponent is $\pi U/2\Gamma$. Second order perturbation theory and the fRG with the full frequency dependent self-energy feedback (compare section VI.D) do not yield an exponential increase.

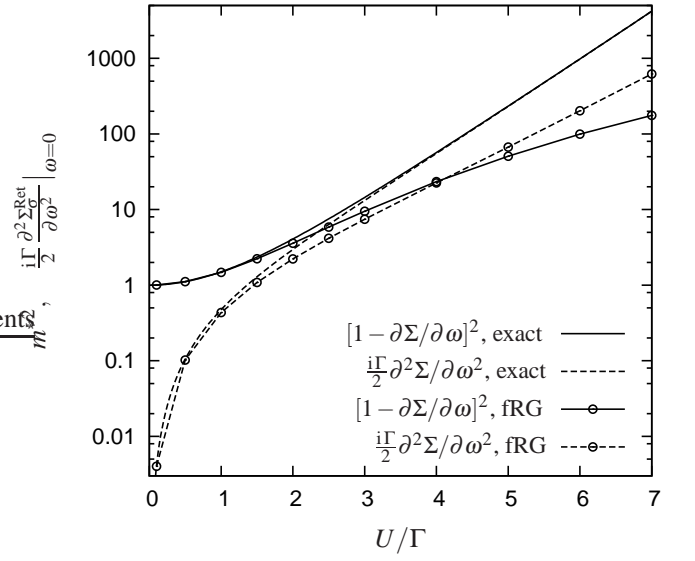


FIG. 4: Comparison of the square of the effective mass and of the second derivative of the self-energy as function of U for $V_g = 0, T = 0, B = 0, V = 0$. In the exact solution both have identical large U asymptotics, m^{*2} being always the larger one of both. In the fRG data the curves cross at U slightly above 4Γ .

equation (159). Given (172b) and (168) the exponential behaviour found there corresponds to a Kondo scale

$$[T_K]_{\text{fRG}} = 4\sqrt{\frac{U\Gamma}{3\pi}} \exp\left(-\frac{2U}{\pi\Gamma}\right). \quad (173)$$

The identical exponential behaviour has been found to govern the pinning of the spectral weight to the chemical potential in the Matsubara fRG with frequency independent truncation scheme^{50,51}. With $2/\pi \simeq 0.64$ the prefactor is slightly smaller than the correct one in equation (170), $\pi/4 \simeq 0.79$. Figure 3 also shows that the fRG with feedback of the full frequency dependent self-energy into the flow does not produce an exponential scale in the second derivative of the self-energy. This illustrates again that the static feedback scheme which we use as standard is advantageous, compare section VI.D.

The fact that the fRG produces an exponential behaviour in $\text{Im}\Sigma''$ but not in the effective mass constitutes an inconsistency which manifests that the method captures Kondo physics only partly. The exact result satisfies

$$m^{*2} = \frac{(\tilde{\chi}_s + \tilde{\chi}_c)^2}{4} > \frac{(\tilde{\chi}_s - \tilde{\chi}_c)^2}{4} = \frac{i\Gamma}{2} \frac{\partial^2 \Sigma_{\sigma}^{\text{Ret}}}{\partial \omega^2} \Big|_{\omega=0}, \quad (174)$$

where both sides asymptotically approach $\tilde{\chi}_s^2/4$. Figure 4 illustrates that the fRG result violates this inequality for $U > 4\Gamma$. Therefore we restrict the following discussions to $U \leq 4\Gamma$.

Figures 5–7 show spectral functions in the particle-hole symmetric case at $B = 0, T = 0$, in equilibrium. Results of the fRG and of second order perturbation theory are compared to essentially exact NRG data⁷⁵. For $U \lesssim 2\Gamma$ all three methods yield nearly identical results. For $U = 2\Gamma$ the shape of the peak

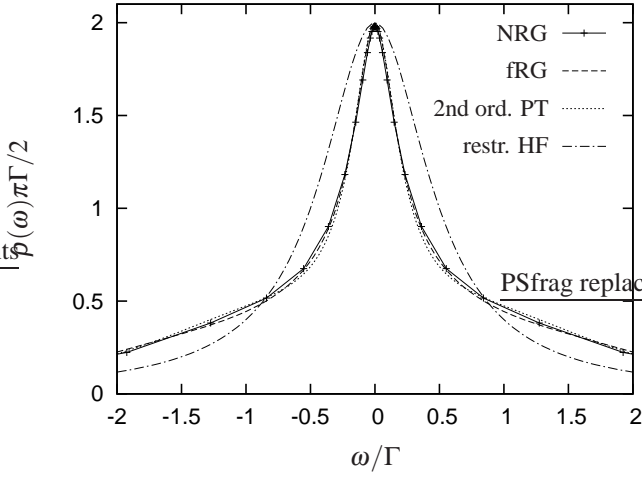


FIG. 5: Spectral function for $V_g = 0, T = 0, B = 0, V = 0$ and $U = 2\Gamma$. The results of fRG and second order perturbation theory agree very well with NRG data. The peak shape differs already significantly from the Lorentzian form produced by static approximations like restricted Hartree-Fock.

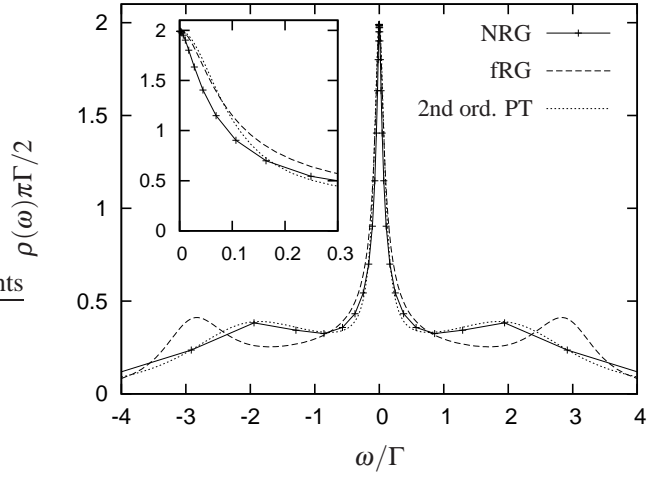


FIG. 7: Spectral function for $V_g = 0, T = 0, B = 0, V = 0$ and $U = 4\Gamma$. The resonance at $\omega = 0$ produced by fRG and by second order perturbation theory is too broad. The side peaks resulting from the fRG calculation are situated at too large $|\omega|$.

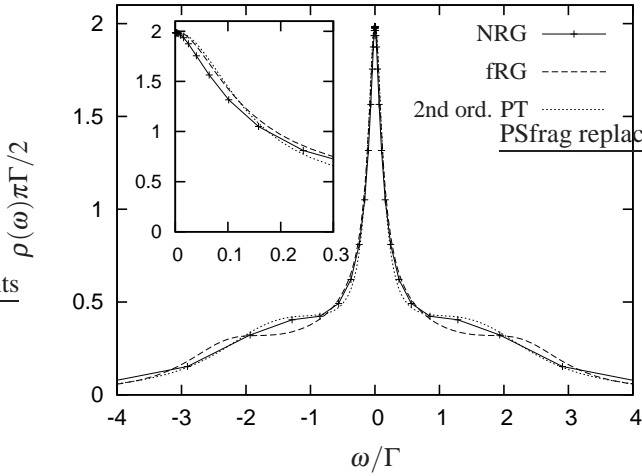


FIG. 6: Spectral function for $V_g = 0, T = 0, B = 0, V = 0$ and $U = 3\Gamma$.

differs already significantly from the Lorentzian form produced by static approximations like restricted Hartree-Fock. At this interaction strength the difference is almost exclusively due to the second order self-energy diagrams which are also captured exactly by the fRG. For $U = 3\Gamma, 4\Gamma$ the resonance peaks produced by fRG and second order perturbation theory are too broad, see insets of Figures 6 and 7, which is a consequence of the effective mass being too small as discussed above. The overall shape of the spectral function is reproduced better by second order perturbation theory than by fRG. The fRG has a tendency to shift spectral weight too far away from the central peak; in Figure 7 the side peaks computed by fRG are situated at $|\omega| \simeq 3\Gamma$ whereas they are expected to be at $|\omega| \simeq U/2 = 2\Gamma$. For the computation of equilibrium spectra it is hence preferable to resort to the frequency dependent

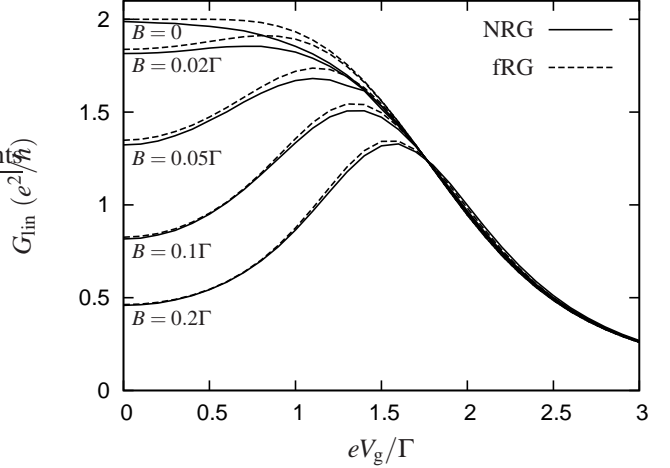


FIG. 8: Linear conductance as function of gate voltage for $T = 0, U = 4\Gamma$ and different magnetic fields.

Matsubara fRG which has been found to be clearly superior in this respect to second order perturbation theory at $U = 2.5\Gamma$.⁵³

The linear conductance as function of gate voltage for different magnetic fields at $T = 0$ and $U = 4\Gamma$ is shown in Figure 8. The very good agreement of the fRG data with NRG results is an interesting success of the frequency dependent Keldysh fRG. It has been shown that an excellent description of $G_{\text{lin}}(V_g, B; T = 0)$ is provided already by the fRG with frequency independent truncation scheme^{50,51}. It is a remarkable observation that the frequency dependent Keldysh fRG yields data of comparable quality, since the frequency dependent Matsubara fRG seems to have lost that ability.

Figures 9 and 10 present the linear conductance as function of gate voltage for different temperatures at $B = 0$ and $U = 2\Gamma, 3\Gamma$. In contrast to second order perturbation the-

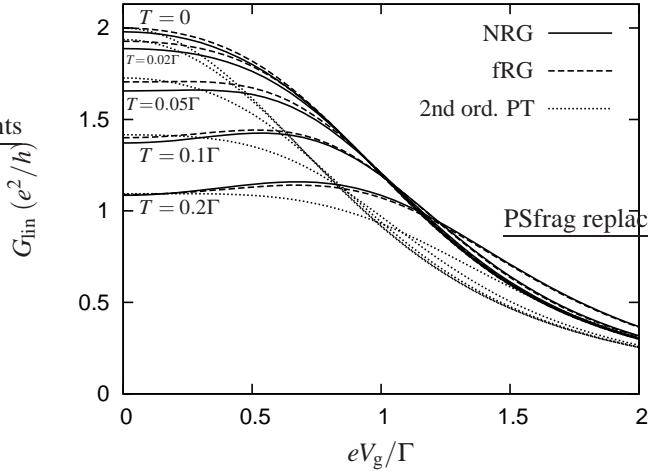


FIG. 9: Linear conductance as function of gate voltage for $B = 0$, $U = 2\Gamma$ and different temperatures.

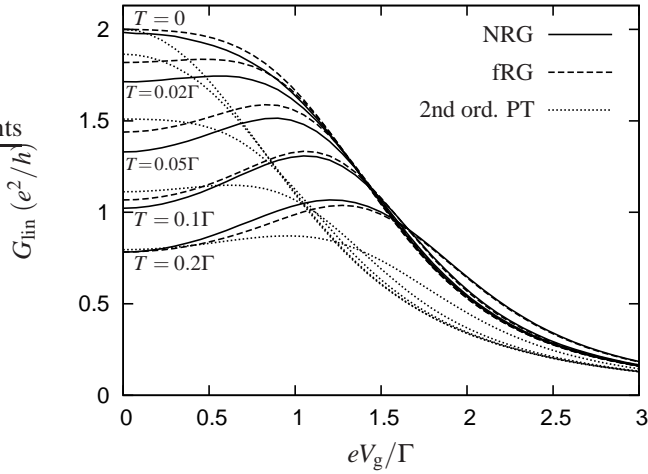


FIG. 10: Linear conductance as function of gate voltage for $B = 0$, $U = 3\Gamma$ and different temperatures.

ory the fRG reproduces the NRG results for the width of the plateau at $T = 0$ and the position of the maxima for $T > 0$ quite accurately. The decrease of the conductance at $V_g = 0$ with increasing temperature is captured not completely correct by the fRG but distinctively better than by second order perturbation theory. The fRG provides an altogether acceptable description of $G_{\text{lin}}(V_g, T)$ for $U \lesssim 3$. This is an important improvement compared to previous fRG approaches. The static fRG^{50,51} is in principle unable to reproduce the minimum of G_{lin} at $V_g = 0$. The reason is that the linear conductance is given by

$$G_{\text{lin}} = e^2 \frac{\Gamma^L \Gamma^R}{\Gamma} \int d\omega \left(-\frac{\partial n_-(\omega)}{\partial \omega} \right) \rho(\omega), \quad (175)$$

as follows from the current formula (21). In any static approximation at $B = 0$ the spectral function $\rho(\omega)$ is a single Lorentzian of fixed width and height, centered at the renor-

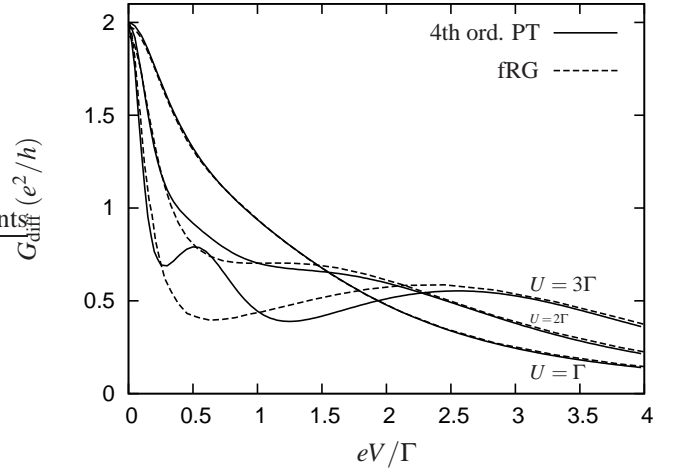


FIG. 11: Differential conductance as function of bias voltage for $V_g = 0$, $B = 0$ and different values of U . The temperature is zero except for the two fRG curves with $U = \Gamma, 2\Gamma$ where $T = 0.02\Gamma$; the corresponding two data sets for the current at $T = 0$ have not been sufficiently smooth to allow for numerical differentiation. The fourth order perturbation theory results have been extracted from the preprint arXiv:cond-mat/0211616v1 to Ref. [55].

malized level position. Obviously equation (175) can produce a single maximum of $G_{\text{lin}}(V_g)$ when the renormalized level is aligned with the chemical potential, but no local minimum. For the frequency dependent Matsubara fRG on the other hand it turned out that the analytic continuation from the imaginary to the real frequency axis constitutes a major obstacle at $T > 0$,⁵³ so that the linear conductance is not accessible systematically so far. A static fRG scheme based on a real frequency cut-off in Keldysh formalism has also been found to reproduce qualitatively the shape of $G_{\text{lin}}(V_g, T)$.³⁸ In view of the argument presented after equation (175) this has to be the consequence of a renormalization of the level broadening. The latter however can be achieved only in a dynamic approximation as can be seen from the fluctuation dissipation theorem (93) that manifestly requires a frequency dependent Keldysh component of the self-energy if Σ^{Ret} has nonvanishing imaginary part. Therefore we suspect that the corresponding result of the static flow scheme used in Ref. [38] is an artifact connected to the violation of causality as consequence of the real frequency cut-off.

The results of our Keldysh fRG for the current as function of bias voltage at $V_g = 0$, $B = 0$, $T = 0$ have been compared in Ref. [13] to data obtained by a TD-DMRG treatment. Excellent agreement between both methods has been found for $U \leq 4\Gamma$. A more sensitive quantity for comparisons is however the differential conductance. Unfortunately the TD-DMRG-results for the current do not yet allow for a reliable numerical differentiation. In Figure 11 we compare the differential conductance as computed by fRG to the fourth order perturbation theory results of Ref. [55]. The agreement for small and large voltages is rather good. A discrepancy is found at intermediate V where the fRG does not reproduce the anomalous peak found by Ref. [55] for sufficiently large

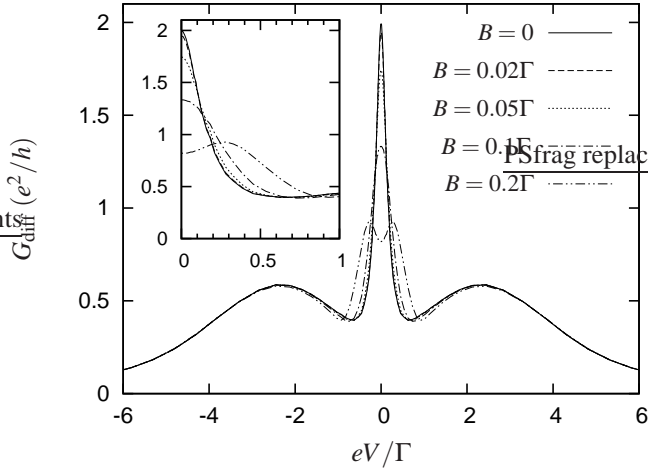


FIG. 12: FRG results for the differential conductance as function of bias voltage for $V_g = 0$, $T = 0$, $U = 3\Gamma$ and different values of the magnetic field.

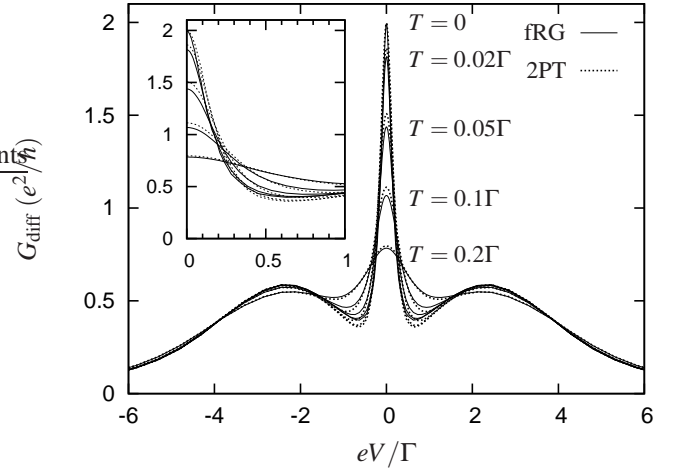


FIG. 14: FRG results for the differential conductance as function of bias voltage for $V_g = 0$, $B = 0$, $U = 3\Gamma$ and different values of temperature.

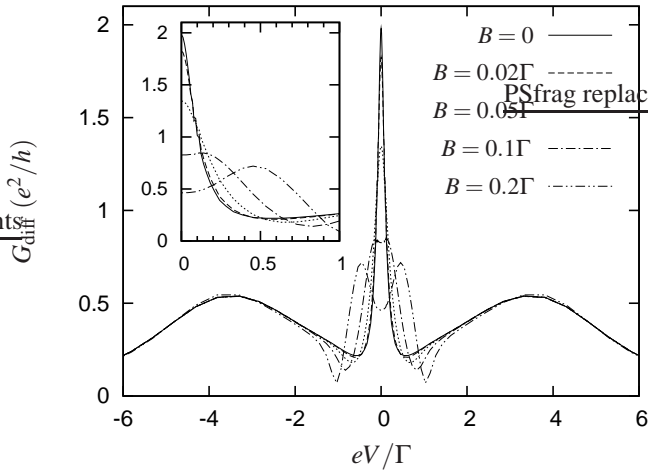


FIG. 13: FRG results for the differential conductance as function of bias voltage for $V_g = 0$, $T = 0$, $U = 4\Gamma$ and different values of the magnetic field.

U . Probably the anomalous peak is an artifact of fourth order perturbation theory; we are not aware of any other investigation indicating its existence.

The data for $G_{\text{diff}}(V)$ at different magnetic fields presented in Figures 12 and 13 could in principle be compared to results of the recently introduced scattering states NRG¹². The data of the latter approach is however is still too noisy to allow for definite conclusions. Figures 14 and 15 finally present the differential conductance for different temperatures in comparison to second order perturbation theory.

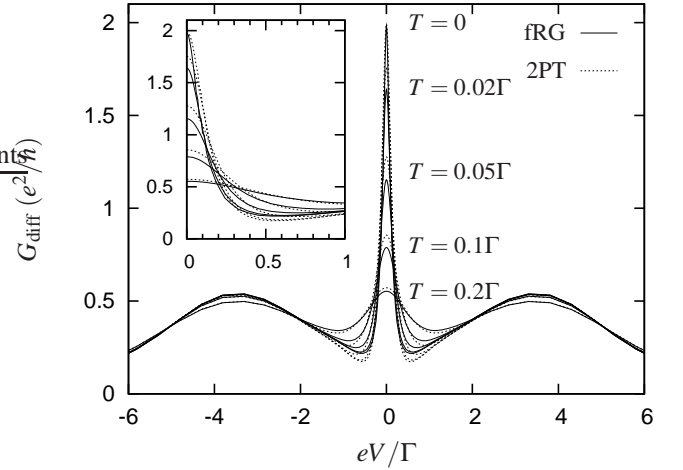


FIG. 15: FRG results for the differential conductance as function of bias voltage for $V_g = 0$, $B = 0$, $U = 4\Gamma$ and different values of temperature.

IX. CONCLUSION

In this paper we studied a frequency dependent fRG approximation for the Anderson impurity model. In equilibrium this model provides the possibility to compare our results to reliable data from Bethe Ansatz or the NRG. Existing studies of the model within Matsubara fRG yield inspiration on how to approach the problem within Keldysh formalism. The non-equilibrium properties of the model are subject of numerous investigations in recent time; however, a consistent picture did not yet emerge.

In order to preserve the Fermi liquid properties of the model we have chosen as flow parameter the level broadening $\Gamma/2 = \Delta$. In the more basic approximation scheme with static vertex renormalization we found it to reproduce exactly

the results of the static Matsubara fRG. For the more advanced dynamic second order truncation scheme it was necessary to simplify the frequency dependence of the vertex in order to obtain treatable equations. The self-energy which we feed back into the flow is static and hence without interaction induced decay rates. Nevertheless, it turned out that the results can be trusted up to values of the Coulomb interaction $U \lesssim 3\Gamma = 6\Delta$, which are typical parameter regimes also used in recent nonequilibrium NRG calculations on the basis of scattering waves¹². For technical reasons we restricted our study furthermore to $T_L = T_R$ and $\Gamma_L = \Gamma_R$.

At the particle-hole symmetric point the description of the spectral function obtained by our fRG is comparable to second order perturbation theory at weak interactions, getting inferior for increasing values of U . But in contrast to perturbation theory the fRG generates exponential behaviour in certain observables. The exponent of the Kondo temperature extracted from the second order derivative of the self-energy is identical to that found from the pinning mechanism in the static fRG and not far from the exact value. The fact that the effective mass derived from the fRG does not exhibit an exponential scale is related to the missing renormalization of the static part of the two-particle vertex in the present second-order truncation scheme. An extension which takes into account contributions from the flow of the three-particle vertex could probably cure this deficiency.

A big success of the method is the very good description of the linear conductance as function of gate voltage, temperature and magnetic field. While, for finite magnetic field and zero temperature, this quality has already been achieved by the static Matsubara fRG, the frequency dependent Matsubara fRG seems to have lost that ability. The description of the linear conductance as function of gate voltage and temperature is of acceptable quality for $U \lesssim 3\Gamma$ and much better than in perturbation theory. This provides a utile complement to the frequency dependent Matsubara fRG which cannot yet access this quantity due to problems with the analytic continuation at $T > 0$. Concerning non-equilibrium properties the results of the fRG compare rather good to those of other methods for $U \lesssim 3\Gamma$ as far as comparisons are possible. In particular, we obtained very good agreement for the nonlinear current $I(V)$ with TD-DMRG data at the most critical point $V_g = T = B = 0$. Together with the fact that our equilibrium results agree well with NRG at finite magnetic field and finite temperature, we expect our results for the nonlinear conductance $G(V)$ to be reliable at finite T and B , although no exact benchmark has been obtained yet by other techniques.

An issue to be adressed for future research is the problem of conservation of current by the fRG. For the finite bias data which we presented in section VIII current conservation is given as a consequence of the complete symmetry established by $eV_g = (\mu_L + \mu_R)/2$, $T_L = T_R$, $\Gamma_L = \Gamma_R$. In more general cases the fRG is not expected to be a current conserving method. Similar problems are known for other methods, for example perturbation theory⁵⁴. Whether the violation of current conservation leads to a significant error for the nonlinear conductance $G(V)$, so that more elaborate parametrizations have to be used within nonequilibrium fRG, can only be

studied when reliable benchmarks are available.

The comparison of the frequency dependent Keldysh and Matsubara fRG reveals that in spite of being closely related, the two methods are far from being equivalent in equilibrium. The choice of an imaginary frequency cut-off as used in Matsubara fRG is not possible in the Keldysh fRG without destroying the Fermi liquid property at the particle-hole symmetric point. For the Keldysh fRG the static self-energy feedback into the flow is preferable to the full one, as opposed to the Matsubara fRG. And while the Matsubara fRG yields better results for the form of the spectral function at the particle-hole symmetric point, the Keldysh fRG produces better data for the linear conductance as function of gate voltage, making accessible finite temperatures where the Matsubara fRG is handicapped by the problem of analytic continuation.

In total our investigation gave insight on how a frequency dependent approximation to the Keldysh fRG can be constructed, and produced a flexible method to compute properties of the Anderson impurity model for moderate interactions. A fundamental problem of applying the fRG in the considered truncation scheme to that model is that the justification for the performed approximations can only be given by perturbative arguments. This difficulty is rooted in the regular perturbative expansion of the model and should not be given in models with low energy divergencies which typically allow to distinguish relevant and irrelevant contributions to the RG flow by power counting. It will be an interesting subject of future research whether perturbative RG techniques are nevertheless capable of finding the exponentially small scale of the Kondo temperature in the effective mass for large Coulomb interactions. Within our proposed approximation scheme, this scale appeared already in the second order derivative of the self-energy, showing that our perturbative RG scheme is in principle capable of obtaining this scale. Therefore, it might be possible that certain contributions of the 3-particle vertex will reveal the same scale also for the effective mass. Alternatively, it might be interesting to access the Kondo limit of the Anderson model by an approach based on Hubbard-Stratonovich fields as proposed in Ref. [57] and combine this method with nonequilibrium fRG. Despite this interesting issue, the method proposed in the present paper seems to be sufficient to describe Coulomb interactions up to the order of the band width D of the local system. For a single-level quantum dot, the band width is given by $D \sim \Gamma$, whereas in quantum wires it is given by $D \sim t$, where t is the hopping matrix element. In both cases, the nonequilibrium fRG schemes of this paper and of Ref. [24] seem to be reliable for $U \lesssim D$, providing the hope for a unified approach describing the whole crossover from small to large quantum systems.

Acknowledgments

We are especially grateful to Theo Costi for providing us with a program to produce NRG data for comparison with the results of the fRG. We thank Sabine Andergassen, Frithjof Anders, Johannes Bauer, Christoph Karrasch, Volker Meden, and Frank Reininghaus for helpful discussions. This work was

supported by the DFG-Forschergruppe 723.

APPENDIX A: IDENTIFICATION OF INDEPENDENT COMPONENTS OF $\varphi_\lambda^{\text{p,x,d}}$

The numerous Keldysh and spin components of the functions $\varphi_\lambda^{\text{p,x,d}}$ are not independent of each other. In this section we isolate a set of independent components from which all the others can be determined. For that purpose we make extensive use of the relations for the vertex functions which are connected to permutation of particles, complex conjugation, causality and the KMS conditions and which are described in reference [39]. We explained in section IV that the hybridization flow parameter preserves these relations during the truncated RG flow. This is as well the case under the additional approximation induced by the replacement (76) since the static renormalized vertices appearing in the flow equation (80) have the same spin and Keldysh structure as the original bare vertex. The relations can be even used for the three individual functions $\varphi_\lambda^{\text{p,x,d}}$ since the diagrammatic structure of the three corresponding flow equations is closed with respect to the manipulations done in the proof of those relations, cf. reference [39]. As the single exception, permutation of either the incoming or the outgoing indices maps φ^{x} onto φ^{d} and vice versa.

1. Analysis of the spin structure

Due to the spin structure of \bar{v} , $(\Phi_\lambda^{\text{p,x,d}})$, and $(I_\lambda^{\text{pp,xph}})$ certain spin components of $\varphi_\lambda^{\text{p,x,d}}$ vanish: Knowing that

$$\left. \begin{aligned} \bar{v}_{\sigma'_1 \sigma'_2 | \sigma_1 \sigma_2} &= 0 \\ (\Phi_\lambda^{\text{p}})_{\sigma'_1 \sigma'_2 | \sigma_1 \sigma_2} &= 0 \\ (\Phi_\lambda^{\text{x}})_{\sigma'_1 \sigma'_2 | \sigma_1 \sigma_2} + (\Phi_\lambda^{\text{d}})_{\sigma'_1 \sigma'_2 | \sigma_1 \sigma_2} &= 0 \end{aligned} \right\} \text{if } \sigma_1 \neq \bar{\sigma}_2 \text{ or } \sigma'_1 \neq \bar{\sigma}'_2, \quad (\text{A1a})$$

$$(\Phi_\lambda^{\text{x,d}})_{\sigma'_1 \sigma'_2 | \sigma_1 \sigma_2} = 0 \quad \text{if } \sigma'_1 + \sigma'_2 \neq \sigma_1 + \sigma_2, \quad (\text{A1b})$$

we conclude from the flow equation (80) that

$$(\varphi_\lambda^{\text{p}})_{\sigma'_1 \sigma'_2 | \sigma_1 \sigma_2} = 0, \quad \text{if } \sigma_1 \neq \bar{\sigma}_2 \text{ or } \sigma'_1 \neq \bar{\sigma}'_2, \quad (\text{A2a})$$

$$(\varphi_\lambda^{\text{x}})_{\sigma'_1 \sigma'_2 | \sigma_1 \sigma_2} = 0, \quad \text{if } \sigma_1 + \sigma_2 \neq \sigma'_1 + \sigma'_2, \quad (\text{A2b})$$

$$(\varphi_\lambda^{\text{d}})_{\sigma'_1 \sigma'_2 | \sigma_1 \sigma_2} = 0, \quad \text{if } \sigma_1 + \sigma_2 \neq \sigma'_1 + \sigma'_2. \quad (\text{A2c})$$

Concerning the remaining spin components, we can restrict our study to

$$(\varphi_\lambda^{\text{p}})_{\sigma \bar{\sigma} | \sigma \bar{\sigma}}, (\varphi_\lambda^{\text{x}})_{\sigma \bar{\sigma} | \sigma \bar{\sigma}}, (\varphi_\lambda^{\text{d}})_{\sigma \bar{\sigma} | \sigma \bar{\sigma}}, (\varphi_\lambda^{\text{d}})_{\sigma \sigma | \sigma \sigma}, \quad (\text{A3})$$

because the other ones can be derived from them by permutations of particle indices,

$$(\varphi_\lambda^{\text{p}})_{\sigma \bar{\sigma} | \sigma \bar{\sigma}}^{\alpha'_1 \alpha'_2 | \alpha_1 \alpha_2}(\Pi) = -(\varphi_\lambda^{\text{p}})_{\sigma \bar{\sigma} | \sigma \bar{\sigma}}^{\alpha'_1 \alpha'_2 | \alpha_2 \alpha_1}(\Pi), \quad (\text{A4a})$$

$$(\varphi_\lambda^{\text{x}})_{\sigma \bar{\sigma} | \sigma \bar{\sigma}}^{\alpha'_1 \alpha'_2 | \alpha_1 \alpha_2}(X) = -(\varphi_\lambda^{\text{x}})_{\sigma \bar{\sigma} | \sigma \bar{\sigma}}^{\alpha'_1 \alpha'_2 | \alpha_2 \alpha_1}(-X), \quad (\text{A4b})$$

$$(\varphi_\lambda^{\text{d}})_{\sigma \bar{\sigma} | \sigma \bar{\sigma}}^{\alpha'_1 \alpha'_2 | \alpha_1 \alpha_2}(\Delta) = -(\varphi_\lambda^{\text{d}})_{\sigma \bar{\sigma} | \sigma \bar{\sigma}}^{\alpha'_1 \alpha'_2 | \alpha_2 \alpha_1}(-\Delta), \quad (\text{A4c})$$

$$(\varphi_\lambda^{\text{x}})_{\sigma \sigma | \sigma \sigma}^{\alpha'_1 \alpha'_2 | \alpha_1 \alpha_2}(X) = -(\varphi_\lambda^{\text{x}})_{\sigma \sigma | \sigma \sigma}^{\alpha'_1 \alpha'_2 | \alpha_2 \alpha_1}(-X). \quad (\text{A4d})$$

2. Analysis of the Keldysh structure

In the following it is convenient to describe the Keldysh components of two-particle functions in terms of block matrices, in which they are arranged according to the scheme

$$\left(\begin{array}{cc|cc} (11|11) & (11|21) & (11|12) & (11|22) \\ (21|11) & (21|21) & (21|12) & (21|22) \\ \hline (12|11) & (12|21) & (12|12) & (12|22) \\ (22|11) & (22|21) & (22|12) & (22|22) \end{array} \right). \quad (\text{A5})$$

The indices α'_2, α_2 of an index tuple $(\alpha'_1 \alpha'_2 | \alpha_1 \alpha_2)$ indicate which of the blocks is to be chosen, while α'_1, α_1 defines the position inside a block. The bare interaction vertex (39) for example is described by the block matrix

$$\frac{1}{\bar{v}} \alpha'_1 \alpha'_2 | \alpha_1 \alpha_2 = \frac{1}{2} \bar{v}_{\sigma'_1 \sigma'_2 | \sigma_1 \sigma_2} \left(\begin{array}{cc|cc} 0 & 1 & 1 & 0 \\ 1 & 0 & 0 & 1 \\ \hline 1 & 0 & 0 & 1 \\ 0 & 1 & 1 & 0 \end{array} \right)_{\alpha'_1 \alpha'_2 | \alpha_1 \alpha_2}. \quad (\text{A6})$$

From the flow equation (80a) it follows that $\varphi_\lambda^{\text{p}}(\Pi)$ has the Keldysh structure

$$\varphi_\lambda^{\text{p}} = \left(\begin{array}{cc|cc} c & d & d & c \\ a & b & b & a \\ \hline a & b & b & a \\ c & d & d & c \end{array} \right)_\lambda, \quad (\text{A7})$$

which can be seen as follows: the initial value $\varphi_{\lambda=\infty}^{\text{p}} \equiv 0$ is consistent with the structure (A7). When $\varphi_\lambda^{\text{p}}(\Pi)$ has this structure, then also $[\bar{v} + \varphi_\lambda^{\text{p}}(\Pi) + \Phi_\lambda^{\text{x}} + \Phi_\lambda^{\text{d}}]$. From equation (80a) it can then be derived that $d\varphi_\lambda^{\text{p}}/d\lambda$ has the structure (A7) as well. Therefore this structure is conserved during the flow.

Exploiting the causality relation $(\varphi_\lambda^{\text{p}})^{22|22} \equiv 0$ and the transformation properties with respect to complex conjugation we find

$$(\varphi_\lambda^{\text{p}})_{\sigma \bar{\sigma} | \sigma \bar{\sigma}}(\Pi) = \left(\begin{array}{cc|cc} 0 & a_\lambda^{\text{p}*} & a_\lambda^{\text{p}*} & 0 \\ a_\lambda^{\text{p}} & b_\lambda^{\text{p}} & b_\lambda^{\text{p}} & a_\lambda^{\text{p}} \\ \hline a_\lambda^{\text{p}} & b_\lambda^{\text{p}} & b_\lambda^{\text{p}} & a_\lambda^{\text{p}} \\ 0 & a_\lambda^{\text{p}*} & a_\lambda^{\text{p}*} & 0 \end{array} \right)_{\sigma \bar{\sigma}}(\Pi), \quad (\text{A8})$$

where $(a_\lambda^p)_{\sigma\bar{\sigma}}(\Pi)$ is a complex valued function while $(b_\lambda^p)_{\sigma\bar{\sigma}}(\Pi)$ is purely imaginary. As a consequence of causality, $(a_\lambda^p)_{\sigma\bar{\sigma}}(\Pi)$ is analytic in the upper half plane of Π . The relations for exchange of particle indices yield

$$(a_\lambda^p)_{\sigma\bar{\sigma}}(\Pi) = (a_\lambda^p)_{\bar{\sigma}\sigma}(\Pi), \quad (\text{A9a})$$

$$(b_\lambda^p)_{\sigma\bar{\sigma}}(\Pi) = (b_\lambda^p)_{\bar{\sigma}\sigma}(\Pi). \quad (\text{A9b})$$

In case of thermal equilibrium at temperature T and chemical potential $\mu = 0$ the only nontrivial component of the generalized fluctuation dissipation theorem of reference [39] reads

$$(b_\lambda^p)_{\sigma\bar{\sigma}}(\Pi) = i2 \coth\left(\frac{\Pi}{2T}\right) \text{Im}(a_\lambda^p)_{\sigma\bar{\sigma}}(\Pi). \quad (\text{A10})$$

The same reasoning as used for $(\varphi_\lambda^p)_{\sigma\bar{\sigma}|\sigma\bar{\sigma}}(\Pi)$ shows that the Keldysh structure of $(\varphi_\lambda^x)_{\sigma\bar{\sigma}|\sigma\bar{\sigma}}(X)$ is

$$(\varphi_\lambda^x)_{\sigma\bar{\sigma}|\sigma\bar{\sigma}}(X) = \left(\begin{array}{cc|cc} 0 & a_\lambda^{x*} & a_\lambda^x & b_\lambda^x \\ a_\lambda^x & b_\lambda^x & 0 & a_\lambda^{x*} \\ \hline a_\lambda^{x*} & 0 & b_\lambda^x & a_\lambda^x \\ b_\lambda^x & a_\lambda^x & a_\lambda^{x*} & 0 \end{array} \right)_{\sigma\bar{\sigma}}(X), \quad (\text{A11})$$

with a complex valued function $(a_\lambda^x)_{\sigma\bar{\sigma}}(X)$ and a purely imaginary function $(b_\lambda^x)_{\sigma\bar{\sigma}}(X)$. $(a_\lambda^x)_{\sigma\bar{\sigma}}(X)$ is analytic in the lower half plane of X . The behaviour of a_λ^x and b_λ^x under exchange of particle indices is

$$(a_\lambda^x)_{\sigma\bar{\sigma}}(X) = (a_\lambda^x)_{\bar{\sigma}\sigma}(-X)^*, \quad (\text{A12a})$$

$$(b_\lambda^x)_{\sigma\bar{\sigma}}(X) = (b_\lambda^x)_{\bar{\sigma}\sigma}(-X). \quad (\text{A12b})$$

In case of thermal equilibrium the KMS conditions are

$$(b_\lambda^x)_{\sigma\bar{\sigma}}(X) = -i2 \coth\left(\frac{X}{2T}\right) \text{Im}(a_\lambda^x)_{\sigma\bar{\sigma}}(X). \quad (\text{A13})$$

The Keldysh structure of $(\varphi_\lambda^d)_{\sigma\bar{\sigma}|\sigma\bar{\sigma}}(\Delta)$ has the form

$$(\varphi_\lambda^d)_{\sigma\bar{\sigma}|\sigma\bar{\sigma}}(\Delta) = \left(\begin{array}{cc|cc} 0 & (a_\lambda^d)_{\sigma\bar{\sigma}} & (a_\lambda^d)_{\bar{\sigma}\sigma}^* & (b_\lambda^d)_{\sigma\bar{\sigma}} \\ (a_\lambda^d)_{\sigma\bar{\sigma}} & 0 & (b_\lambda^d)_{\sigma\bar{\sigma}} & (a_\lambda^d)_{\bar{\sigma}\sigma}^* \\ \hline (a_\lambda^d)_{\bar{\sigma}\sigma}^* & (b_\lambda^d)_{\sigma\bar{\sigma}} & 0 & (a_\lambda^d)_{\sigma\bar{\sigma}} \\ (b_\lambda^d)_{\sigma\bar{\sigma}} & (a_\lambda^d)_{\bar{\sigma}\sigma}^* & (a_\lambda^d)_{\sigma\bar{\sigma}} & 0 \end{array} \right)_{\sigma\bar{\sigma}}(\Delta), \quad (\text{A14})$$

where $(a_\lambda^d)_{\sigma\bar{\sigma}}(\Delta)$ and $(b_\lambda^d)_{\sigma\bar{\sigma}}(\Delta)$ are complex valued functions which satisfy

$$(a_\lambda^d)_{\sigma\bar{\sigma}}(\Delta) = (a_\lambda^d)_{\bar{\sigma}\sigma}(-\Delta)^*, \quad (\text{A15a})$$

$$(b_\lambda^d)_{\sigma\bar{\sigma}}(\Delta) = -(b_\lambda^d)_{\bar{\sigma}\sigma}(-\Delta)^*, \quad (\text{A15b})$$

$$(b_\lambda^d)_{\sigma\bar{\sigma}}(\Delta) = (b_\lambda^d)_{\bar{\sigma}\sigma}(-\Delta). \quad (\text{A15c})$$

The function $(a_\lambda^d)_{\sigma\bar{\sigma}}(\Delta)$ is analytic in the upper half plane of Δ . In case of thermal equilibrium the KMS conditions demand

$$\text{Re}(b_\lambda^d)_{\sigma\bar{\sigma}}(\Delta) = \tanh\left(\frac{\Delta}{2T}\right) \text{Re}\left[(a_\lambda^d)_{\sigma\bar{\sigma}}(\Delta) - (a_\lambda^d)_{\bar{\sigma}\sigma}(\Delta)\right], \quad (\text{A16a})$$

$$\text{Im}(b_\lambda^d)_{\sigma\bar{\sigma}}(\Delta) = \coth\left(\frac{\Delta}{2T}\right) \text{Im}\left[(a_\lambda^d)_{\sigma\bar{\sigma}}(\Delta) + (a_\lambda^d)_{\bar{\sigma}\sigma}(\Delta)\right]. \quad (\text{A16b})$$

Finally the Keldysh structure of $(\varphi_\lambda^d)_{\sigma\sigma|\sigma\sigma}(\Delta)$ is

$$(\varphi_\lambda^d)_{\sigma\sigma|\sigma\sigma}(\Delta) = \left(\begin{array}{cc|cc} 0 & a_\lambda^d & a_\lambda^{d*} & b_\lambda^d \\ a_\lambda^d & 0 & b_\lambda^d & a_\lambda^{d*} \\ \hline a_\lambda^{d*} & b_\lambda^d & 0 & a_\lambda^d \\ b_\lambda^d & a_\lambda^{d*} & a_\lambda^d & 0 \end{array} \right)_{\sigma\sigma}(\Delta), \quad (\text{A17})$$

where $(a_\lambda^d)_{\sigma\sigma}(\Delta)$ is a complex valued and $(b_\lambda^d)_{\sigma\sigma}(\Delta)$ a purely imaginary function; they satisfy

$$(a_\lambda^d)_{\sigma\sigma}(\Delta) = (a_\lambda^d)_{\sigma\sigma}(-\Delta)^*, \quad (\text{A18a})$$

$$(b_\lambda^d)_{\sigma\sigma}(\Delta) = (b_\lambda^d)_{\sigma\sigma}(-\Delta). \quad (\text{A18b})$$

$(a_\lambda^d)_{\sigma\sigma}(\Delta)$ is analytic in the upper half plane of Δ . In case of thermal equilibrium the KMS conditions are

$$(b_\lambda^d)_{\sigma\sigma}(\Delta) = i2 \coth\left(\frac{\Delta}{2T}\right) \text{Im}(a_\lambda^d)_{\sigma\sigma}(\Delta). \quad (\text{A19})$$

In summary we conclude that all spin and Keldysh components of the functions $\varphi^{p,x,d}$ can be determined from the selection

$$(a_\lambda^{p,x,d})_{\uparrow\downarrow}, (b_\lambda^{p,x,d})_{\uparrow\downarrow}, (a_\lambda^d)_{\downarrow\uparrow}, (a_\lambda^d)_{\sigma\sigma}, (b_\lambda^d)_{\sigma\sigma}, \quad \sigma = \uparrow, \downarrow \quad (\text{A20})$$

The precise form of the flow equations shows, that $(a_\lambda^d)_{\downarrow\uparrow}$ can even be omitted, compare equation (C8) below.

APPENDIX B: FLOW EQUATION FOR THE SELF-ENERGY

In our approximation the two-particle vertex acquires a special structure described in section VI.B and Appendix A. When we insert this structure into equation (26) we obtain as flow equation for the retarded component of the self-energy

$$\begin{aligned} \frac{d\Sigma_{\sigma}^{\text{Ret}\lambda}(\omega)}{d\lambda} = & -\frac{i}{2\pi} \int d\omega' \left\{ \left[(b_{\lambda}^x)_{\sigma\bar{\sigma}}(\omega' - \omega) + (b_{\lambda}^d)_{\sigma\bar{\sigma}}(0) \right] S_{\sigma}^{\text{Ret}\lambda}(\omega') - \left[(b_{\lambda}^d)_{\sigma\sigma}(\omega - \omega') - (b_{\lambda}^d)_{\sigma\sigma}(0) \right] S_{\sigma}^{\text{Ret}\lambda}(\omega') \right. \\ & + \left. \left[(b_{\lambda}^p)_{\sigma\bar{\sigma}}(\omega' + \omega) + (b_{\lambda}^d)_{\sigma\bar{\sigma}}(0) \right] S_{\sigma}^{\text{Av}\lambda}(\omega') + (b_{\lambda}^d)_{\sigma\sigma}(0) S_{\sigma}^{\text{Av}\lambda}(\omega') \right. \\ & \left. + \left[\frac{U}{2} + (a_{\lambda}^p)_{\sigma\bar{\sigma}}(\omega' + \omega) + (a_{\lambda}^x)_{\sigma\bar{\sigma}}(\omega' - \omega) + (a_{\lambda}^d)_{\sigma\bar{\sigma}}(0) \right] S_{\sigma}^{\text{K}\lambda}(\omega') - \left[(a_{\lambda}^d)_{\sigma\sigma}(\omega - \omega') - (a_{\lambda}^d)_{\sigma\sigma}(0) \right] S_{\sigma}^{\text{K}\lambda}(\omega') \right\}. \end{aligned} \quad (\text{B1})$$

As a consequence of equation (35) $S^{\text{Ret}}(\omega')$ [$S^{\text{Av}}(\omega')$] is analytic in the upper [lower] half plane of ω' and vanishes as $|\omega'| \rightarrow \infty$. Hence

$$\int d\omega' S^{\text{Ret, Av}}(\omega') = 0 \quad (\text{B2})$$

and equation (B1) is reduced to

$$\begin{aligned} \frac{d\Sigma_{\sigma}^{\text{Ret}\lambda}(\omega)}{d\lambda} = & -\frac{i}{2\pi} \int d\omega' \left\{ (b_{\lambda}^x)_{\sigma\bar{\sigma}}(\omega' - \omega) S_{\sigma}^{\text{Ret}\lambda}(\omega') - (b_{\lambda}^d)_{\sigma\sigma}(\omega - \omega') S_{\sigma}^{\text{Ret}\lambda}(\omega') + (b_{\lambda}^p)_{\sigma\bar{\sigma}}(\omega' + \omega) S_{\sigma}^{\text{Av}\lambda}(\omega') \right. \\ & \left. + \left[\frac{U}{2} + (a_{\lambda}^p)_{\sigma\bar{\sigma}}(\omega' + \omega) + (a_{\lambda}^x)_{\sigma\bar{\sigma}}(\omega' - \omega) + (a_{\lambda}^d)_{\sigma\bar{\sigma}}(0) \right] S_{\sigma}^{\text{K}\lambda}(\omega') - \left[(a_{\lambda}^d)_{\sigma\sigma}(\omega - \omega') - (a_{\lambda}^d)_{\sigma\sigma}(0) \right] S_{\sigma}^{\text{K}\lambda}(\omega') \right\}. \end{aligned} \quad (\text{B3})$$

Since the relation $\Sigma_{\sigma}^{\text{Av}\lambda}(\omega) = \Sigma_{\sigma}^{\text{Ret}\lambda}(\omega)^*$ is maintained during the flow, it is not necessary to compute the flow of $\Sigma_{\sigma}^{\text{Av}\lambda}(\omega)$ separately. Using similar steps as for Σ^{Ret} we acquire the following flow equation for Σ^{K} ,

$$\begin{aligned} \frac{d\Sigma_{\sigma}^{\text{K}\lambda}(\omega)}{d\lambda} = & -\frac{i}{2\pi} \int d\omega' \left\{ 2\text{Re} \left[\left(\frac{U}{2} + (a_{\lambda}^p)_{\sigma\bar{\sigma}}(\omega' + \omega)^* + (a_{\lambda}^x)_{\sigma\bar{\sigma}}(\omega' - \omega) \right) S_{\sigma}^{\text{Ret}\lambda}(\omega') \right] - 2\text{Re} \left[(a_{\lambda}^d)_{\sigma\sigma}(\omega - \omega') S_{\sigma}^{\text{Ret}\lambda}(\omega') \right] \right. \\ & \left. + \left[(b_{\lambda}^p)_{\sigma\bar{\sigma}}(\omega' + \omega) + (b_{\lambda}^x)_{\sigma\bar{\sigma}}(\omega' - \omega) \right] S_{\sigma}^{\text{K}\lambda}(\omega') - (b_{\lambda}^d)_{\sigma\sigma}(\omega - \omega') S_{\sigma}^{\text{K}\lambda}(\omega') \right\}. \end{aligned} \quad (\text{B4})$$

APPENDIX C: FLOW EQUATION FOR THE TWO-PARTICLE VERTEX

Due to the structure of the two-particle vertex function described in section VI.B and Appendix A, its flow is determined completely by the flow of the components (A20). The flow equations of these components can be formulated as a closed set, if the other components are eliminated by use of the relations found in Appendix A. Setting up this set of flow equations is cumbersome but not complicated. This section is restricted to sketching briefly some simplifications which can be made during the calculation and indicating the result.

The flow equations for $(a_{\lambda}^p)_{\sigma\bar{\sigma}} = (\varphi_{\lambda}^p)_{\sigma\bar{\sigma}|\sigma\bar{\sigma}}^{12|22}$ and $(b_{\lambda}^p)_{\sigma\bar{\sigma}} = (\varphi_{\lambda}^p)_{\sigma\bar{\sigma}|\sigma\bar{\sigma}}^{12|21}$ follow from equation (80a). Due to equations (78), (81), and (A2a) the implicit summation over spin indices in equation (80a) is reduced to the two contributions $(\sigma_3\sigma_4|\sigma_3'\sigma_4') = (\sigma\bar{\sigma}|\sigma\bar{\sigma}), (\bar{\sigma}\sigma|\bar{\sigma}\sigma)$. The summation over Keldysh indices is also largely reduced: first because of the vanishing components in equation (A8), and second because of

$$(I_{\lambda}^{\text{PP}})^{\alpha_1\alpha_2|\alpha_1'\alpha_2'} = 0, \quad \text{if } \alpha_1 = \alpha_1' = 1 \text{ or } \alpha_2 = \alpha_2' = 1, \quad (\text{C1a})$$

$$(I_{\lambda}^{\text{PP}})^{12|21} = (I_{\lambda}^{\text{PP}})^{21|12} = 0. \quad (\text{C1b})$$

Equation (C1a) is a consequence of $G^{1|1} = 0, S^{1|1} = 0$, while equation (C1b) follows from $G^{\text{Ret}}(\omega), S^{\text{Ret}}(\omega)$ [$G^{\text{Av}}(\omega), S^{\text{Av}}(\omega)$] being analytic in the upper [lower] half plane of ω . Making further use of

$$(I_{\lambda}^{\text{PP}})^{\alpha_1'\alpha_2'|\alpha_1\alpha_2}(\omega) = -(-1)^{\alpha_1'+\alpha_2'+\alpha_1+\alpha_2} (I_{\lambda}^{\text{PP}})^{\alpha_1\alpha_2|\alpha_1'\alpha_2'}(\omega)^* \quad (\text{C2})$$

for the remaining components, which follows from $G_\sigma^{\text{Ret}}(\omega)^* = G_\sigma^{\text{Av}}(\omega)$, $S_\sigma^{\text{Ret}}(\omega)^* = S_\sigma^{\text{Av}}(\omega)$ and $G_\sigma^{\text{K}}(\omega)^* = -G_\sigma^{\text{K}}(\omega)$, $S_\sigma^{\text{K}}(\omega)^* = -S_\sigma^{\text{K}}(\omega)$, we find

$$\frac{d(a_\lambda^{\text{p}})_{\sigma\bar{\sigma}}(\Pi)}{d\lambda} = \left[\frac{U + U_\lambda^{\text{x}} + U_\lambda^{\text{d}}}{2} + (a_\lambda^{\text{p}})_{\sigma\bar{\sigma}}(\Pi) \right]^2 \left[(I_\lambda^{\text{pp}})_{\sigma\bar{\sigma}}^{22|12}(\Pi) + (I_\lambda^{\text{pp}})_{\sigma\bar{\sigma}}^{22|21}(\Pi) \right], \quad (\text{C3a})$$

$$\begin{aligned} \frac{d(b_\lambda^{\text{p}})_{\sigma\bar{\sigma}}(\Pi)}{d\lambda} = 2i \text{Im} \left\{ \left| \frac{U + U_\lambda^{\text{x}} + U_\lambda^{\text{d}}}{2} + (a_\lambda^{\text{p}})_{\sigma\bar{\sigma}}(\Pi) \right|^2 \left[(I_\lambda^{\text{pp}})_{\sigma\bar{\sigma}}^{22|11}(\Pi) + \frac{1}{2} (I_\lambda^{\text{pp}})_{\sigma\bar{\sigma}}^{22|22}(\Pi) \right] \right. \\ \left. + \left[\frac{U + U_\lambda^{\text{x}} + U_\lambda^{\text{d}}}{2} + (a_\lambda^{\text{p}})_{\sigma\bar{\sigma}}(\Pi) \right] (b_\lambda^{\text{p}})_{\sigma\bar{\sigma}}(\Pi) \left[(I_\lambda^{\text{pp}})_{\sigma\bar{\sigma}}^{22|12}(\Pi) + (I_\lambda^{\text{pp}})_{\sigma\bar{\sigma}}^{22|21}(\Pi) \right] \right\}. \quad (\text{C3b}) \end{aligned}$$

The flow equations for $(a_\lambda^{\text{x}})_{\sigma\bar{\sigma}}(X)$ and $(b_\lambda^{\text{x}})_{\sigma\bar{\sigma}}(X)$ can be derived in an analogous way. Instead of equations (C1) and (C2) we use

$$(I_\lambda^{\text{ph}})^{\alpha_1 \alpha_2 | \alpha'_1 \alpha'_2} = 0, \quad \text{if } \alpha_1 = \alpha'_1 = 1 \text{ or } \alpha_2 = \alpha'_2 = 1, \quad (\text{C4a})$$

$$(I_\lambda^{\text{ph}})^{11|22} = (I_\lambda^{\text{ph}})^{22|11} = 0, \quad (\text{C4b})$$

and

$$(I_\lambda^{\text{ph}})^{\alpha'_1 \alpha'_2 | \alpha_1 \alpha_2}(\omega) = -(-1)^{\alpha'_1 + \alpha'_2 + \alpha_1 + \alpha_2} (I_\lambda^{\text{ph}})^{\alpha_1 \alpha_2 | \alpha'_1 \alpha'_2}(\omega)^*, \quad (\text{C5})$$

and find

$$\frac{d(a_\lambda^{\text{x}})_{\sigma\bar{\sigma}}(X)}{d\lambda} = \left[\frac{U + U_\lambda^{\text{p}} + U_\lambda^{\text{d}}}{2} + (a_\lambda^{\text{x}})_{\sigma\bar{\sigma}}(X) \right]^2 \left[(I_\lambda^{\text{ph}})_{\sigma\bar{\sigma}}^{21|22}(X) + (I_\lambda^{\text{ph}})_{\sigma\bar{\sigma}}^{22|12}(X) \right], \quad (\text{C6a})$$

$$\begin{aligned} \frac{d(b_\lambda^{\text{x}})_{\sigma\bar{\sigma}}(X)}{d\lambda} = 2i \text{Im} \left\{ \left| \frac{U + U_\lambda^{\text{p}} + U_\lambda^{\text{d}}}{2} + (a_\lambda^{\text{x}})_{\sigma\bar{\sigma}}(X) \right|^2 \left[(I_\lambda^{\text{ph}})_{\sigma\bar{\sigma}}^{12|21}(X) + \frac{1}{2} (I_\lambda^{\text{ph}})_{\sigma\bar{\sigma}}^{22|22}(X) \right] \right. \\ \left. + \left[\frac{U + U_\lambda^{\text{p}} + U_\lambda^{\text{d}}}{2} + (a_\lambda^{\text{x}})_{\sigma\bar{\sigma}}(X) \right] (b_\lambda^{\text{x}})_{\sigma\bar{\sigma}}(X) \left[(I_\lambda^{\text{ph}})_{\sigma\bar{\sigma}}^{21|22}(X) + (I_\lambda^{\text{ph}})_{\sigma\bar{\sigma}}^{22|12}(X) \right] \right\}. \quad (\text{C6b}) \end{aligned}$$

The flow equations for $(a_\lambda^{\text{d}})_{\sigma\bar{\sigma}}(\Delta)$ and $(b_\lambda^{\text{d}})_{\sigma\bar{\sigma}}(\Delta)$ are

$$\frac{d(a_\lambda^{\text{d}})_{\sigma\bar{\sigma}}(\Delta)}{d\lambda} = - \left[\frac{U + U_\lambda^{\text{p}} + U_\lambda^{\text{x}}}{2} + (a_\lambda^{\text{d}})_{\sigma\bar{\sigma}}(\Delta) \right] \sum_{s=\uparrow, \downarrow} \left[(a_\lambda^{\text{d}})_{ss}(\Delta) - \frac{W_{\lambda s}^{\text{d}}}{2} \right] \left[(I_\lambda^{\text{ph}})_{ss}^{22|21}(\Delta) + (I_\lambda^{\text{ph}})_{ss}^{12|22}(\Delta) \right], \quad (\text{C7a})$$

$$\begin{aligned} \frac{d(b_\lambda^{\text{d}})_{\sigma\bar{\sigma}}(\Delta)}{d\lambda} = - \left[\frac{U + U_\lambda^{\text{p}} + U_\lambda^{\text{x}}}{2} + (a_\lambda^{\text{d}})_{\sigma\bar{\sigma}}(\Delta) \right] \left[(a_\lambda^{\text{d}})_{\sigma\bar{\sigma}}(\Delta)^* - \frac{W_{\lambda\bar{\sigma}}^{\text{d}}}{2} \right] \left[(I_\lambda^{\text{ph}})_{\sigma\bar{\sigma}}^{12|21}(\Delta) + (I_\lambda^{\text{ph}})_{\sigma\bar{\sigma}}^{21|12}(\Delta) + (I_\lambda^{\text{ph}})_{\sigma\bar{\sigma}}^{22|22}(\Delta) \right] \\ - \left[\frac{U + U_\lambda^{\text{p}} + U_\lambda^{\text{x}}}{2} + (a_\lambda^{\text{d}})_{\bar{\sigma}\sigma}(\Delta)^* \right] \left[(a_\lambda^{\text{d}})_{\sigma\sigma}(\Delta) - \frac{W_{\lambda\sigma}^{\text{d}}}{2} \right] \left[(I_\lambda^{\text{ph}})_{\sigma\sigma}^{12|21}(\Delta) + (I_\lambda^{\text{ph}})_{\sigma\sigma}^{21|12}(\Delta) + (I_\lambda^{\text{ph}})_{\sigma\sigma}^{22|22}(\Delta) \right] \\ - \left[\frac{U + U_\lambda^{\text{p}} + U_\lambda^{\text{x}}}{2} + (a_\lambda^{\text{d}})_{\sigma\bar{\sigma}}(\Delta) \right] (b_\lambda^{\text{d}})_{\sigma\bar{\sigma}}(\Delta) \left[(I_\lambda^{\text{ph}})_{\sigma\bar{\sigma}}^{22|21}(\Delta) + (I_\lambda^{\text{ph}})_{\sigma\bar{\sigma}}^{12|22}(\Delta) \right] \\ - \left[\frac{U + U_\lambda^{\text{p}} + U_\lambda^{\text{x}}}{2} + (a_\lambda^{\text{d}})_{\bar{\sigma}\sigma}(\Delta)^* \right] (b_\lambda^{\text{d}})_{\sigma\sigma}(\Delta) \left[(I_\lambda^{\text{ph}})_{\sigma\sigma}^{21|22}(\Delta) + (I_\lambda^{\text{ph}})_{\sigma\sigma}^{22|12}(\Delta) \right] \\ - \left[(a_\lambda^{\text{d}})_{\sigma\bar{\sigma}}(\Delta)^* - \frac{W_{\lambda\bar{\sigma}}^{\text{d}}}{2} \right] (b_\lambda^{\text{d}})_{\sigma\bar{\sigma}}(\Delta) \left[(I_\lambda^{\text{ph}})_{\sigma\bar{\sigma}}^{21|22}(\Delta) + (I_\lambda^{\text{ph}})_{\sigma\bar{\sigma}}^{22|12}(\Delta) \right] \\ - \left[(a_\lambda^{\text{d}})_{\sigma\sigma}(\Delta) - \frac{W_{\lambda\sigma}^{\text{d}}}{2} \right] (b_\lambda^{\text{d}})_{\sigma\sigma}(\Delta) \left[(I_\lambda^{\text{ph}})_{\sigma\sigma}^{22|21}(\Delta) + (I_\lambda^{\text{ph}})_{\sigma\sigma}^{12|22}(\Delta) \right]. \quad (\text{C7b}) \end{aligned}$$

Since $(a_\lambda^{\text{d}})_{\sigma\bar{\sigma}}$ and $(a_\lambda^{\text{d}})_{\bar{\sigma}\sigma}$ have the same initial value zero at $\lambda = \infty$ we conclude from equation (C7a) that

$$(a_\lambda^{\text{d}})_{\sigma\bar{\sigma}}(\Delta) = (a_\lambda^{\text{d}})_{\bar{\sigma}\sigma}(\Delta). \quad (\text{C8})$$

Finally the flow equations for $(a_\lambda^d)_{\sigma\sigma}(\Delta)$ and $(b_\lambda^d)_{\sigma\sigma}(\Delta)$ turn out to be

$$\begin{aligned} \frac{d(a_\lambda^d)_{\sigma\sigma}(\Delta)}{d\lambda} = & - \left[\frac{U + U_\lambda^p + U_\lambda^x}{2} + (a_\lambda^d)_{\sigma\bar{\sigma}}(\Delta) \right]^2 \left[(I_\lambda^{\text{ph}})_{\bar{\sigma}\sigma}^{22|21}(\Delta) + (I_\lambda^{\text{ph}})_{\bar{\sigma}\sigma}^{12|22}(\Delta) \right] \\ & - \left[(a_\lambda^d)_{\sigma\sigma}(\Delta) - \frac{W_{\lambda\sigma}^d}{2} \right]^2 \left[(I_\lambda^{\text{ph}})_{\bar{\sigma}\sigma}^{22|21}(\Delta) + (I_\lambda^{\text{ph}})_{\bar{\sigma}\sigma}^{12|22}(\Delta) \right], \end{aligned} \quad (\text{C9a})$$

$$\begin{aligned} \frac{d(b_\lambda^d)_{\sigma\sigma}(\Delta)}{d\lambda} = & -2i \text{Im} \left\{ \left| \frac{U + U_\lambda^p + U_\lambda^x}{2} + (a_\lambda^d)_{\sigma\bar{\sigma}}(\Delta) \right|^2 \left[(I_\lambda^{\text{ph}})_{\bar{\sigma}\sigma}^{12|21}(\Delta) + \frac{1}{2} (I_\lambda^{\text{ph}})_{\bar{\sigma}\sigma}^{22|22}(\Delta) \right] \right. \\ & + \left| (a_\lambda^d)_{\sigma\sigma}(\Delta) - \frac{W_{\lambda\sigma}^d}{2} \right|^2 \left[(I_\lambda^{\text{ph}})_{\bar{\sigma}\sigma}^{12|21}(\Delta) + \frac{1}{2} (I_\lambda^{\text{ph}})_{\bar{\sigma}\sigma}^{22|22}(\Delta) \right] \\ & + \left[\frac{U + U_\lambda^p + U_\lambda^x}{2} + (a_\lambda^d)_{\sigma\bar{\sigma}}(\Delta) \right] (b_\lambda^d)_{\sigma\bar{\sigma}}(\Delta) \left[(I_\lambda^{\text{ph}})_{\bar{\sigma}\sigma}^{21|22}(\Delta) + (I_\lambda^{\text{ph}})_{\bar{\sigma}\sigma}^{22|12}(\Delta) \right] \\ & \left. + \left[(a_\lambda^d)_{\sigma\sigma}(\Delta)^* - \frac{W_{\lambda\sigma}^d}{2} \right] (b_\lambda^d)_{\sigma\sigma}(\Delta) \left[(I_\lambda^{\text{ph}})_{\bar{\sigma}\sigma}^{21|22}(\Delta) + (I_\lambda^{\text{ph}})_{\bar{\sigma}\sigma}^{22|12}(\Delta) \right] \right\}. \end{aligned} \quad (\text{C9b})$$

APPENDIX D: NONEQUILIBRIUM FERMI-LIQUID COEFFICIENT

In this evaluation we make the same assumptions as in the section VII, i.e. $\Gamma_L = \Gamma_R$ and $\mu_L = -\mu_R = \frac{eV}{2}$, $B = eV_g = 0$. We remind that these conditions are important to ensure the real value of the static component of the vertex as well as the current conservation.

Let us define a nonequilibrium distribution function

$$\begin{aligned} h_F^{\text{neq}}(\omega) &= \alpha_L h_{F,L}(\omega) + \alpha_R h_{F,R}(\omega) \\ &= \frac{1}{2} h_F \left(\omega - \frac{eV}{2} \right) + \frac{1}{2} h_F \left(\omega + \frac{eV}{2} \right), \end{aligned} \quad (\text{D1})$$

where $\alpha_L + \alpha_R = 1$.

The nonequilibrium equation for the self-energy (B1) in the particle-hole symmetric case reads

$$\begin{aligned} \frac{\partial}{\partial \lambda} \Sigma_\sigma^{\text{Ret}}(\omega) &= \frac{1}{\pi} \int d\tilde{\omega} \left[-\gamma_0 h_F^{\text{neq}}(\tilde{\omega}) \text{Im} s_{\bar{\sigma}}^{\text{Ret}}(\tilde{\omega}) \right. \\ &+ h_F^{\text{neq}}(\tilde{\omega}) a_1(\tilde{\omega} + \omega) \text{Im} s_{\bar{\sigma}}^{\text{Ret}}(\tilde{\omega}) + b_1(\tilde{\omega} + \omega) s_{\bar{\sigma}}^{\text{Av}}(\tilde{\omega}) \\ &+ h_F^{\text{neq}}(\tilde{\omega}) a_3(\tilde{\omega} - \omega) \text{Im} s_{\bar{\sigma}}^{\text{Ret}}(\tilde{\omega}) + b_3(\tilde{\omega} - \omega) s_{\bar{\sigma}}^{\text{Ret}}(\tilde{\omega}) \\ &\left. + h_F^{\text{neq}}(\tilde{\omega}) \bar{a}_{2\sigma}(\tilde{\omega} - \omega) \text{Im} s_{\bar{\sigma}}^{\text{Ret}}(\tilde{\omega}) + \bar{b}_{2\sigma}(\tilde{\omega} - \omega) s_{\bar{\sigma}}^{\text{Ret}}(\tilde{\omega}) \right], \end{aligned} \quad (\text{D2})$$

where the vertex functions a and b components are no longer related to each other by the KMS equalities.

The product of the two distribution functions (D1) evaluated at different frequency arguments can be equivalently rewritten as

$$\begin{aligned} & \left(\alpha_L h_{F,L}^+ + \alpha_R h_{F,R}^+ \right) \left(\alpha_L h_{F,L}^- + \alpha_R h_{F,R}^- \right) \\ &= \alpha_L h_{F,L}^+ h_{F,L}^- + \alpha_R h_{F,R}^+ h_{F,R}^- \\ &- \alpha_L \alpha_R \left(h_{F,L}^+ - h_{F,R}^+ \right) \left(h_{F,L}^- - h_{F,R}^- \right) \\ &\approx \alpha_L h_{F,L}^+ h_{F,L}^- + \alpha_R h_{F,R}^+ h_{F,R}^- \\ &- 4\alpha_L \alpha_R (eV)^2 \delta(\omega_+) \delta(\omega_-), \end{aligned} \quad (\text{D3})$$

where $h_\eta^\pm = h_{F,\eta}(\omega_\pm)$, and $\eta = \pm$ for $\eta = L/R$.

Let us consequently analyze the contribution of each channel.

1. Particle-particle channel

For the PP channel we use the identity

$$h_{F,\eta}^+ h_{F,\eta}^- = -1 + h_{B,\eta}(\omega_+ + \omega_-) \left(h_{F,\eta}^+ + h_{F,\eta}^- \right), \quad (\text{D4})$$

where $h_{B,\eta}(\Pi) = h_B(\Pi - \eta eV)$. It leads to

$$\begin{aligned} \sum_{\eta=\pm} \alpha_\eta h_{F,\eta}^+ h_{F,\eta}^- &= -1 + \frac{1}{2} \sum_{\eta=\pm} h_{B,\eta}(\Pi) \left(h_F^{\text{neq},+} + h_F^{\text{neq},-} \right) \\ &+ \frac{1}{2} \sum_{\eta=\pm} \eta h_{B,\eta}(\Pi) \left[\alpha_L (h_{F,L}^+ + h_{F,L}^-) - \alpha_R (h_{F,R}^+ + h_{F,R}^-) \right] \end{aligned} \quad (\text{D5})$$

where

$$\sum_{\eta=\pm} \frac{\eta h_{B,\eta}(\Pi)}{2} \equiv h_B^{\text{mean}}(\Pi), \quad (\text{D6})$$

$$\sum_{\eta=\pm} \frac{\eta h_{B,\eta}(\Pi)}{2} \approx -2eV \delta(\Pi), \quad (\text{D7})$$

as well as

$$\alpha_L (h_{F,L}^+ + h_{F,L}^-) - \alpha_R (h_{F,R}^+ + h_{F,R}^-) \approx -eV [\delta(\omega_+) + \delta(\omega_-)] \quad (\text{D8})$$

for $\alpha_L = \alpha_R = \frac{1}{2}$. Therefore, the second line of (D5) approximately equals $\approx 4(eV)^2 \delta(\omega') \delta(\Pi)$.

We can represent

$$H_1(\Pi) = H_1^I(\Pi) + H_1^{II}(\Pi), \quad (\text{D9})$$

where

$$H_1^I(\Pi) = h_B^{\text{mean}}(\Pi) \{F_1(\Pi) - F_1^*(\Pi)\}, \quad (\text{D10})$$

$$H_1^{II}(\Pi) \approx i(s_1^a + s_1^b) \delta(\Pi), \quad (\text{D11})$$

and

$$s_1^a = \frac{8}{\pi} \alpha_L \alpha_R (eV)^2 \frac{\partial}{\partial \lambda} [\text{Im} G_\sigma^R(0)]^2, \quad (\text{D12})$$

$$s_1^b = -4s_1^a. \quad (\text{D13})$$

Therefore the solution of Eq. (110) has the form

$$b_1(\Pi) = b_1^I(\Pi) + i(b_1^{IIa} + b_1^{IIb})\delta(\Pi), \quad (\text{D14})$$

where

$$b_1(\Pi) = h_B^{\text{mean}}(\Pi) \{a_1(\Pi) - a_1^*(\Pi)\}, \quad (\text{D15})$$

and b_1^{IIa} and b_1^{IIb} correspond to the inhomogeneity terms in the second line of (D3) and in the second line of (D5), respectively. They can be found from the equation

$$\frac{\partial b_1^{II,a/b}}{\partial \lambda} = |a_1(0)|^2 s_1^{a/b} + 2a_1(0)F_1(0)b_1^{II,a/b}. \quad (\text{D16})$$

2. Particle-hole channel

For the PH channel we use the identity

$$h_{F,\eta}^+ h_{F,\eta}^- = 1 - h_B(\omega_+ - \omega_-) (h_{F,\eta}^+ - h_{F,\eta}^-) \quad (\text{D17})$$

Then

$$H_3(X) = H_3^I(X) + H_3^{II}(X), \quad (\text{D18})$$

where

$$H_3^I(X) = -h_B(X) \{F_3(X) - F_3^*(X)\}, \quad (\text{D19})$$

$$H_3^{II}(X) = is_3 \delta(X), \quad (\text{D20})$$

and

$$s_3 = \frac{8}{\pi} \alpha_L \alpha_R (eV)^2 \frac{\partial}{\partial \lambda} [\text{Im} G_\sigma^R(0)]^2. \quad (\text{D21})$$

The solution of Eq. (111) has the form

$$b_3(X) = b_3^I(X) + ib_3^{II}\delta(X), \quad (\text{D22})$$

where

$$b_3^I(X) = -h_B(X) \{a_3(X) - a_3^*(X)\}, \quad (\text{D23})$$

and

$$\frac{\partial b_3^{II}}{\partial \lambda} = |a_3(0)|^2 s_3 + 2a_3(0)F_3(0)b_3^{II}. \quad (\text{D24})$$

Analogously,

$$H_{2\sigma}^I(\Delta) = h_B(\Delta) \{F_{2\sigma}(\Delta) - F_{2\sigma}^*(\Delta)\}, \quad (\text{D25})$$

$$H_{2\sigma}^{II}(\Delta) = is_{2\sigma} \delta(\Delta), \quad (\text{D26})$$

where

$$s_{2\sigma} = \frac{8}{\pi} \alpha_L \alpha_R (eV)^2 \frac{\partial}{\partial \lambda} [\text{Im} G_\sigma^R(0)]^2. \quad (\text{D27})$$

Note that

$$s_1^a = s_3 = s_{2\sigma} = -(eV)^2 \text{Im} F_3'(0), \quad (\text{D28})$$

which follows from (123).

The solution of Eqs. (136) and (137) takes the form

$$b_{20/2\sigma}(\Delta) = b_{20/2\sigma}^I(\Delta) + ib_{20/2\sigma}^{II}\delta(\Delta), \quad (\text{D29})$$

where

$$b_{20/2\sigma}^I(\Delta) = h_B(\Delta) \{F_{20/2\sigma}(\Delta) - F_{20/2\sigma}^*(\Delta)\}, \quad (\text{D30})$$

and

$$\frac{\partial b_{20}^{II}}{\partial \lambda} = -2a_{20}(0)F_{2\sigma}(0)b_{2\sigma}^{II}, \quad (\text{D31})$$

$$\frac{\partial b_{2\sigma}^{II}}{\partial \lambda} = -|a_{20}(0)|^2 s_{2\sigma} - 2a_{20}(0)F_{2\sigma}(0)b_{20}^{II}. \quad (\text{D32})$$

One can prove the relations

$$b_{2\sigma}^{II} = -\frac{b_1^{IIa} + b_3^{II}}{2}, \quad b_{20}^{II} = \frac{b_3^{II} - b_1^{IIa}}{2}, \quad (\text{D33})$$

which follows from comparison of Eqs. (D31) and (D32) with Eqs. (D16) and (D24) using (D28).

3. Self-energy

An equation for the imaginary part of the self-energy in nonequilibrium reads

$$\begin{aligned} \frac{\partial}{\partial \lambda} \text{Im} \Sigma_\sigma^{\text{Ret}}(0) &= \frac{1}{\pi} \int d\tilde{\omega} \\ &\times \left[h_F^{\text{neq}}(\tilde{\omega}) \text{Im} a_1(\tilde{\omega}) \text{Im} s_\sigma^{\text{Ret}}(\tilde{\omega}) - \frac{i}{2} b_1^I(\tilde{\omega}) \text{Im} s_\sigma^{\text{Av}}(\tilde{\omega}) \right. \\ &+ h_F^{\text{neq}}(\tilde{\omega}) \text{Im} a_3(\tilde{\omega}) \text{Im} s_\sigma^{\text{Ret}}(\tilde{\omega}) - \frac{i}{2} b_3^I(\tilde{\omega}) \text{Im} s_\sigma^{\text{Ret}}(\tilde{\omega}) \\ &+ h_F^{\text{neq}}(\tilde{\omega}) \text{Im} \bar{a}_{2\sigma}(\tilde{\omega}) \text{Im} s_\sigma^{\text{Ret}}(\tilde{\omega}) - \frac{i}{2} \bar{b}_{2\sigma}^I(\tilde{\omega}) \text{Im} s_\sigma^{\text{Ret}}(\tilde{\omega}) \left. \right] \\ &+ \frac{1}{2\pi} [(b_1^{IIa} + b_1^{IIb}) \text{Im} s^{\text{Av}}(0) + (b_3^{II} - b_{2\sigma}^{II}) \text{Im} s^{\text{Ret}}(0)], \end{aligned} \quad (\text{D34})$$

which simplifies due to the particle-hole symmetry to the form

$$\begin{aligned} \frac{\partial}{\partial \lambda} \text{Im} \Sigma_\sigma^{\text{Ret}}(0) &= \frac{1}{\pi} \int d\tilde{\omega} \\ &\times \left[(h_F^{\text{neq}}(\tilde{\omega}) - h_B^{\text{mean}}(\tilde{\omega})) \text{Im} \bar{a}_1(\tilde{\omega}) \text{Im} s_\sigma^{\text{Ret}}(\tilde{\omega}) \right. \\ &+ (h_F^{\text{neq}}(\tilde{\omega}) - h_B(\tilde{\omega})) \text{Im} \{a_3(\tilde{\omega}) + \bar{a}_{2\sigma}(\tilde{\omega})\} \text{Im} s_\sigma^{\text{Ret}}(\tilde{\omega}) \\ &+ \frac{1}{2\pi} \left[-2b_1^{IIa} - b_1^{IIb} + \frac{3}{2}(b_1^{IIa} + b_3^{II}) \right] \text{Im} s^{\text{Ret}}(0). \end{aligned} \quad (\text{D35})$$

Expanding it in eV , we obtain

$$\begin{aligned}
\frac{\partial}{\partial \lambda} \text{Im} \Sigma_{\sigma}^{\text{Ret}}(0) &= \frac{3}{2\pi} \left(\frac{eV}{2} \right)^2 \\
&\times \int d\tilde{\omega} \delta'(\tilde{\omega}) \text{Im} \{ \bar{a}_1(\tilde{\omega}) + a_3(\tilde{\omega}) \} \text{Im} s^{\text{Ret}}(\tilde{\omega}) \\
&- \frac{1}{\pi} (eV)^2 \int d\tilde{\omega} \delta'(\tilde{\omega}) \text{Im} \bar{a}_1(\tilde{\omega}) \text{Im} s^{\text{Ret}}(\tilde{\omega}) \\
&+ \frac{1}{2\pi} \left[-2b_1^{IIa} - b_1^{IIb} + \frac{3}{2}(b_1^{IIa} + b_3^{II}) \right] \text{Im} s^{\text{Ret}}(0) \\
&= -\frac{3}{2\pi} \left(\frac{eV}{2} \right)^2 \text{Im} \left[\frac{\partial \bar{a}_1}{\partial \omega} + \frac{\partial a_3}{\partial \omega} \right]_{\omega=0} \text{Im} s^{\text{Ret}}(0) \\
&+ \frac{1}{\pi} (eV)^2 \text{Im} \left[\frac{\partial \bar{a}_1}{\partial \omega} \right]_{\omega=0} \text{Im} s^{\text{Ret}}(0) \\
&+ \frac{1}{2\pi} \left[-2b_1^{IIa} - b_1^{IIb} + \frac{3}{2}(b_1^{IIa} + b_3^{II}) \right] \text{Im} s^{\text{Ret}}(0).
\end{aligned} \tag{D36}$$

Comparing Eqs. (D16) and (D24) with (151) and (152) we establish that

$$b_1^{IIa} = -(eV)^2 \text{Im} \left[\frac{\partial \bar{a}_1}{\partial \omega} \right]_{\omega=0}, \tag{D37}$$

$$b_1^{IIb} = -4b_1^{IIa}, \tag{D38}$$

$$b_3^{II} = -(eV)^2 \text{Im} \left[\frac{\partial a_3}{\partial \omega} \right]_{\omega=0}. \tag{D39}$$

These relations allows us to express (D36) as

$$\begin{aligned}
&\frac{\partial}{\partial \lambda} \text{Im} \Sigma_{\sigma}^{\text{Ret}}(0) \\
&= -\frac{3}{2\pi} \frac{3(eV)^2}{4} \text{Im} \left[\frac{\partial \bar{a}_1}{\partial \omega} + \frac{\partial a_3}{\partial \omega} \right]_{\omega=0} \text{Im} s^{\text{Ret}}(0). \tag{D40}
\end{aligned}$$

After comparison with (153) it becomes clear that

$$\text{Im} \frac{\partial^2 \Sigma_{\sigma}^{\text{Ret}}}{\partial V^2} \Big|_{\omega, V=0} = \frac{3}{4} \text{Im} \Sigma'', \tag{D41}$$

which agrees with (31) and Ref. [58].

-
- ¹ U. Weiss, *Quantum Dissipative Systems* (World Scientific, Singapore, 2000); A. J. Leggett *et al.*, *Rev. Mod. Phys.* **59**, 1 (1987).
² *Single Charge Tunneling: Coulomb Blockade Phenomena in Nanostructures*, ed. by H. Grabert and M. H. Devoret (Plenum Press, New York, 1992).
³ *Mesoscopic Electron Transport*, ed. by L. L. Sohn, L. P. Kouwenhoven, and G. Schön (Kluwer, Dordrecht, 1997).
⁴ M. Mayor, H. B. Weber, and R. Waser, in *Nanoelectronics and Information Technology* ed. by R. Waser (Wiley-VCH, Weinheim, 2003), p. 503-525.
⁵ K. Hiruma *et al.*, *J. Appl. Phys.* **77**, 447 (1995).
⁶ S. Huang, X. Cai, and J. Liu, *J. Am. Chem. Soc.* **125**, 5636 (2003).
⁷ F. Lesage and H. Saleur, *Phys. Rev. Lett.* **80**, 4370 (1998); A. Schiller and S. Hershfield, *Phys. Rev. B* **62**, R16271 (2000); A. Komnik, *Phys. Rev. B* **79**, 245102 (2009).
⁸ E. Boulat, H. Saleur, and P. Schmitteckert, *Phys. Rev. Lett.* **101**, 140601 (2008).
⁹ E. Boulat and H. Saleur, *Phys. Rev. B* **77**, 033409 (2008).
¹⁰ P. Mehta and N. Andrei, *Phys. Rev. Lett.* **96**, 216802 (2006); *ibid.*, Erratum cond-mat/0703426.
¹¹ N. Andrei, private communication.
¹² F. B. Anders, *Phys. Rev. Lett.* **101**, 066804 (2008).
¹³ F. Heidrich-Meisner, A. E. Feiguin, and E. Dagotto, *Phys. Rev. B* **79**, 235336 (2009).
¹⁴ J. E. Han and R. J. Heary, *Phys. Rev. Lett.* **99**, 236808 (2007).
¹⁵ S. Weiss, J. Eckel, M. Thorwart, and R. Egger, *Phys. Rev. B* **77**, 195316 (2008).
¹⁶ F. B. Anders and A. Schiller, *Phys. Rev. Lett.* **95**, 196801 (2005); *ibid.*, *Phys. Rev. B* **74**, 245113 (2006); F. B. Anders, R. Bulla, and M. Vojta, *Phys. Rev. Lett.* **98**, 210402 (2007).
¹⁷ D. Roosen, M.R. Wegewijs, and W. Hofstetter, *Phys. Rev. Lett.* **100**, 087201 (2008).
¹⁸ A. Daley, C. Kollath, U. Schollwöck, and G. Vidal, *J. Stat. Mech.: Theor. Exp.* P04005 (2004); S. R. White and A. Feiguin, *Phys. Rev. Lett.* **93**, 076401 (2004); P. Schmitteckert, *Phys. Rev. B* **70**, 121302 (2004).
¹⁹ T. L. Schmidt, P. Werner, L. Mühlbacher, and A. Komnik, *Phys. Rev. B* **78**, 235110 (2008).
²⁰ P. Werner, T. Oka, and A. J. Millis, *Phys. Rev. B* **79**, 035320 (2009); P. Werner, T. Oka, M. Eckstein, and A. J. Millis, arXiv:0911.0587.
²¹ H. Schoeller and J. König, *Phys. Rev. Lett.* **84**, 3686 (2000).
²² H. Schoeller, in *Low-Dimensional Systems* (T. Brandes, Lect. Notes Phys., Springer, 2000) p. 137.
²³ M. Keil and H. Schoeller, *Phys. Rev. B* **63**, 180302(R) (2001).
²⁴ S. G. Jakobs, V. Meden, and H. Schoeller, *Phys. Rev. Lett.* **99**, 150603 (2007).
²⁵ H. Schoeller, *Eur. Phys. J. Special Topics* **168**, 179 (2009).
²⁶ H. Schoeller and F. Reininghaus, *Phys. Rev. B* **80**, 045117 (2009).
²⁷ D. Schuricht and H. Schoeller, *Phys. Rev. B* **80**, 075120 (2009).
²⁸ M. Pletyukhov, D. Schuricht, and H. Schoeller, arXiv:0910.0119.
²⁹ C. Karrasch, S. Andergassen, M. Pletyukhov, D. Schuricht, L. Borda, V. Meden, and H. Schoeller, arXiv:0911.5496.
³⁰ A. Rosch, H. Kroha, and P. Woelfle, *Phys. Rev. Lett.* **87**, 156802 (2001).
³¹ A. Rosch, J. Paaske, H. Kroha, and P. Woelfle, *Phys. Rev. Lett.* **90**,

- (2003) 076804; *ibid.*, J. Phys. Soc. Jpn. **74**, 118 (2005).
- ³² H. Schmidt and P. Woelfle, to be published in Ann. Phys. (Berlin), arXiv:0911.4383.
- ³³ S. Kehrein, Phys. Rev. Lett. **95**, 056602 (2005).
- ³⁴ F. Wegner, Ann. Phys. (Leipzig) **3**, 77 (1994); S. D. Glazek and K. G. Wilson, Phys. Rev. D **48**, 5863 (1993); *ibid.*, **49**, 4214 (1994).
- ³⁵ Ch. Wetterich, Phys. Lett. B **301**, 90 (1993); T. R. Morris, Int. J. Mod. Phys. A **9**, 2411 (1994).
- ³⁶ S. Jakobs, diploma thesis, Aachen 2003.
- ³⁷ R. Gezzi, Th. Pruschke, and V. Meden, Phys. Rev. B **75**, 045324 (2007).
- ³⁸ R. Gezzi, *Functional Renormalization Group for Non-Equilibrium Quantum Many-Body Problems*, PhD-thesis, Göttingen (2007).
- ³⁹ S. G. Jakobs, M. Pletyukhov, and H. Schoeller, arXiv:0902.2350.
- ⁴⁰ P. W. Anderson, Phys. Rev. **124**, 41 (1961).
- ⁴¹ A. C. Hewson, *The Kondo problem to heavy fermions*, (Cambridge University Press, Cambridge, 1993).
- ⁴² L. I. Glazman and M. E. Raikh, Sov. Phys. JETP Lett. **47**, 452 (1988); T. K. Ng and P. A. Lee, Phys. Rev. Lett. **61**, 1768 (1988).
- ⁴³ D. Goldhaber-Gordon *et al.*, Nature **391**, 156 (1998); S.M. Cronenwett *et al.*, Science **281**, 540 (1998); F. Simmel *et al.*, Phys. Rev. Lett. **83**, 804 (1999); J. Schmid *et al.*, Phys. Rev. Lett. **84**, 5824 (2000); W. G. van der Wiel *et al.*, Science **289**, 2105 (2000).
- ⁴⁴ K. Yamada, Prog. Theor. Phys. **53**, 970 (1975).
- ⁴⁵ K. Yosida and K. Yamada, Prog. Theor. Phys. **53**, 1286 (1975).
- ⁴⁶ K. Yamada, Prog. Theor. Phys. **54**, 316 (1975).
- ⁴⁷ V. Zlatić and B. Horvatić, Phys. Rev. B **28**, 6904 (1983).
- ⁴⁸ T. A. Costi, A. C. Hewson, and V. Zlatić, J. Phys.: Condens. Matter **6**, 2519 (1994); R. Bulla, T. A. Costi, and T. Pruschke, Rev. Mod. Phys. **80**, 395 (2008).
- ⁴⁹ A. M. Tsel'ick and P. B. Wiegmann, Adv. Phys. **32**, 453 (1983).
- ⁵⁰ C. Karrasch, T. Enss, and V. Meden, Phys. Rev. B **73**, 235337 (2006).
- ⁵¹ S. Andergassen, T. Enss, C. Karrasch, and V. Meden, in *Quantum Magnetism* ed. by B. Barbara, Y. Imry, G. Sawatzky, and P. C. E. Stamp (Springer, New York, 2008) (arXiv:cond-mat/0612229).
- ⁵² R. Hedden, V. Meden, Th. Pruschke, and K. Schönhammer, J. Phys.: Cond. Mat. **16**, 5279 (2004).
- ⁵³ C. Karrasch, R. Hedden, R. Peters, Th. Pruschke, K. Schönhammer, and V. Meden, J. Phys.: Condens. Matter **20**, 345205 (2008).
- ⁵⁴ S. Hershfield, J. H. Davies, and J. W. Wilkins, Phys. Rev. Lett. **67**, 3720 (1991); Phys. Rev. B **46**, 7046 (1992).
- ⁵⁵ T. Fujii and K. Ueda, Phys. Rev. B **68**, 155310 (2003).
- ⁵⁶ C. D. Spataru, M. S. Hybertsen, S. G. Louie, and A. J. Millis, Phys. Rev. B **79**, 155110 (2009).
- ⁵⁷ L. Bartosch, H. Freire, J. J. R. Cardenas, and P. Kopietz, J. Phys.: Cond. Mat. **21**, 305602 (2009).
- ⁵⁸ A. Oguri, Phys. Rev. B **64**, 153305 (2001).
- ⁵⁹ D. C. Langreth, *Linear and Nonlinear Response Theory with Applications*, NATO Advanced Study Institutes Series B vol. 17, J. T. Devreese and V. E van Doren, eds. (Plenum Press, New York, 1976).
- ⁶⁰ E. M. Lifshitz and L. P. Pitaevskii, *Physical Kinetics*, (Pergamon Press, New York, 1981).
- ⁶¹ J. Rammer and H. Smith, Rev. Mod. Phys. **58**, 323 (1986).
- ⁶² H. Haug, A.-P. Jauho, *Quantum Kinetics in Transport and Optics of Semiconductors* (Springer, Berlin, 1996).
- ⁶³ L. V. Keldysh, Zh. Eksp. Teor. Fiz. **47**, 1515 (1964) [Sov. Phys. JETP **20**, 1018 (1965)].
- ⁶⁴ B.-L. Hao, Physica A **109**, 221 (1981).
- ⁶⁵ J. W. Negele and H. Orland, *Quantum Many-Particle Systems* (Addison-Wesley, Reading, 1988).
- ⁶⁶ M. Salmhofer 1998, *Renormalization: An Introduction* (Springer, Heidelberg, 1998).
- ⁶⁷ M. Salmhofer and C. Honerkamp, Prog. Theor. Phys. **105**, 1 (2001).
- ⁶⁸ W. Metzner, Prog. Theor. Phys. Suppl. **160**, 58 (2005).
- ⁶⁹ V. Meden, in *Advances in Solid State Physics*, Vol. 46, ed. by R. Haug (Springer, New York, 2007); arXiv:cond-mat/0604302.
- ⁷⁰ J. R. Schrieffer, D. C. Mattis, Phys. Rev. **140**, A1412 (1965).
- ⁷¹ Y. Meir, N. S. Wingreen, Phys. Rev. Lett. **68**, 2512 (1992).
- ⁷² V. Janiš and P. Augustinský, Phys. Rev. B **75**, 165108 (2007); V. Janiš and P. Augustinský, Phys. Rev. B **77**, 085106 (2008).
- ⁷³ C. Honerkamp and M. Salmhofer, Phys. Rev. Lett. **87**, 187004 (2001); Phys. Rev. B **64**, 184516 (2001).
- ⁷⁴ D. E. Logan, M. P. Eastwood, and M. A. Tusch, J. Phys.: Condens. Matter **10**, 2673 (1998).
- ⁷⁵ The NRG data presented here and in the following figures have been created with a ready-to-use program that was kindly provided by Dr. Theo Costi, Institute of Solid State Research, Forschungszentrum Jülich.